EFFECT OF FLOOR SLABS AND FLOOR BEAMS ON STATIC AND DYNAMIC BEHAVIOUR OF SHEAR WALL STRUCTURES

by

JAYANTA K. BISWAS, M.E.

A Thesis

Submitted to the Faculty of Graduate Studies

in Partial Fulfilment of the Requirements

for the Degree

Master of Engineering

McMaster University

November 1970

MASTER OF ENGINEERING (1970)
(Civil Engineering)

McMASTER UNIVERSITY
Hamilton, Ontario

TITLE: Effect of Floor Slabs and Floor Beams on Static and Dynamic Behaviour of Shear Wall Structures.

AUTHOR: Jayanta K. Biswas, M.E. (Calcutta University)

SUPERVISOR: Dr. W.K. Tso

NUMBER OF PAGES: vi, 170

SCOPE AND CONTENTS:

This thesis studies the effect of floor slabs on the static and dynamic behaviour of the shear wall structure. A single component has been analysed using the 'Matrix Transfer' technique along with Vlasov's thin walled elastic beam theory. Experimental verification was done on a small scale plexiglas eight storey model in the form of a channel section for both static and dynamic loading.

The thesis also deals with the analysis of the non-planar shear walls coupled through floor beams subjected to static loading. The continuum approach along with Vlasov's theory has been used in the analysis. Experimental verification was done on a small scale plexiglas model in the form of two equal angles connected by eight floor beams at equal spacing.

ACKNOWLEDGEMENTS

I wish to express my profound gratitude to Dr. W.K. Tso for his continued guidance and encouragement in carrying out this thesis.

I would also like to thank Dr. A.C. Heidebrecht for arranging discussions among shear wall group in order to exchange views and ideas.

I thank Dr. A. Ghobarah and Mr. R.K. Raina for their co-operation. Thanks are also due to Mrs. S. McQueen for neatly typing this thesis.

This investigation was made possible through the financial assistance of the National Research Council, to whom I extend my sincere thanks.

TABLE OF CONTENTS

NOTATIONS

The following symbols are used throughout this thesis without further definition. Other symbols are defined when used.

E	Modulus of Elasticity
G	Modulus of rigidity
ν	Poisson's ratio
X,Y	Orthogonal axis
Z	Vertical axis
ω	Principal Sectorial co-ordinate
A	cross sectional area
I_X, I_Y	Moment of Inertia about X and Y axes
J	Torsional rigidity
I_p	Polar moment of inertia about shear center
I_ω	Sectorial moment of inertia
θ	Rotation about Z axis
θ'	Rate of change of rotation about Z axis
u,v	Displacement of shear center in x and y directions
u',v'	Slope in zx and zy planes
V	Shear Force
M	Moment
H	Torque
B	Bimoment
N	Axial Force
a_x, a_y	Co-ordinate of shear center
ρ	Mass density of material
w	Natural frequency
$(\dot{\ })$	Differentiation with respect to time
$(\ ')$	Differentiation with respect to space.

CHAPTER I

INTRODUCTION

1.1 Description of Shear Wall

As buildings increase in height, it becomes necessary to ensure adequate lateral stiffness. This stiffness may be achieved in various ways of which the use of shear wall is very common and popular.

Although shear walls can be arranged in a building in innumerable ways, they can be broadly classified into two basic types. In an apartment building, shear walls are used alone and located on both sides of the corridor as shown in Fig. 1.1.1. In an office building, shear walls are located in the center to form a service core for staircases, elevators etc. This core is surrounded by a structural framing which are interconnected as shown in Fig. 1.1.2. In both the above types, shear walls serve the multipurpose function of supporting vertical and lateral loads, acting as partition walls and serving other useful functions.

Shear walls are normally interconnected by floor slabs at each floor level. These floor slabs act as highly rigid diaphragm in their own plane and bend and twist out of plane. Therefore, the slabs transmit and distribute lateral loads among the walls and also provide some resistance

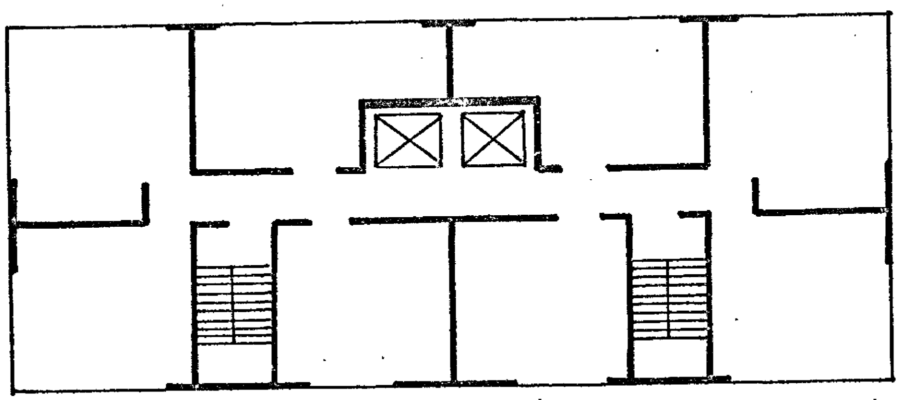

Typical Apartment Building With Shear Wall

FIG. 1.1.1

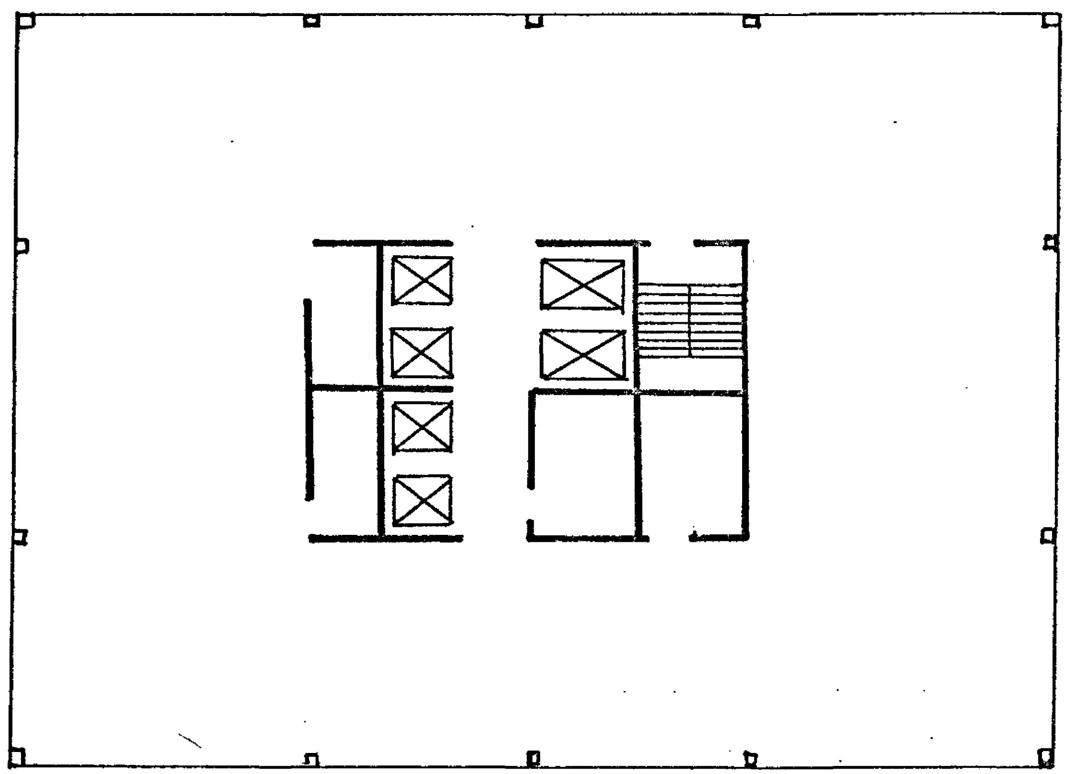

Typical Office Building With Shear Walls in the central Core Surrounded by Structural Framing

FIG. 1.1.2

to the deformation of the walls. The effect of overall interaction between the walls and the floors is to increase the lateral stiffness of the building and to reduce stress level in the walls.

Very often shear walls are pierced to provide openings for doors, windows or corridors. The arrangement may be thought of as two or more sets of walls connected by beams. These beams resist the deformation of the wall and increase the stiffness of the assembly.

Frequently the section of shear walls are in the form of open thin walled sections. Such beams are distinguished from solid beams by experiencing longitudinal stress as a result of torsion due to warping. Appropriate theory should be considered for dealing with such sections.

For these reasons, a complete analysis of a building as shown in Figs. 1.1.1 and 1.1.2 is a most complex problem encountered in structural engineering practice. The complexity is due to various interacting elements. The dynamic analysis is even more complex. Approximate design methods, neglecting complex interaction can be used for proportioning elements which often under estimates the stiffness of building. Therefore, more sophisticated techniques of analysis are required.

The general purpose of research on shear wall structure is firstly to understand fully the behaviour of different elements and secondly, to develop more realistic methods of analysis.

1.2 Shear Wall Project

The Canada Emergency Measures Organization is sponsoring an extensive program into behaviour of shear wall building. This project is conducted in the Department of Civil Engineering and Engineering Mechanics at McMaster University. The experimental part of the project consists of building small scale shear wall structures and studying their response due to static and dynamic lateral loadings. The theoretical part of the project consists of developing theories to explain the behaviour of shear wall structures, comparing theoretical results with experiments and developing simplified design method.

Tests have been carried on an eight feet model having E shaped section and made of non-reinforced micro-concrete. Afsar(1), Quareshi(2), Speirs(3), Raina(4) and Swift(5) studied different aspects of behaviour of shear wall structures.

1.3 Review of Past Works

Coull and Smith (6) compiled a comprehensive summary of the published literature concerning shear wall buildings.

Winokur and Gluck (7) developed a method to form lateral stiffness matrix of asymmetric bulding by combining lateral stiffness matrix of each element. Transverse stiffness of slab and warping torsional stiffness of individual elements has been neglected.

The phenomenon of warping has been known to the aeronotical engineers for a long time but its application to shear wall structure is rather recent. Vlasov (8) developed the theory of thin walled open beams. Zbirohowski-Koscia (9) presented Vlasov's theory in simpler way and with an aim to make it usable by practicing engineers.

Afsar (1) has outlined various analytical and experimental approaches used in the shear wall study.

Quareshi (2) analysed the shear wall with rows of opening by frame analogy method and also conducted experiments on small scale models.

Speirs (3) studied the behaviour of floor slabs introduced in shear wall structure. His theoretical analysis is mainly based on the initial parameter approach of Vlasov.

Raina (4) studied response of shear wall structure under dynamic loading.

Swift (5) developed computer program based on matrix method, to solve asymmetric coupled shear wall. He also developed a program to analyse shear wall with floors.

Qadeer (10) and Qadeer and Smith (11) discussed the interaction between walls and slabs in a cross wall structure. Curves are given for equivalent width of slab. Experimental work on a model was done for verification of the theory.

Taranath (12) studied open section with and without floors. Finite element treatment for floor slab is used. Multiple open section core structure coupled through floor slab is also examined for the case of static loading.

Beck (13), Rosman (14) analysed plane coupled shear wall by continuum method. The connecting beams are replaced by independently acting laminae. Coull and Choudhury (15), (16) developed design curves for different types of loading based on the continuous method of analysis.

Choudhury (17) discussed the solution single shear wall with openings by continuous method, equivalent frame method and finite element method. The behaviour of walls interconnected through floor slab is also examined. A method of complete analysis of shear wall/frame buildings taking into account their three-dimensional behaviour is presented.

Michael (18) made torsion analysis of a core wall consisting of two equal channels tied by beams at equal spacing by the continuum approach.

Jenkins and Harrison (19) analysed tall building with shear walls under bending and torsion. His bending analysis is based on stiffness matrix approach and torsion analysis is based on the theorem of minimum potential energy. The warping stiffness of the open sections are neglected. Experiments are carried out on small scale plexiglas model in different stages.

Holmes and Astill (20) conducted experiments on a small scale shear wall structure under simulated wind load. Comparison of experimental values are made with theoretical consideration of simplified structure using Rosman's (14) theory.

Rosman (21) presented analysis of pierced torsion boxes subjected to torsion loading, arbitrarily distributed along the height. Treatment for two channel box and four angle box is done. Determination of approximate fundamental period of torsional vibration is also included.

Gluck (22) presented a lateral load analysis by three dimensional continuous method for structures consisting of simple or coupled, prismatic or non-prismatic, shear walls and frames arranged asymmetrically in floor plan. Connecting beam on the shear wall is replaced by an 'elastic media' of known stiffness properties. Treatment for thin walled open section is included. Differential equations are obtained for three-generalised displacements. In his derivation of stiffness matrix for 'elastic media', slight inconsistancy of the use of 'thin walled beam theory' was noticed. Modification of few elements of matrix has been suggested by Biswas and Tso (24) in a discussion of Gluck's (22) paper.

Macleod (23) commented on the limitation of the use of continuum method when the bending stiffness of the wall appraoch that of connecting beams. A criterion is developed for assessing when this effect may be important. Comparison is made with more accurate frame analysis.

Coull and Irwin (28) presented a method for the analysis of the distribution of load amongst the shear walls of a three dimensional multistorey building subjected to bending and torsion. The method is based on the continuum approach.

1.4 Present Investigation

In the second and third chapters of this thesis, particular interest is given on shear wall with floors. A shear wall structure consisting of channel section with floor slabs is analysed for static and dynamic loading using the 'Matrix Transfer' method. To the best of the author's knowledge, this method has not been used to solve similar problems before. Experimental study was conducted on a small scale plexiglas model. This model was subjected to lateral loading at different floor levels when the recorded deflections and strains were studied. It was then subjected to lateral vibration to determine the resonant frequencies. The relative strain distribution at resonance is also studied.

In the fourth chapter, particular interest is on the nonplanar shear walls coupled by floor beams where warping due to torsion of piers is taken into account. Differential equations are obtained using the continuum approach. The present formulation is applicable to two shear walls connected by one row of beams and subjected to forces and torques distributed along its height. The experimental study was performed on a small scale plexiglas model consisting of two equal angle sections connected by beams at equal spacing. It was subjected to a force and a torque at top. The resulting strains and deflections are then analysed. A comparison of the experimental results with the theory is made in all three chapters.

CHAPTER II

STATIC STUDY OF SHEAR WALL WITH FLOORS

2.1 Summary

In this chapter, a shear wall structure consisting of a channel section with floor slab is analysed for static lateral load. The 'Matrix Transfer' technique is used. An experiment performed on a small scale plexiglas model Fig. (2.1.1) is described and the experimental results are compared with theoretical predictions.

2.2 Matrix Transfer Method

This method was originally developed by Holtzer(25) for treating torsional vibrations of shafts with lumped system. Myklestad(26) used a similar method for study of beam vibration problems. It was modified by Thomson(27) to extend its applicability to more general problems. Application of such method to static problem is less common.

Consider a system with n points and n elements along its length as shown in Fig.(2.2.1). For any point i there are two sub-point $(i)_-$ and $(i)_+$ denoting position before and after the ith point. Generalised force and displacement quantitites of a sub-point is assembled in a column matrix called state vector $\{Z\}$. The part of the structure between $(i)_-$ and $(i-1)_+$ is defined as ith field and that between $(i)_-$ and $(i)_+$ is defined as ith point. Field transfer matrix $[F_i]$ relates the state vectors of two subpoints in ith field and is obtained from

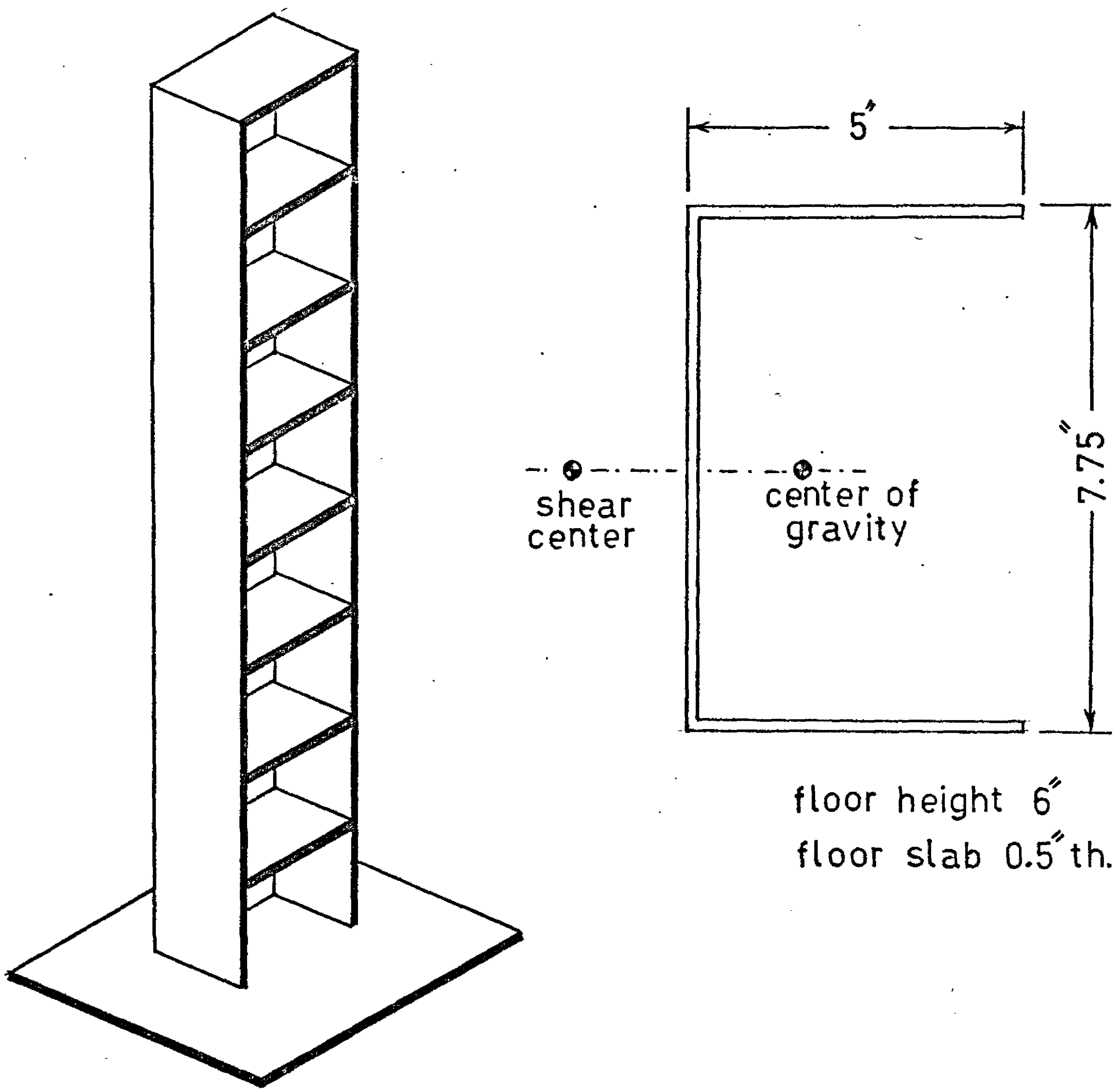

TEST STRUCTURE

FIG. 2.1.1

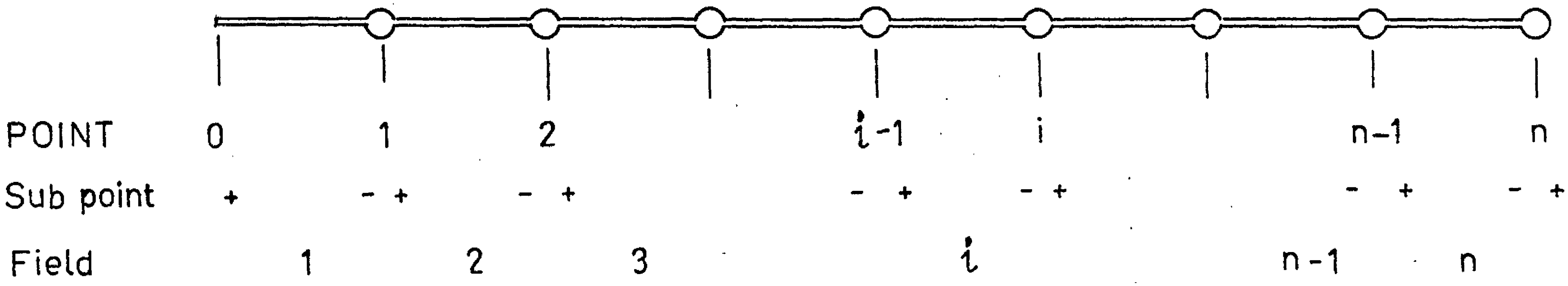

$\{Z_i^+\}$ State Vector at Point i & Sub point +

$[F_i]$ Field Transfer Matrix at i th Field

$[P_i]$ Point Transfer Matrix at i th Point

$[L_i]$ Load Vector at i th Point

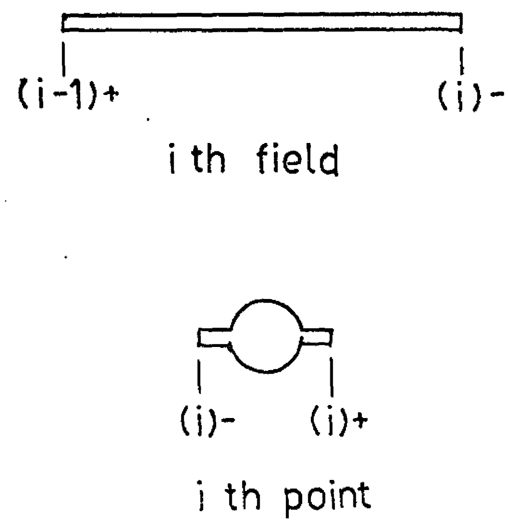

FIG. 2.2.1

solution of differential equation of the element. Point transfer Matrix $[P_i]$ relates the state vectors of two subpoints in ith point. Load vector at ith point is defined as $\{L_i\}$. The relations can be expressed as

$$\{Z_i^-\} = [F_i]\{Z_{i-1}^+\} \tag{2.2.1}$$

$$\{Z_i^+\} = [P_i]\{Z_i^-\} + \{L_i\} \tag{2.2.2}$$

where $i = 1,2,\ldots n$

From these two sets of eqs. (2.2.1) and (2.2.2) it is possible to eliminate the state vectors of the inner points and get a relation between the state vectors of the extreme points $(0)_+$ and $(n)_+$

$$\{Z_n^+\} = [A]\{Z_o^+\} + \{N\} \tag{2.2.3}$$

Where [A] is combined transfer matrix and {N} is combined load vector obtained from multiplication of appropriate matrices.

Mathematically, they are given by

$$[A] = [P_n][F_n]\ldots.[P_2][F_2][P_1][F_1] \tag{2.2.3a}$$

$$\begin{aligned}\{N\} = {} & [P_n][F_n]\ldots.[P_2][F_2]\{L_1\} \\ & + [P_n][F_n]\ldots.[P]2[F_3]\{L_2\} \\ & \ldots\ldots\ldots\ldots\ldots\ldots\ldots\ldots \\ & + [P_n][F_n][P_{n-1}][F_{n-1}]\{L_{n-2}\} \\ & + [P_n][F_n]\{L_{n-1}\} + \{L_n\}\end{aligned} \tag{2.2.3b}$$

The next step is to substitute the boundary conditions in the boundary state vectors, namely $\{Z_n^+\}$ and $\{Z_o^+\}$ in eq. 2.2.3.

Simplification of this matrix equation will yield a set of linear simultaneous equation which can be solved. The solution will give the values of boundary state vectors $\{Z_n^+\}$ and $\{Z_o^+\}$. The state vector at other points follow from the eq. 2.2.1 and 2.2.2 as,

$$\{Z_1^-\} = [F_1]\{Z_o^+\}$$

$$\{Z_1^+\} = [P_1][F_1]\{Z_o^+\} + \{L_1\}$$

$$\{Z_2^-\} = [F_2][P_1][F_1]\{Z_o^+\} + [F_2]\{L_1\}$$

$$\{Z_2^+\} = [P_2][F_2][P_1][F_1]\{Z_o^+\} + [P_2][F_2]\{L_1\} + \{L_2\}$$

$$\begin{aligned}\{Z_n^-\} = {} & [F_n][P_{n-1}][F_{n-1}]\ldots.[P_1][F_1]\{Z_o^+\} \\ & + [F_n][P_{n-1}][F_{n-1}]\ldots.[P_2][F_2]\{L_1\} \\ & + [F_n][P_{n-1}][F_{n-1}]\ldots.[P_3][F_3]\{L_2\} \\ & \ldots\ldots\ldots\ldots + [F_n]\{L_{n-1}\}\end{aligned} \qquad (2.2.4)$$

2.3 Application of Matrix Transfer Method

The structure considered consists of a prismatic mono symmetric section with equally spaced slabs. The floor slab represents 'point' and the part of the beam in between floor slabs represents 'field' as defined earlier. The simplified model to be used in Matrix Transfer method is shown in Fig. 2.3.1. In this case n equals eight and all field transfer matrices and points transfer matrices are identical.

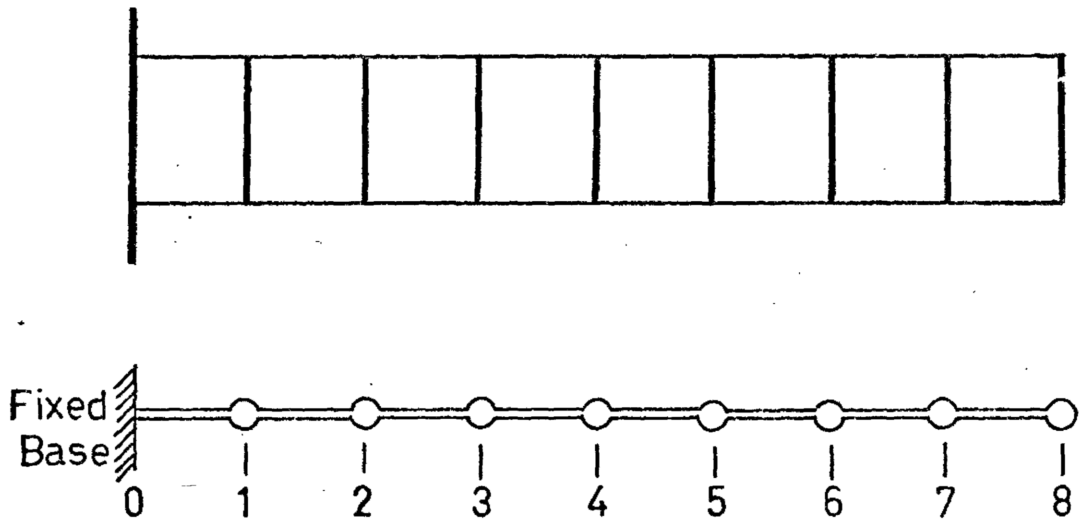

SIMPLIFIED MODEL

FIG. 2.3.1

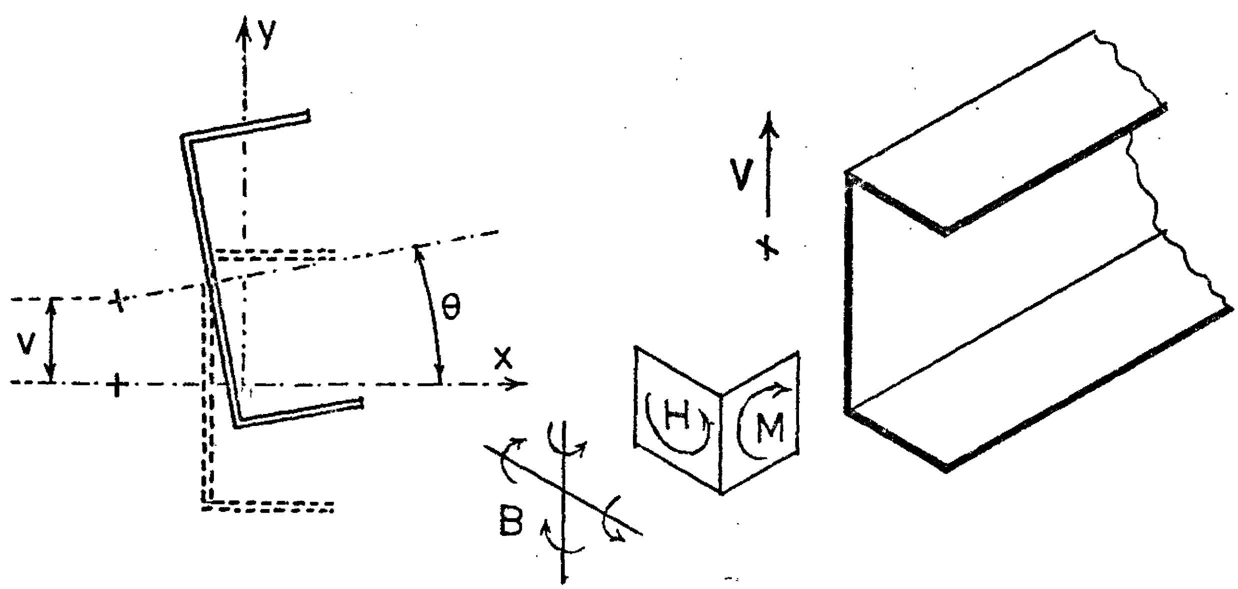

FORCE & DISPLACEMENT QUANTITIES

FIG. 2.3.2

2.3.1 State Vector

The state vector is an eighth order column matrix consisting of the following terms

$$Z = \begin{Bmatrix} v \\ v' \\ M \\ V \\ \theta \\ \theta' \\ B \\ H \end{Bmatrix}$$

The notations are explained and illustrated in fig. 2.3.2.

2.3.2 Field Transfer Matrix

The field is a prismatic thin walled beam of length ℓ and its transfer matrix is obtained from the solution of the differential equations. When refered to principal axes, the uncoupled differential equations for bending in y-direction and rotation are (Eq. A.4, Appendix-A):

$$EI_x v^{IV} = 0 \tag{2.3.1}$$

$$EI_\omega \theta^{IV} - GJ\theta'' = 0 \tag{2.3.2}$$

The solution of the first equation yields the following expressions for displacement, slope, moment and shear.

$$\left.\begin{aligned} v(Z) &= D_1 Z^3/6 + D_2 Z^2/2 + D_3 Z + D_4 \\ v'(Z) &= D_1 Z^2/2 + D_2 Z + D_3 \\ M(Z)/EI_x &= v'' = D_1 Z + D_2 \\ V(Z)/EI_x &= -v''' = -D_1 \end{aligned}\right\} \tag{2.3.3}$$

Where D_1, D_2, D_3 and D_4 are constants of integration determined from the boundary condition at Z=0 namely

$$v = v(0),\ v' = v'(0),\ M = M(0) \text{ and } V = V(0)$$

The state vector at Z = ℓ can be expressed in terms of state vector at Z = 0 by the relation,

$$\left.\begin{aligned} v(\ell) &= (0) + \ell v'(0) + \frac{\ell^2}{2EI_x} M(0) - \frac{\ell^3}{6EI_x} V(0) \\ v'(\ell) &= v'(0) + \frac{\ell}{EI_x} M(0) - \frac{\ell^2}{2EI_x} V(0) \\ M(\ell) &= M(0) + \ell.V(0) \\ V(\ell) &= V(0) \end{aligned}\right\} \qquad (2.3.4)$$

The solution of the second equation yields the following expresssions for rotation, warping, bimoment and torque.

$$\left.\begin{aligned} \theta(Z) &= C_1 + C_2 Z + C_3 \sinh KZ + C_4 \cosh KZ \\ \theta'(Z) &= C_2 + C_3 K \cosh KZ + C_4 K \sinh KZ \\ B(Z)/EI_\omega &= -\theta'' = -C_3 K^2 \sinh K^2 - C_4 K^2 \cosh KZ \\ H(Z) &= -EI_\omega \theta^{111} + CJ\theta^1 = C_2.GJ \end{aligned}\right\} \qquad (2.3.5)$$

$$\text{Where} \quad K = \sqrt{\frac{GJ}{EI_\omega}}$$

The constants C_1, C_2, C_3 and $C_4$are constants of integration determined from the boundary condition at Z = 0 namely

$$\theta = \theta(0),\ \theta' = \theta'(0),\ B = B(0) \text{ and } H = H(0)$$

The boundary condition at Z = ℓ are

$$\theta = \theta(\ell),\ \theta' = \theta'(\ell),\ B = B(\ell) \text{ and } H = H(\ell)$$

They can be expressed in terms of $\theta(0)$ $\theta'(0)$, $B(0)$ and $H(0)$ by the following expressions

$$\left.\begin{aligned}
\theta(\ell) &= \theta(0) - \frac{1}{K}\sinh K\ell\ \theta'(0) - \frac{1}{GJ}(1-\cosh K\ell)\ B(0) \\
&\qquad + \frac{1}{GJ}\left(\ell - \frac{1}{K}\sinh K\ell\right) H(0) \\
\theta'(\ell) &= \cosh K\ell\ \theta'(0) - \frac{K}{GJ}\sinh K\ell\ B(0) \\
&\qquad + \frac{1}{GJ}(1 - \cosh K\ell)\ H(0) \\
B(\ell) &= -\frac{GJ}{K}\sin K\ell\ \theta'(0) + \cosh K\ell\ B(0) \\
&\qquad + \frac{1}{K}\sinh K\ell\ H(0) \\
H(\ell) &= H(0)
\end{aligned}\right\} \quad (2.3.6)$$

Eq. 2.3.4 and eq. 2.3.6 can be combined in a single matrix eq. as

$$\{Z(\ell)\} = [F]\{Z(0)\} \qquad (2.3.7)$$

where

$$\{Z(\ell)\} = \begin{Bmatrix} v(\ell) \\ v'(\ell) \\ M(\ell) \\ V(\ell) \\ \theta(\ell) \\ \theta'(\ell) \\ B(\ell) \\ H(\ell) \end{Bmatrix} \quad \text{and} \quad Z(0) = \begin{Bmatrix} v(0) \\ v'(0) \\ M(0) \\ V(0) \\ \theta(0) \\ \theta'(0) \\ B(0) \\ H(0) \end{Bmatrix}$$

Field transfer matrix is an eigth order square matrix

$$[F] = \begin{bmatrix} f_{11} & f_{12} & f_{13} & f_{14} & 0 & 0 & 0 & 0 \\ 0 & f_{22} & f_{23} & f_{24} & 0 & 0 & 0 & 0 \\ 0 & 0 & f_{33} & f_{34} & 0 & 0 & 0 & 0 \\ 0 & 0 & 0 & f_{44} & 0 & 0 & 0 & 0 \\ 0 & 0 & 0 & 0 & f_{55} & f_{56} & f_{57} & f_{58} \\ 0 & 0 & 0 & 0 & 0 & f_{66} & f_{67} & f_{68} \\ 0 & 0 & 0 & 0 & 0 & f_{76} & f_{77} & f_{78} \\ 0 & 0 & 0 & 0 & 0 & 0 & 0 & f_{88} \end{bmatrix} \tag{2.3.8}$$

Where the non zero elements are

$f_{11} = 1,\ f_{12} = \ell,\ f_{13} = \ell^2/2EI_x,\ f_{14} = -\ \ell^3/6EI_x,$

$f_{22} = 1,\ f_{23} = \ell/EI_x,\ f_{24} = -\ \ell^2/2EI_x,$

$f_{33} = 1,\ f_{34} = \ell,\ f_{44} = 1,$

$f_{55} = 1,\ f_{56} = \sinh K\ell/K,$

$f_{57} = (1 - \cosh K\ell)/GJ,\ f_{58} = (\ell - \frac{1}{K} \sinh K\ell)/GJ$

$f_{66} = \cosh K\ell,\ f_{67} = -\ K \sinh K\ell/GJ$

$f_{68} = (1 - \cosh K\ell)/GJ,\ f_{76} = -\ GJ \sin K\ell/K$

$f_{77} = \cosh K\ell,\ f_{78} = \sinh K\ell/K,\ f_{88} = 1.$

2.3.3 Action of Floor Slab

Vlasov (1) considered the effect of a diaphragm on the behaviour of a thin walled beam. In a shear wall structure, floor slab is equivalent to diaphragm. Vlasov assumed that the diaphragm acts as a plate in torsion and derived the following relationship for the bimoment applied to the shear wall by the action of the slab (Fig. 2.3.4(a)).

$$B_t = \frac{Et^3 bd}{6(1+\nu)} \theta' \qquad (2.3.9)$$

Where b = width of slab

d = length of slab

t = thickness of slab

ν = Poisson's ratio

E = modulus of elasticity of slab

θ' = warping of the shear wall at the level of slab.

In this derivation Vlasov neglected the effect of bending of slab (Fig. 2.3.4 (b)) due to fixity of walls. This can be considered by treating the slab as a series of beams running between the flanges. The center line of the beams is the locus of point of contraflexure for each beam. If a cut is made along that line, there will be relative displacement to the left and right of the cut. (Fig. 2.3.4(c)). Shear force q will develop along the line to maintain continuity (Fig. 2.3.4 (d)). For an element of beam at a distance ξ from the wall, the sectorial areas at the center

FIG. 2.3.4

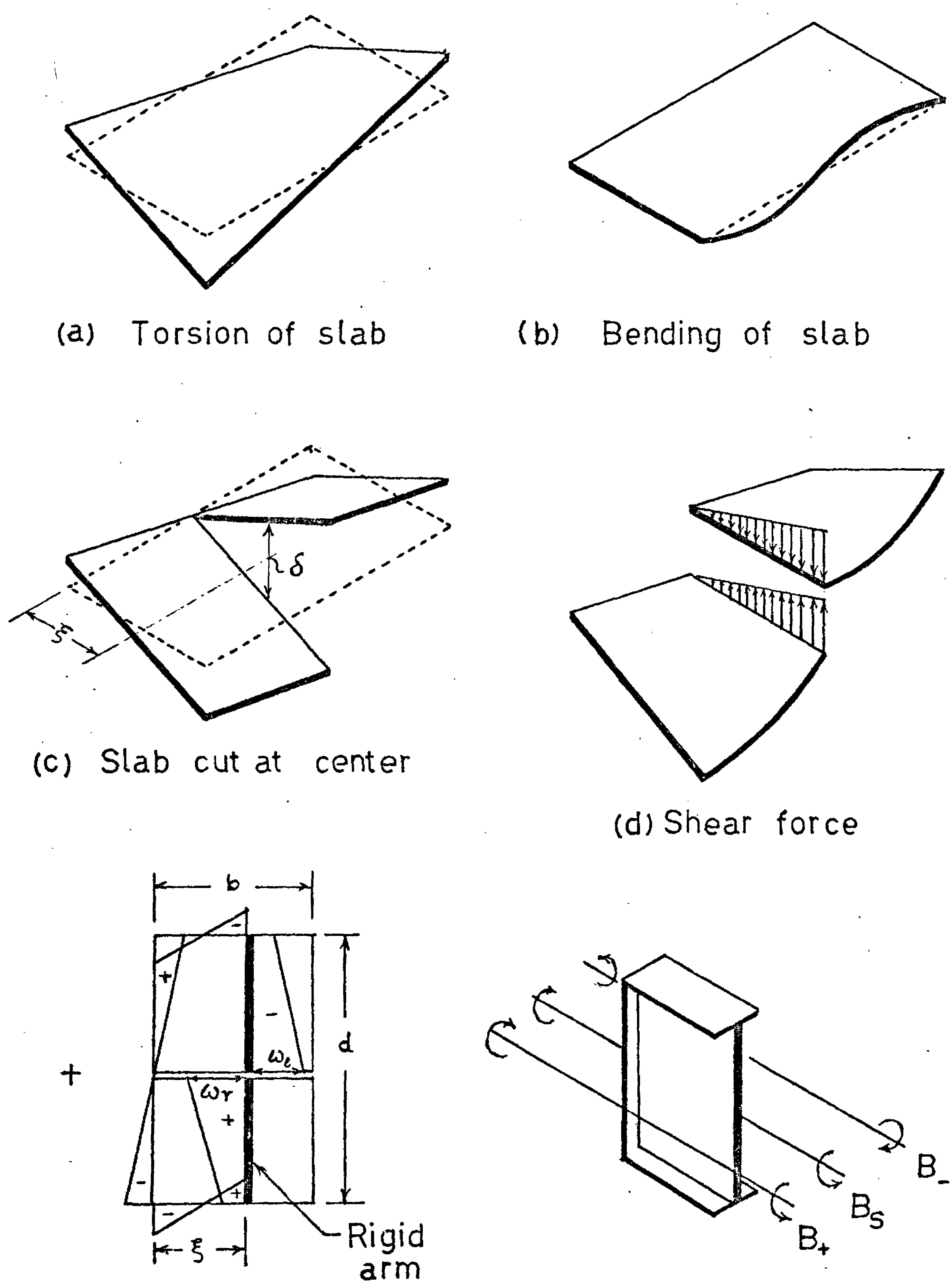

(a) Torsion of slab (b) Bending of slab

(c) Slab cut at center (d) Shear force

(e) Sectorial area (f) Bimoment from slab

(Fig. 2.3.4(e)) considering rigid arms attached to thin walled beam are:

$$\omega_r = \xi d, \ \omega_\ell = -\xi d.$$

Discrepancy of displacement is

$$\delta = (\omega_r - \omega_\ell)\theta' = 2\xi d\theta'$$

Shear force develops to maintain continuity considering bending deformation only

$$q = \frac{2Et^3\xi}{(1-\nu^2)d^2}\theta'$$

The bimoment due to the shear force is

$$dB = q(\omega_r - \omega_\ell)d\xi = 2\ q\ \xi d\ d\xi$$

The total bimoment due to bending is obtained on integration

$$B_b = \int_o^b dB = \frac{4Et^3b^3}{3d(1-\nu^2)}\theta' \qquad (2.3.10)$$

The combined bimoment due to torsion and bending is

$$B_s = B_t + B_b = D\ \theta' \qquad (2.3.11)$$

Where

$$D = \left(\frac{Et^3bd}{6(1+\nu)} + \frac{4Et^3b^3}{3d(1-\nu^2)} \right) \qquad (2.3.12)$$

From Fig. 2.3.4 (a), the bimoment contribution from slab is related to the bimoments in the walls immediately above and below the floor slab.

$$B_+ = B_- - B_s = B_- - D\ \theta' \qquad (2.3.13)$$

2.3.4. Point Transfer Matrix and Load Vector

The Point transfer matrix [P] is a square matrix of order eigth. It is obtained from the consideration of equilibrium and compatibility:

$$[P] = \begin{bmatrix} 1 & 0 & 0 & 0 & 0 & 0 & 0 & 0 \\ 0 & 1 & 0 & 0 & 0 & 0 & 0 & 0 \\ 0 & 0 & 1 & 0 & 0 & 0 & 0 & 0 \\ 0 & 0 & 0 & 1 & 0 & 0 & 0 & 0 \\ 0 & 0 & 0 & 0 & 1 & 0 & 0 & 0 \\ 0 & 0 & 0 & 0 & 0 & 1 & 0 & 0 \\ 0 & 0 & 0 & 0 & 0 & -D & 1 & 0 \\ 0 & 0 & 0 & 0 & 0 & 0 & 0 & 1 \end{bmatrix}$$

The load vector is a column matrix of order eight.

$$\{L_i\} = \begin{Bmatrix} 0 \\ 0 \\ 0 \\ -P_i \\ 0 \\ 0 \\ 0 \\ -Q_i \end{Bmatrix}$$

Where $i = 1,2....8$

and P_i is applied load

and Q_i is the applied

torque at ith level.

2.3.5 Boundary Conditions

The shear wall is fixed at the base and free at top. Therefore, the state vectors at the base and the top can be written as

$$\{Z_o^+\} = \begin{Bmatrix} 0 \\ 0 \\ M_o^+ \\ V_o^+ \\ 0 \\ 0 \\ B_o^+ \\ H_o^+ \end{Bmatrix} \quad \text{and} \quad \{Z_8^+\} = \begin{Bmatrix} v_8^+ \\ v_8'^+ \\ 0 \\ 0 \\ \theta_8^+ \\ \theta_8'^+ \\ 0 \\ 0 \end{Bmatrix}$$

Substituting the above conditions in eq. 2.2.3 and making some rearangment of terms the following eq. is obtained.

$$[B]\{Y\} = \{N\} \tag{2.3.14}$$

Where

$$\{Y\} = \begin{Bmatrix} v_8^+ \\ v_8'^+ \\ M_o^+ \\ V_o^+ \\ \theta_8^+ \\ \theta_8'^+ \\ B_o^+ \\ H_o^+ \end{Bmatrix}$$

and $\{N\}$ is defined in eq. 2.2.3b

and

$$[B] = \begin{bmatrix} 1 & 0 & -a_{13} & -a_{14} & 0 & 0 & 0 & 0 \\ 0 & 1 & -a_{23} & -a_{24} & 0 & 0 & 0 & 0 \\ 0 & 0 & -a_{33} & -a_{34} & 0 & 0 & 0 & 0 \\ 0 & 0 & -a_{43} & -a_{44} & 0 & 0 & 0 & 0 \\ 0 & 0 & 0 & 0 & 1 & 0 & -a_{57} & -a_{58} \\ 0 & 0 & 0 & 0 & 0 & 1 & -a_{67} & -a_{68} \\ 0 & 0 & 0 & 0 & 0 & 0 & -a_{77} & -a_{78} \\ 0 & 0 & 00 & 0 & 0 & 0 & -a_{87} & -a_{88} \end{bmatrix}$$

Here 'a' denotes the elements of matrix [A] as defined in eq. 2.2.3 (a). The solution is obtained by inversion

$$\{Y\} = [B]^{-1}\{N\} \tag{2.3.15}$$

Knowing {Y}, $\{Z_o^+\}$ and $\{Z_8^+\}$ can be formed. State vector at other points are obtained from expressions in eq. 2.2.4.

2.4 Computer Program

A computer program based on the above analysis has been written. The input data are the geometric and elastic properties and loading of the structure. The output quantitites are the state vectors at all floor levels. The present program is for identical floor slabs, equal storey heights and prismatic section. Extension for stepped cases or different storey heights and floor slabs can be made with little modification.

The flow chart is given in Fig. 2.4.1 and the computer program is included in Appendix-B.

2.5 Experiment

An experiment was done on a small scale plexiglas model (Fig. 2.1.1). It was made by assembling different components representing walls and floors. The base of the model was connected to a thick base plate which in turn was fixed to two heavy I sections to achieve fixity (Fig. 2.5.1), It was loaded at the 8th, 6th and 4th floor respectively, one floor at a time, by hanging weights over

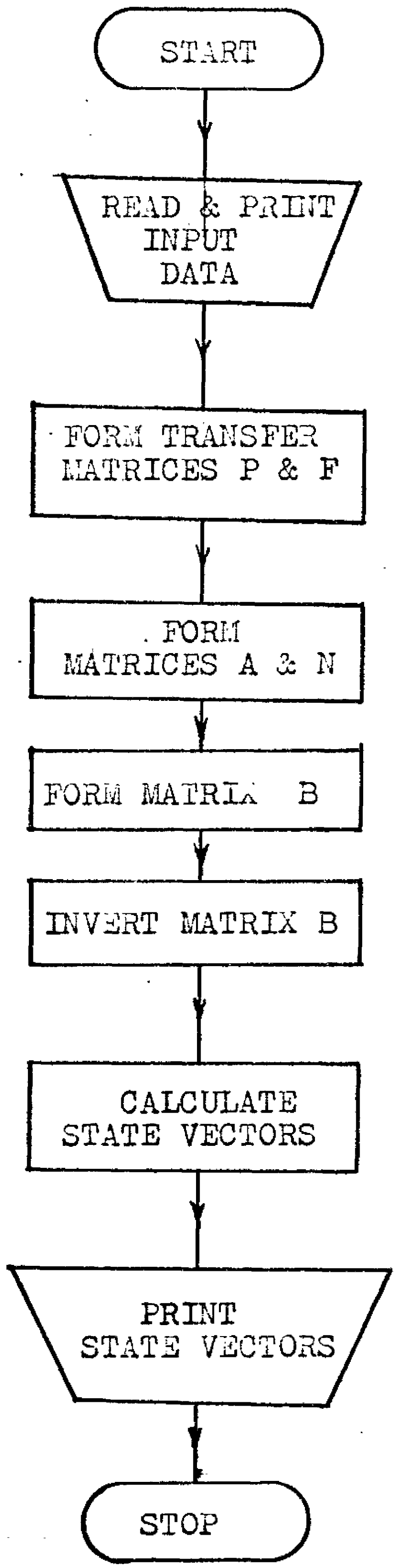

FLOW CHART

FIG. 2.4.1

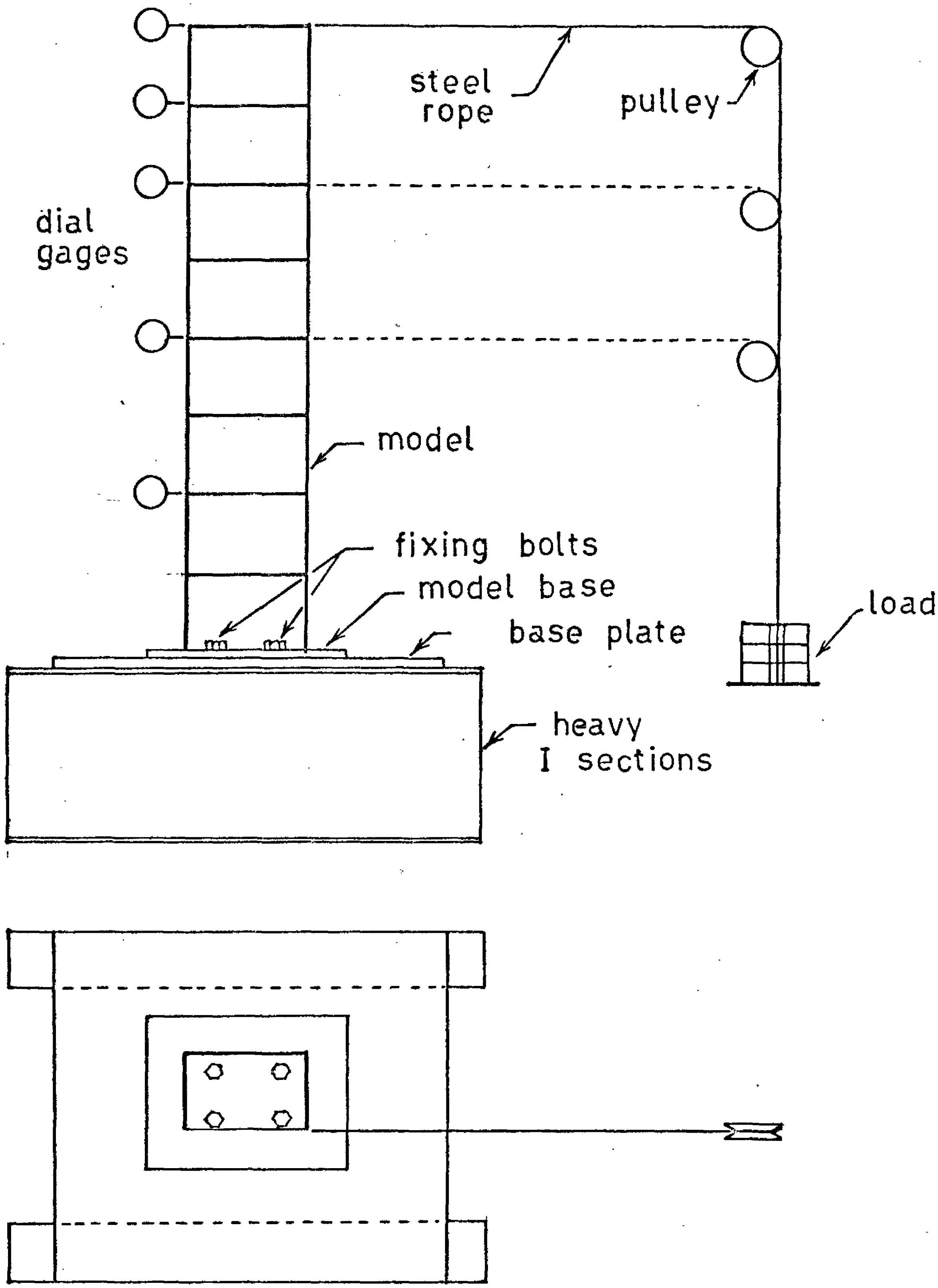

EXPERIMENTAL SET UP

FIG. 2.5.1

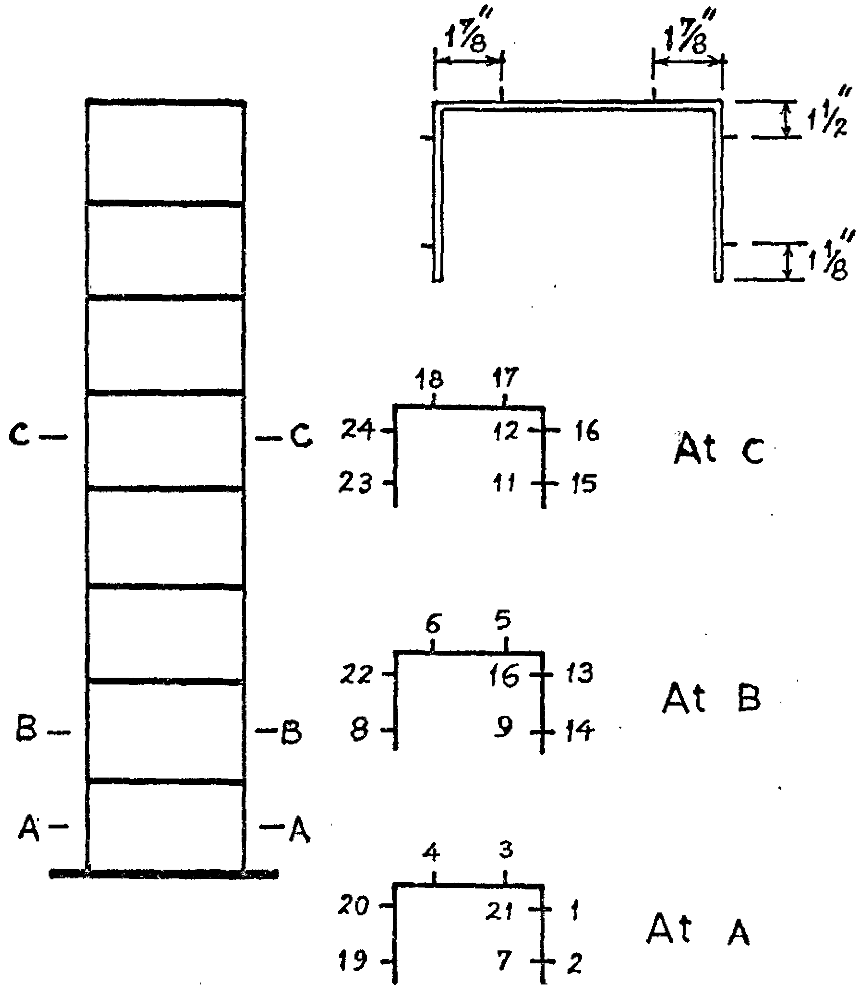

(a) Strain Gauge Positions

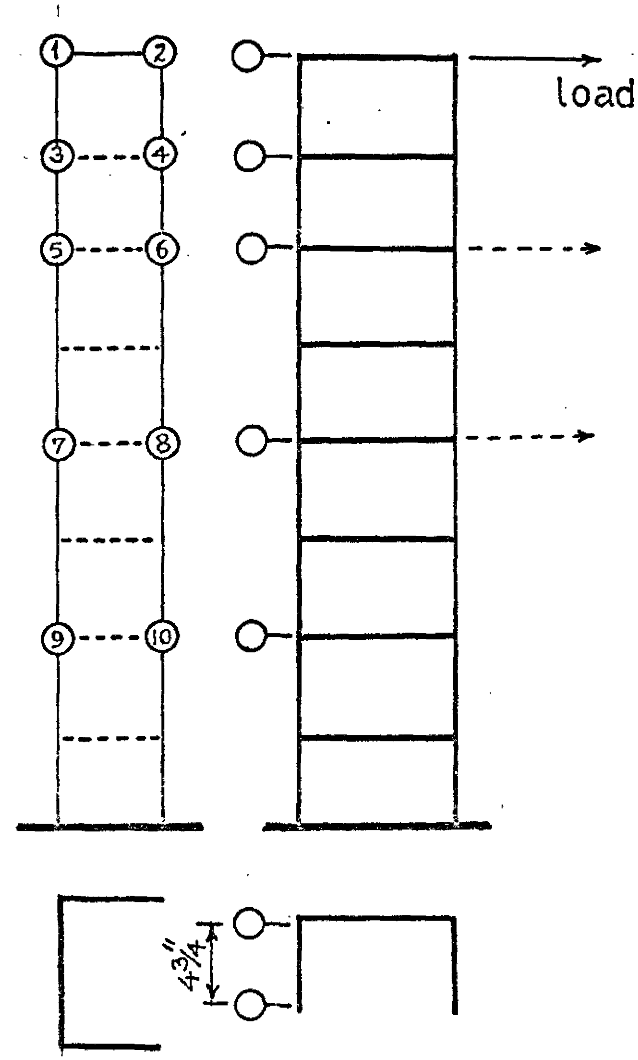

(b) Dial Gauge Positions

FIG. 2.5.2

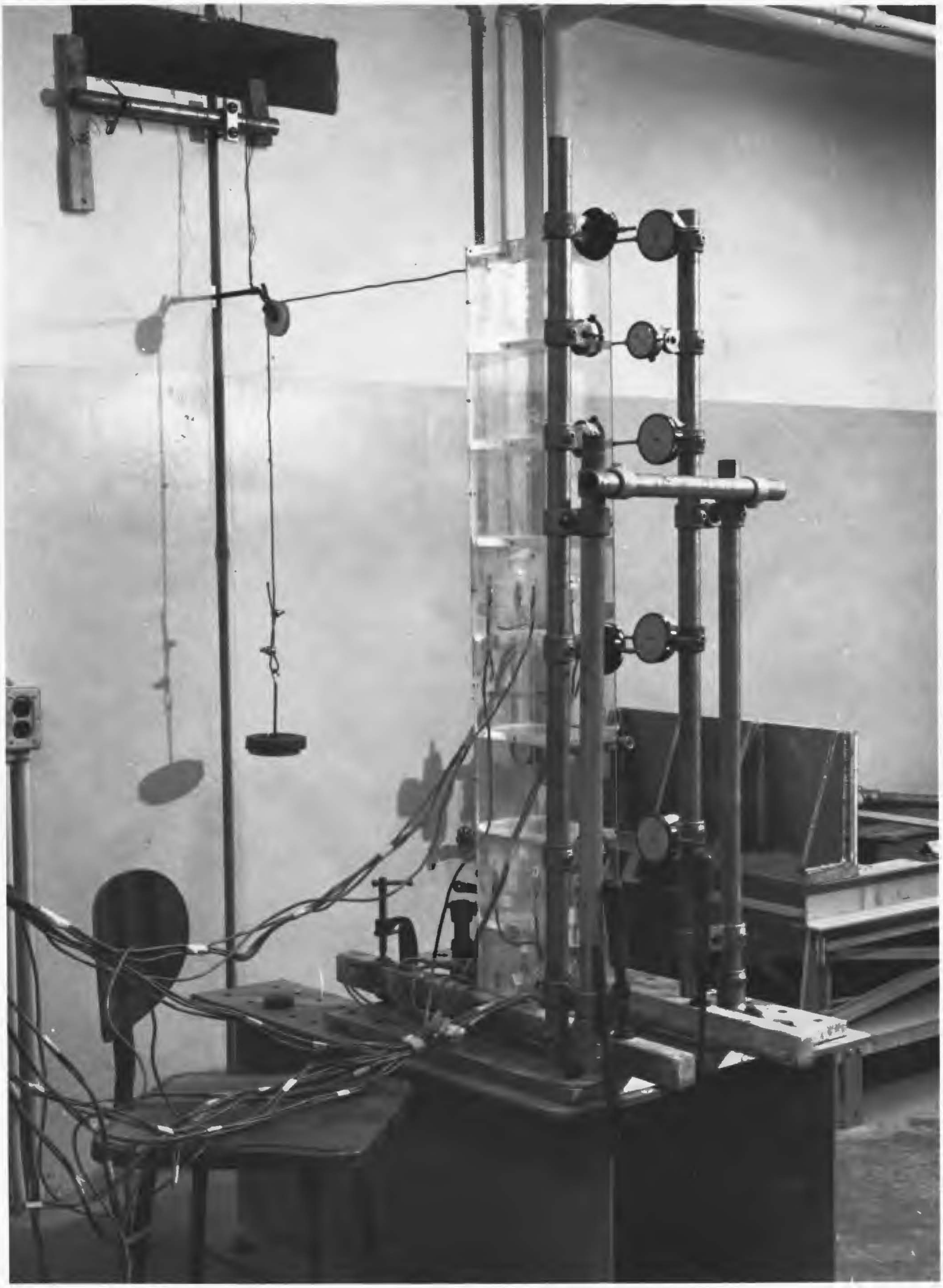

Fig. 2.5.3

EXPERIMENTAL SET UP FOR STATIC TEST

a pulley. Strain gauges were attached at the middle of 1st, 2nd and 5th storey. Leads from the strain gauges were hooked up to a strain indicator through switch boxes and strain readings at every increment of loading were taken. Deflections are measured from readings of dial gauges mounted at different points of the structure (Fig. 2.5.2). The strain gauge and dial gauge readings are tabulated in Appendix C. Fig. 2.5.3 shows the experimental set up for the case with loading at top.

The following is a list of equipment and materials used in this experimental work.

A. Model Material: Plexiglas
   Elastic properties: $E = 0.40 \times 10^6$ psi, $\nu = 0.35$

B. Electric Resistance Strain Gauges
   Make: Micro Measurement
   Type: EA-41-25086-120
   suitable for plastic
   Resistance: 120 $\Omega \pm 0.15\%$
   Gauge Factor: $2.01 \pm 0.5\%$

C. Dial Gauges:
   Make: Baty
   Reading: .001 in and .0001 in

D. Strain Indicator:
   Make: Budd Corporation
   Reading: Directly calbirated to strain in μin/in
   Range: $\pm$ 40,000 μ in/in

2.6 Results and Discussion

The linearity of the test structure is checked in fig. 2.6.18. The comparison of theoretical and experimental data as plotted in fig. 2.6.3 to 2.6.11 shows that the structure is not so stiff as predicted by considering both torsional and flexural stiffness of floor slabs. If only the torsional stiffness of floor slab is taken, the theoretical analysis gives a mathematical model which is more flexible than the actual structure. The difference between theory and experiment attributed to the local bending of the wall section at the joint of the floor slab as shown in fig. 2.6.1. As a result of this bending, the joint is not rigid which in turn reduces the shear force q at the centerline of slab (Fig. 2.3.4d). To allow for this effect, the bimoment contribution from flexure of the floor slab is modified by a factor K. The effect of the floor is then expressed as.

$$D = \left[\frac{Et^3bd}{6(1+\nu)} + K \frac{4Et^3b^3}{3d(1-\nu^2)} \right] \qquad (2.6.1)$$

An approximate method to assess the value of K is given below. Consider a one bay multistory frame as in fig. 2.6.1. Assuming points of contraflexure are at the center of storey height. Let M be the moment induced at the end of the slab strip if the joints do not rotate locally. Due to the local bending of the joints the final moment is KM where K is obtained as

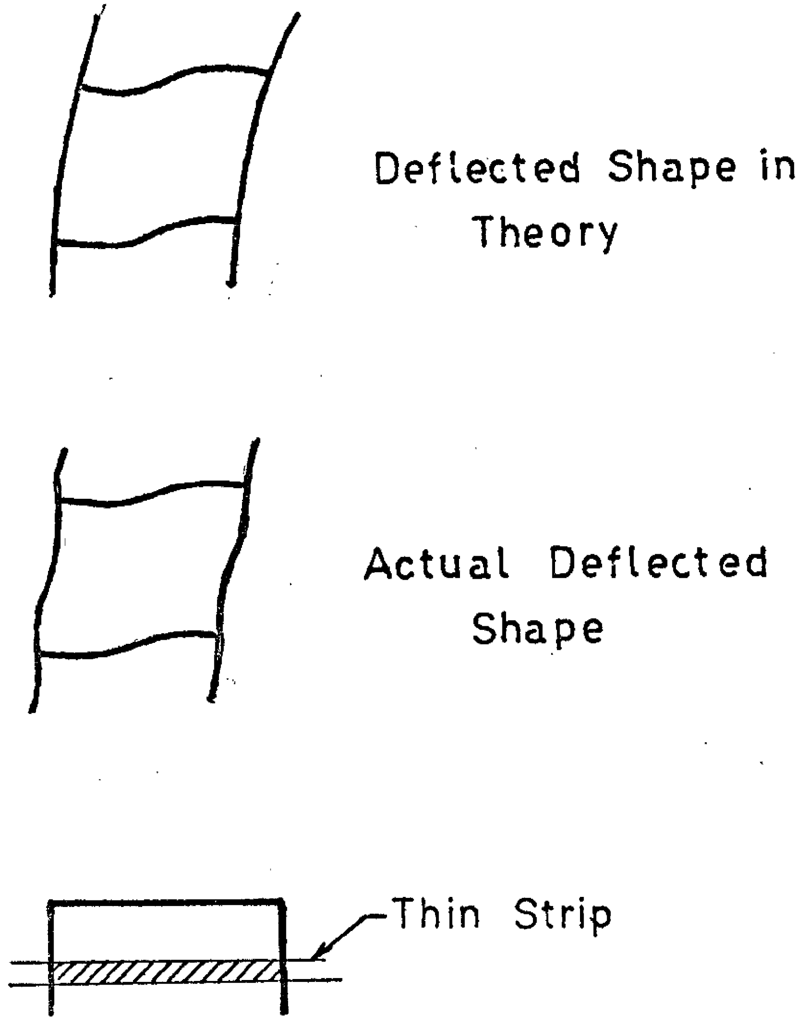

FIG. 2.6.1

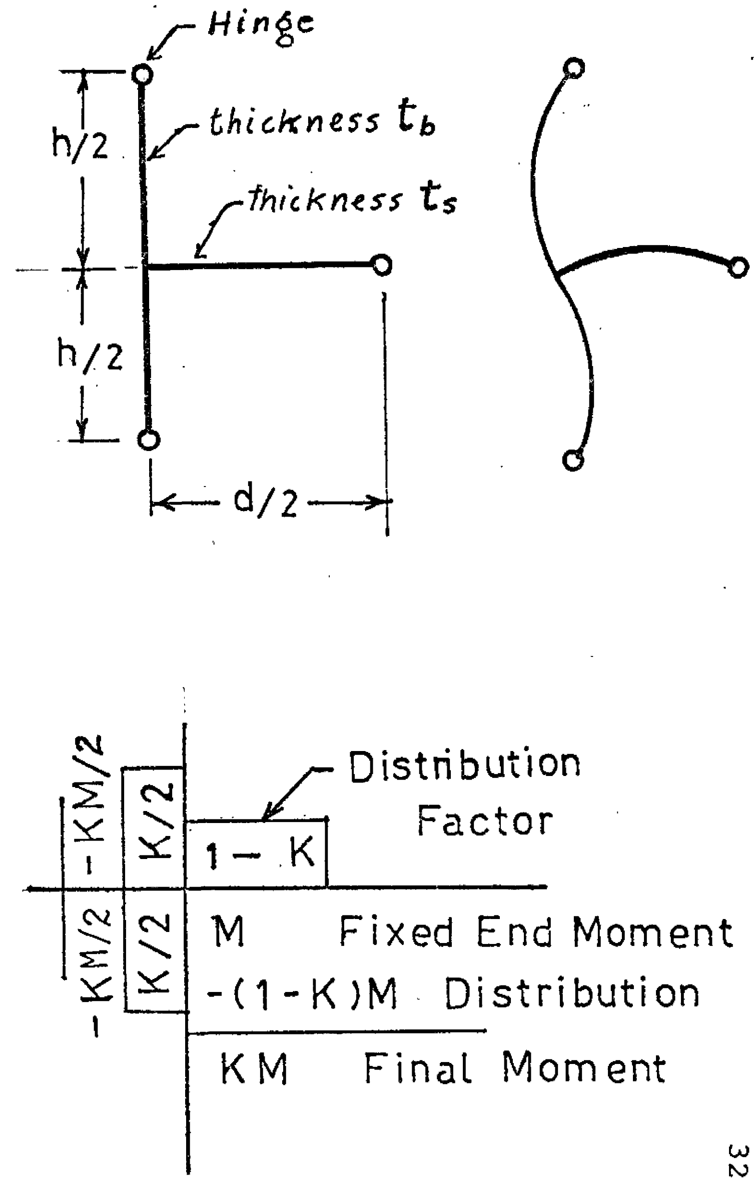

MOMENT DISTRIBUTION

FIG. 2.6.2

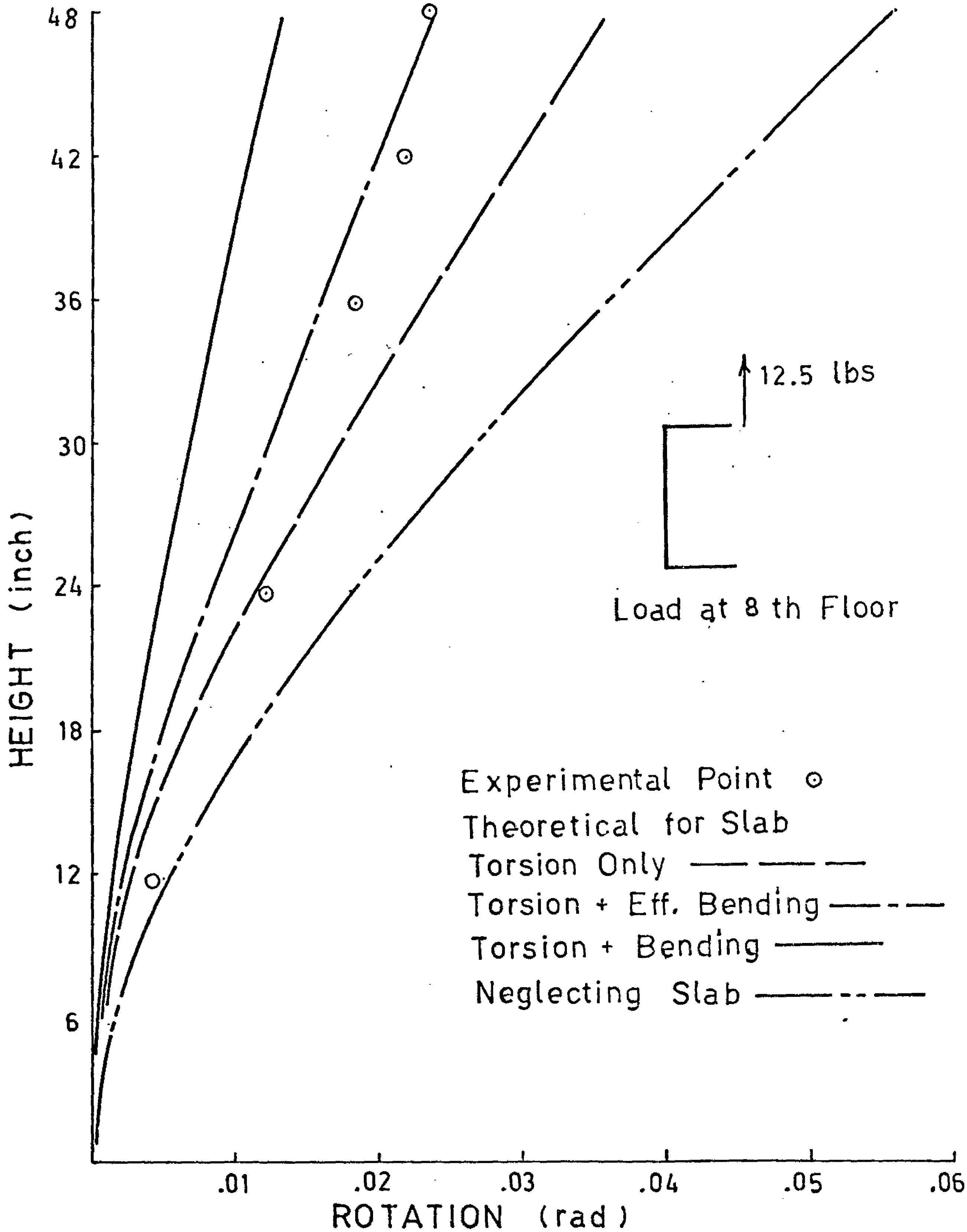

48
42
36
30
24
18
12
6
HEIGHT (inch)
.01
.02
.03
.04
.05
.06
ROTATION (rad)
12.5 lbs
Load at 8 th Floor
Experimental Point
Theoretical for Slab
Torsion Only
Torsion + Eff. Bending
Torsion + Bending
Neglecting Slab

FIG. 2.6.3

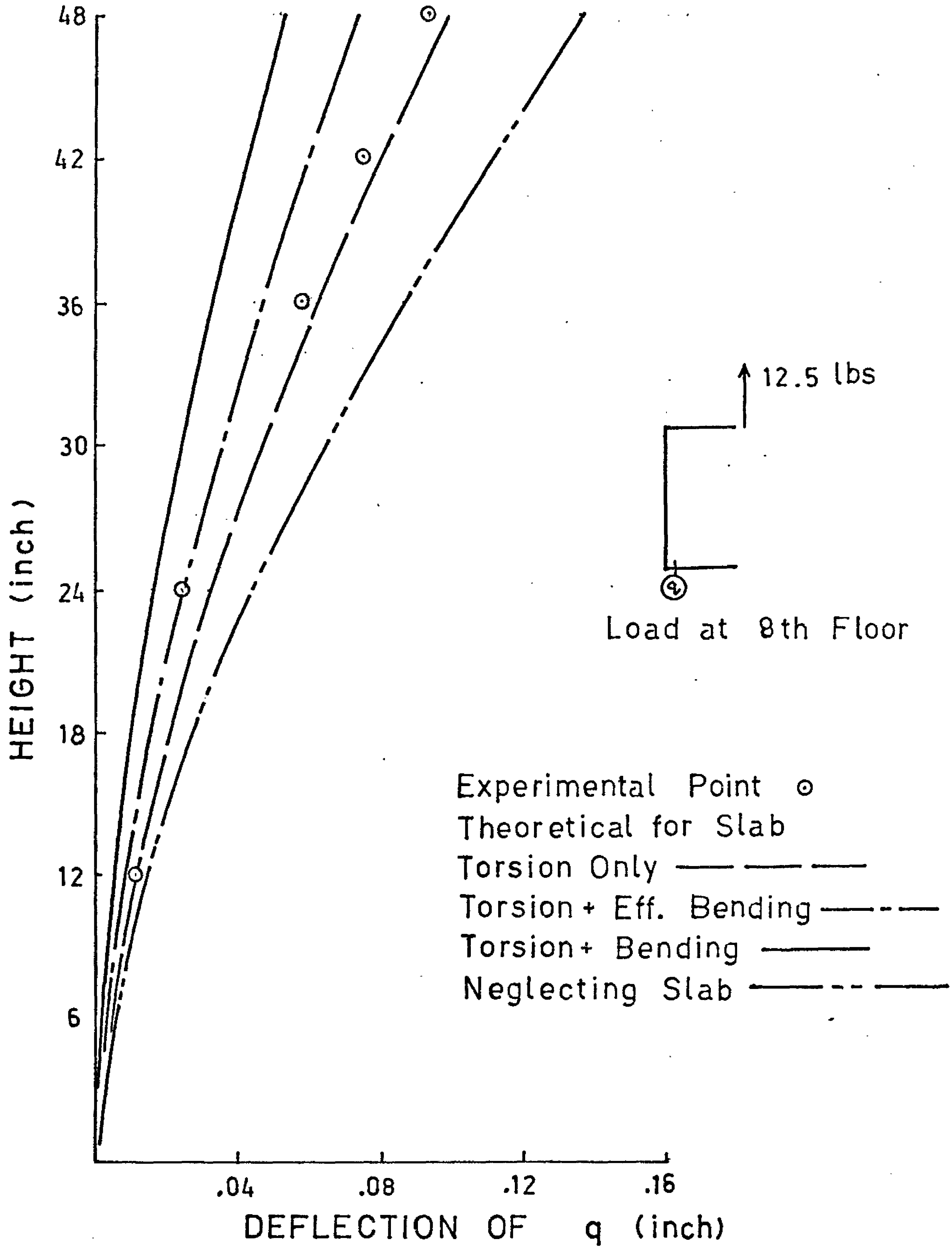
48
42
36
30
24
18
12
6
HEIGHT (inch)
12.5 lbs
q
Load at 8th Floor
Experimental Point
Theoretical for Slab
Torsion Only
Torsion + Eff. Bending
Torsion + Bending
Neglecting Slab
.04
.08
.12
.16
DEFLECTION OF q (inch)

FIG. 2.6.4

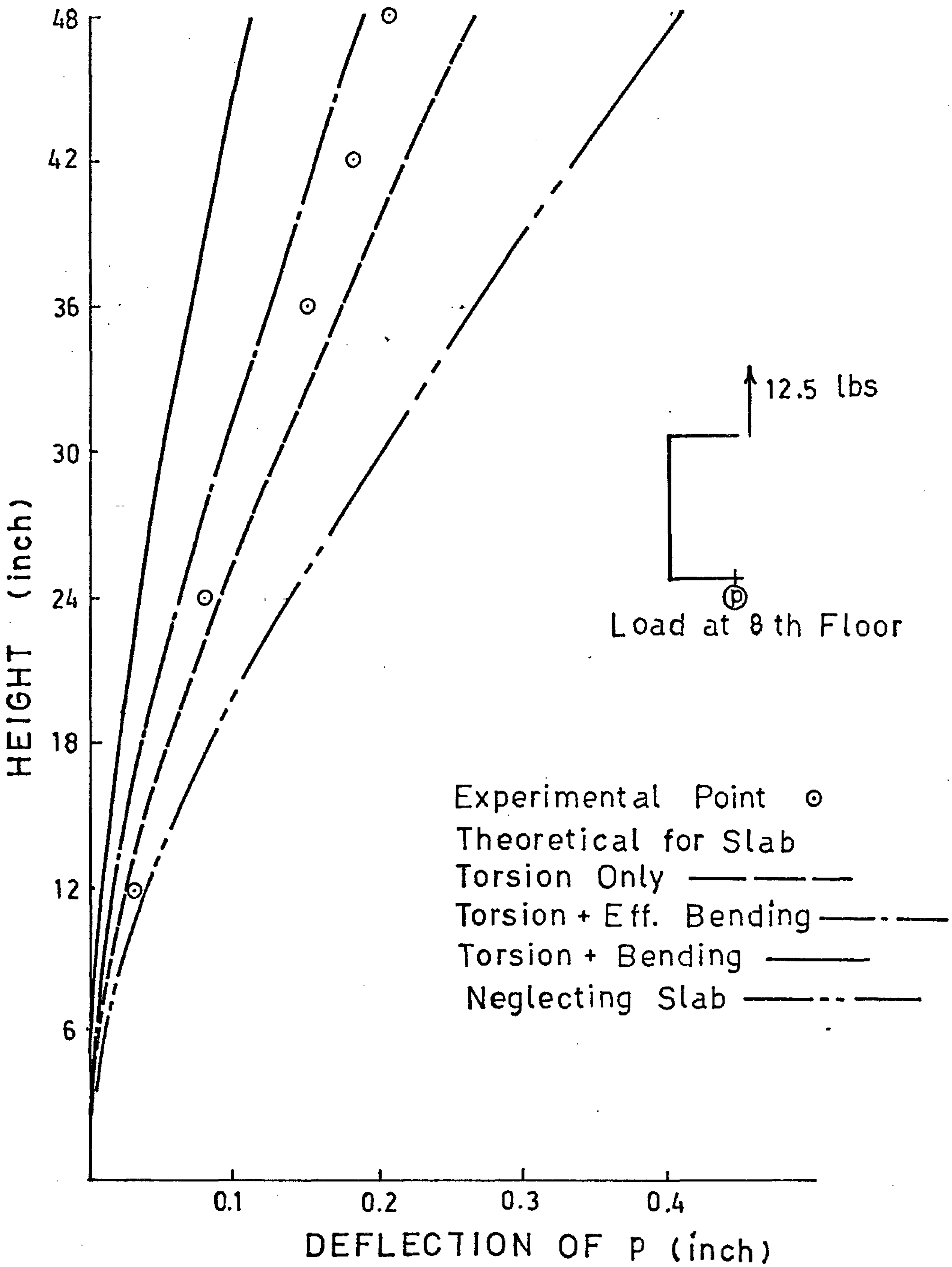
48
42
36
30
24
18
12
6
HEIGHT (inch)
0.1
0.2
0.3
0.4
DEFLECTION OF P (inch)
12.5 lbs
P
Load at 8 th Floor
Experimental Point
Theoretical for Slab
Torsion Only
Torsion + Eff. Bending
Torsion + Bending
Neglecting Slab

FIG. 2.6.5

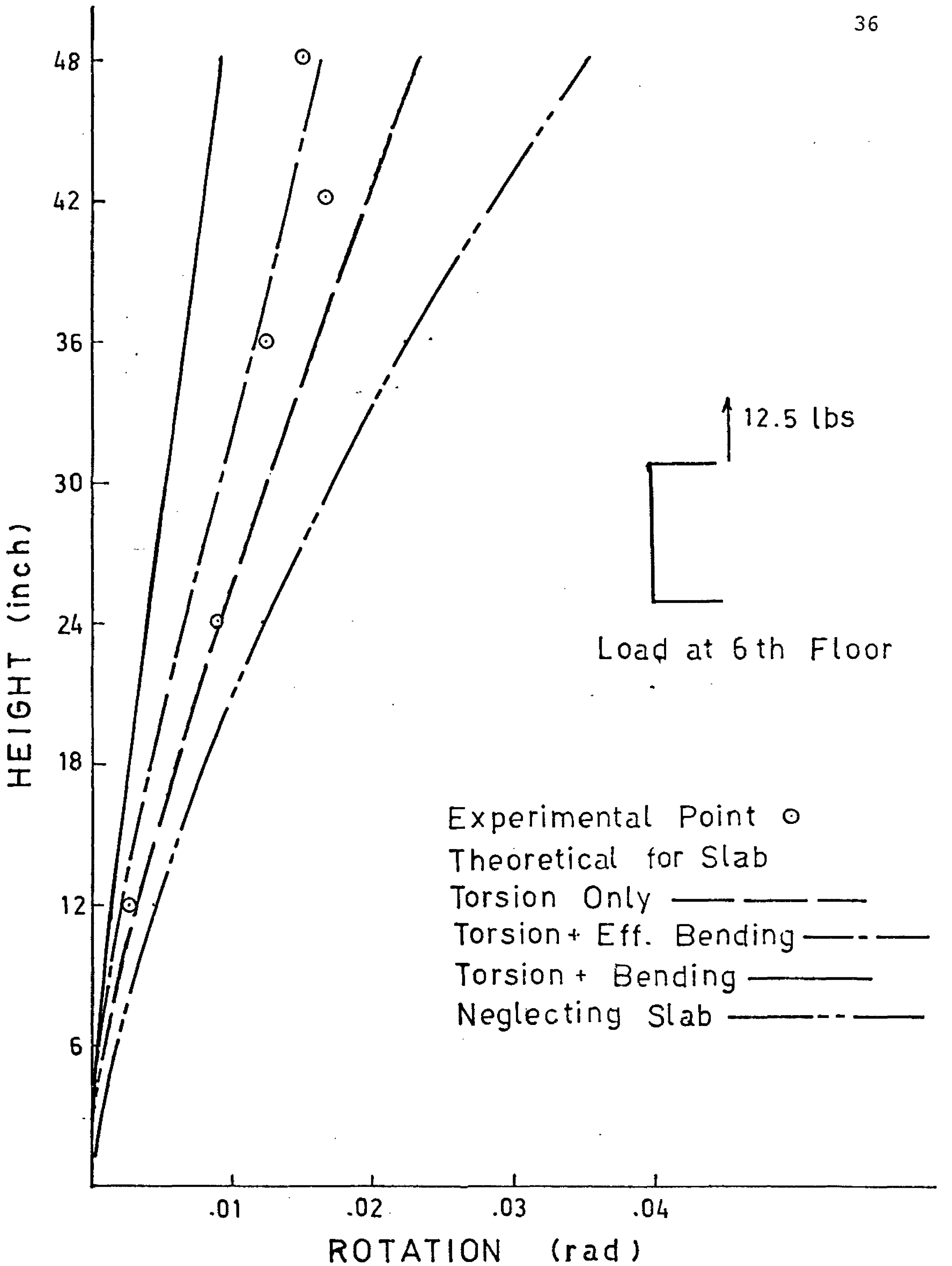
48
42
36
30
24
18
12
6
HEIGHT (inch)
.01
.02
.03
.04
ROTATION (rad)
12.5 lbs
Load at 6th Floor
Experimental Point
Theoretical for Slab
Torsion Only
Torsion + Eff. Bending
Torsion + Bending
Neglecting Slab

FIG. 2.6.6

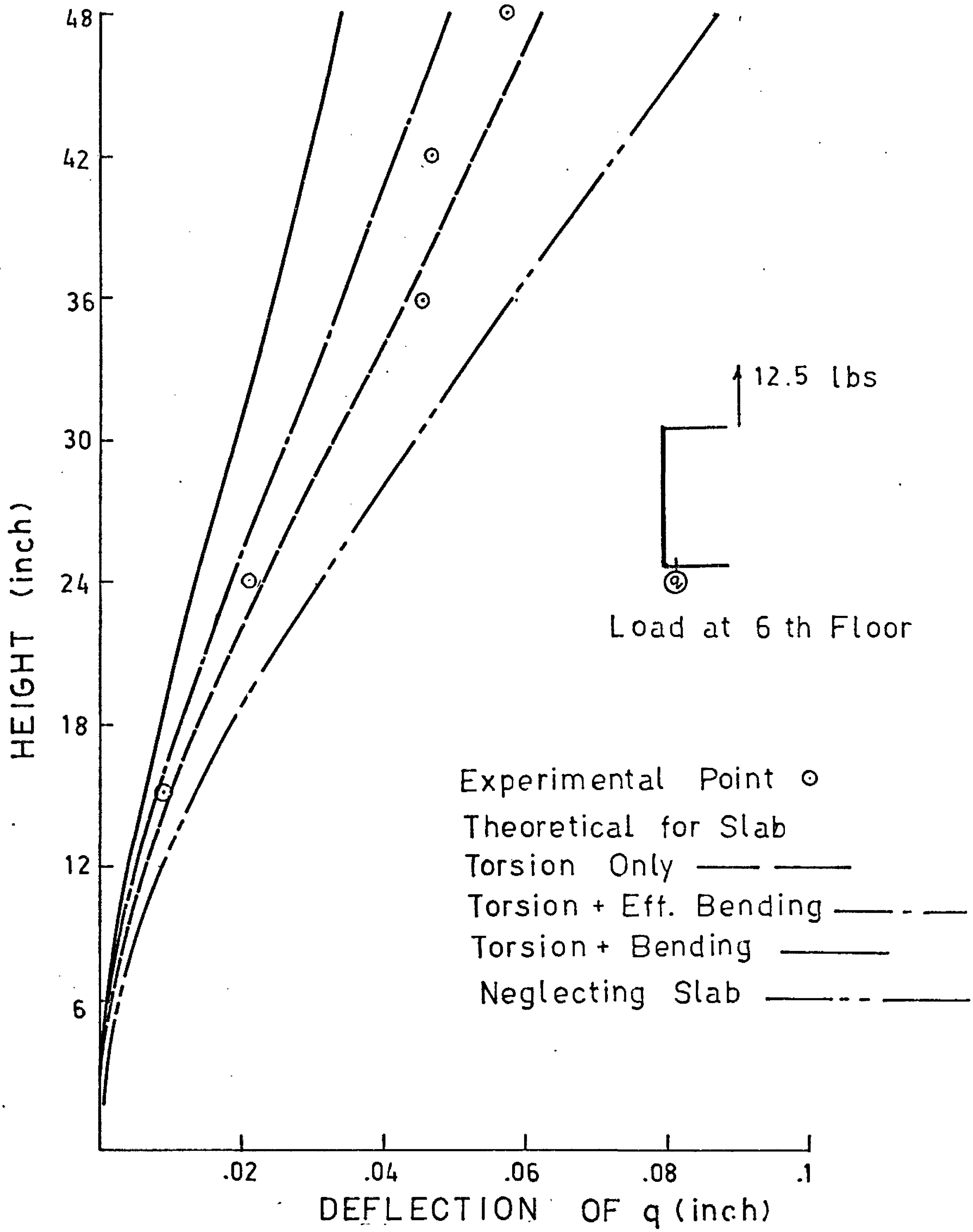
48
42
36
30
24
18
12
6
HEIGHT (inch)
.02
.04
.06
.08
.1
DEFLECTION OF q (inch)
12.5 lbs
q
Load at 6 th Floor
Experimental Point
Theoretical for Slab
Torsion Only
Torsion + Eff. Bending
Torsion + Bending
Neglecting Slab

FIG. 2.6.7

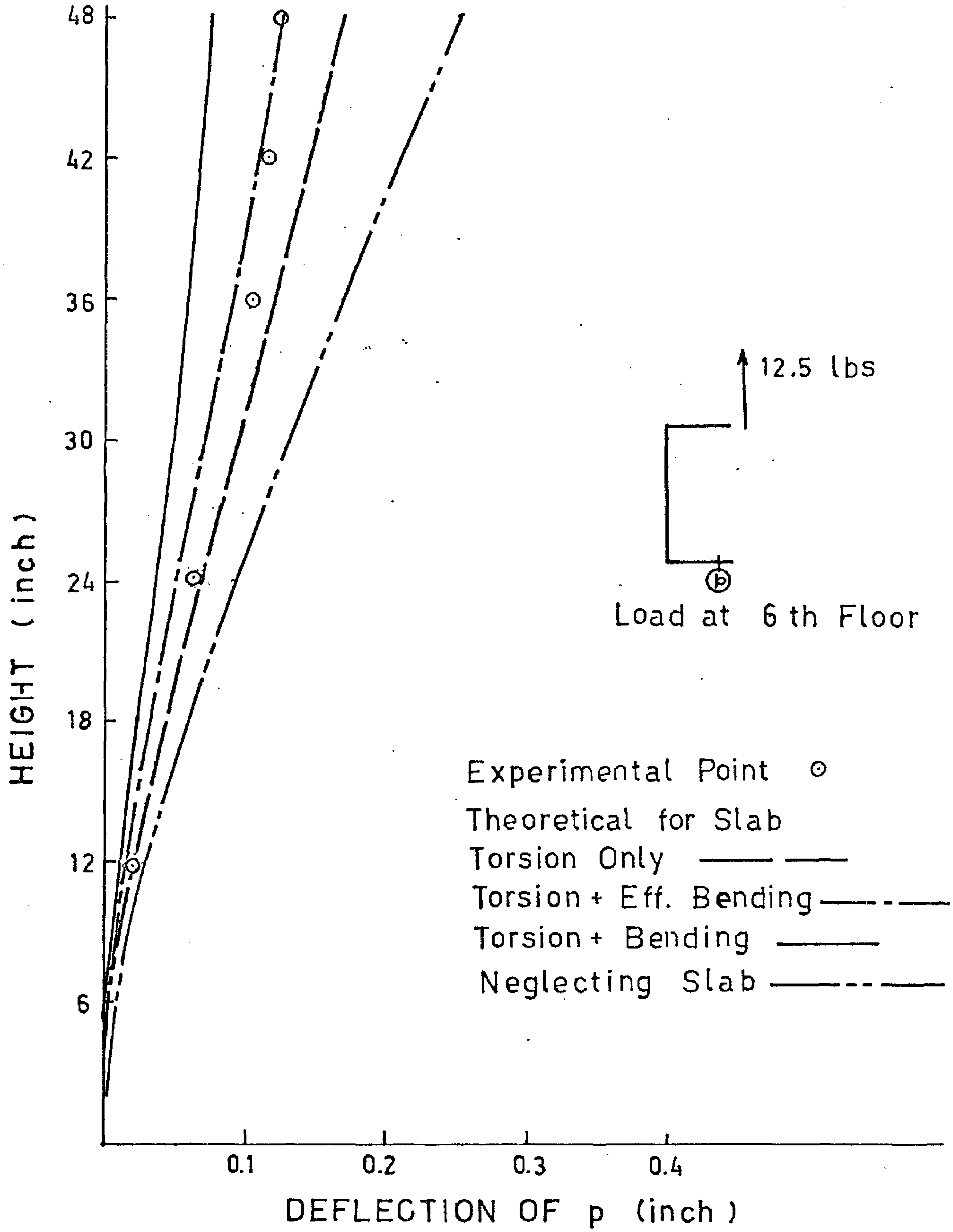

48
42
36
30
24
18
12
6
HEIGHT (inch)
0.1
0.2
0.3
0.4
DEFLECTION OF p (inch)
12.5 lbs
p
Load at 6 th Floor
Experimental Point
Theoretical for Slab
Torsion Only
Torsion + Eff. Bending
Torsion + Bending
Neglecting Slab

FIG. 2.6.8

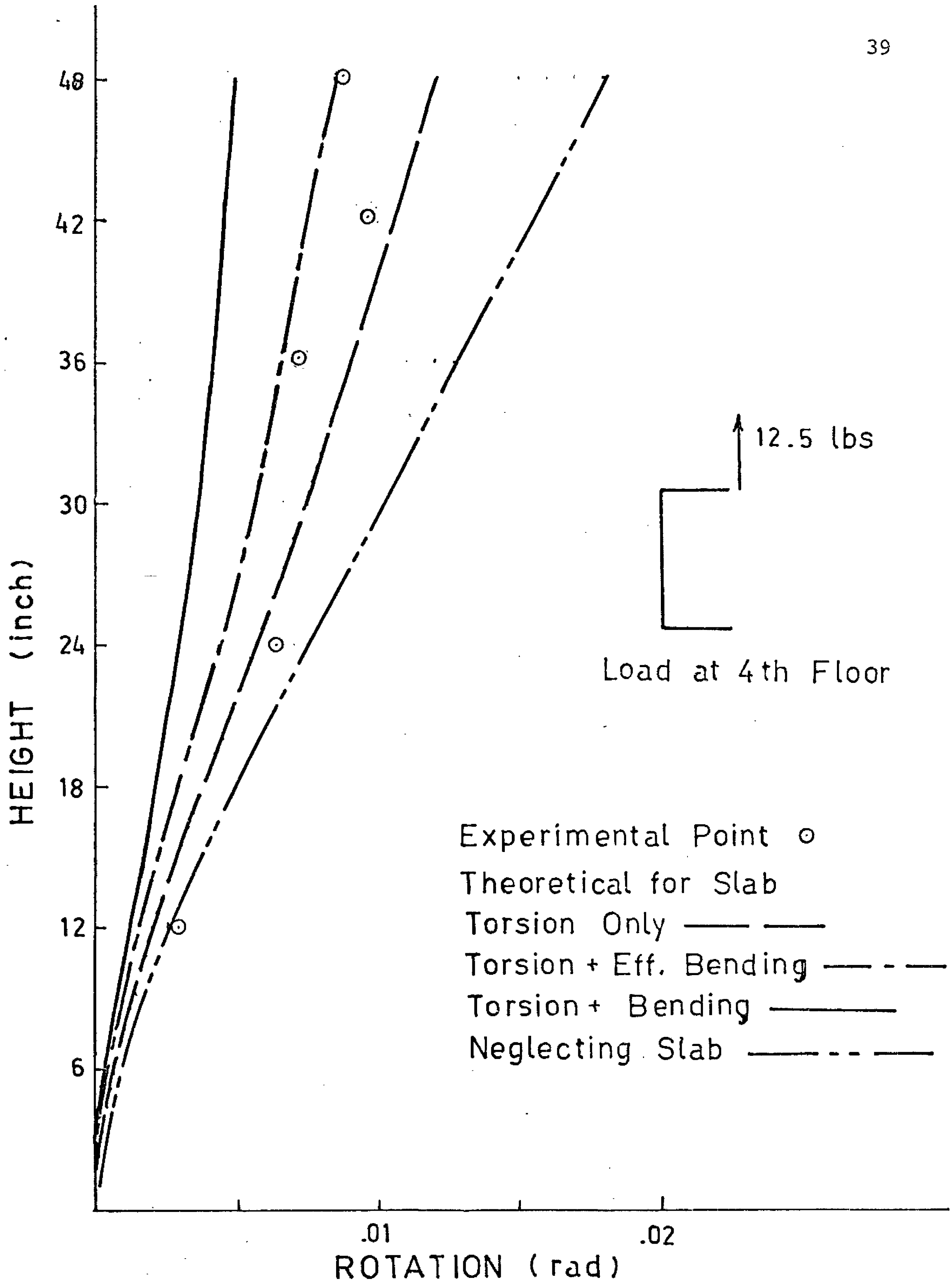
48
42
36
30
24
18
12
6
HEIGHT (inch)
.01
.02
ROTATION (rad)
12.5 lbs
Load at 4th Floor
Experimental Point
Theoretical for Slab
Torsion Only
Torsion + Eff. Bending
Torsion + Bending
Neglecting Slab

FIG. 2.6.9

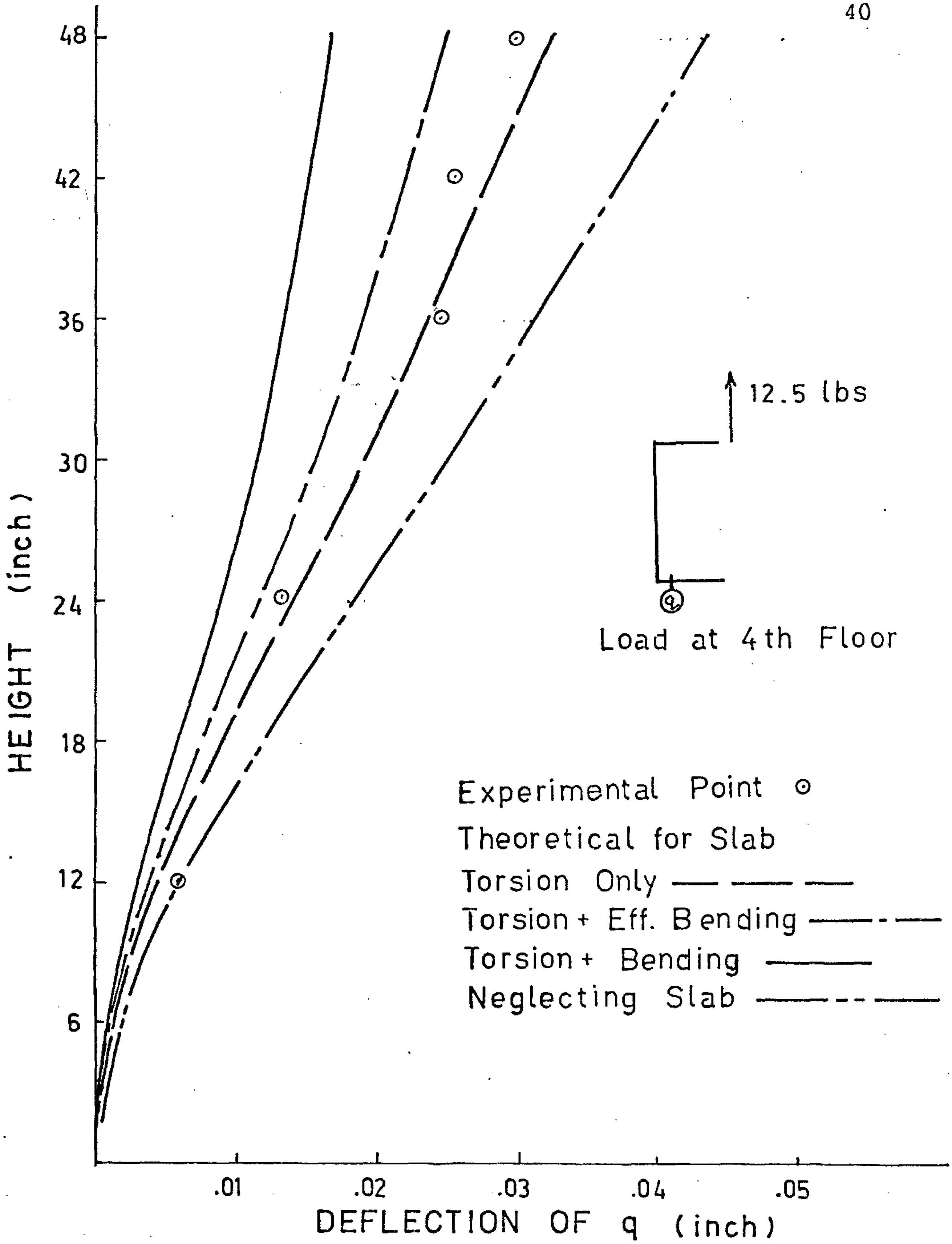

48
42
36
30
24
18
12
6
HEIGHT (inch)
.01
.02
.03
.04
.05
DEFLECTION OF q (inch)
12.5 lbs
q
Load at 4th Floor
Experimental Point
Theoretical for Slab
Torsion Only
Torsion + Eff. Bending
Torsion + Bending
Neglecting Slab

FIG. 2.6.10

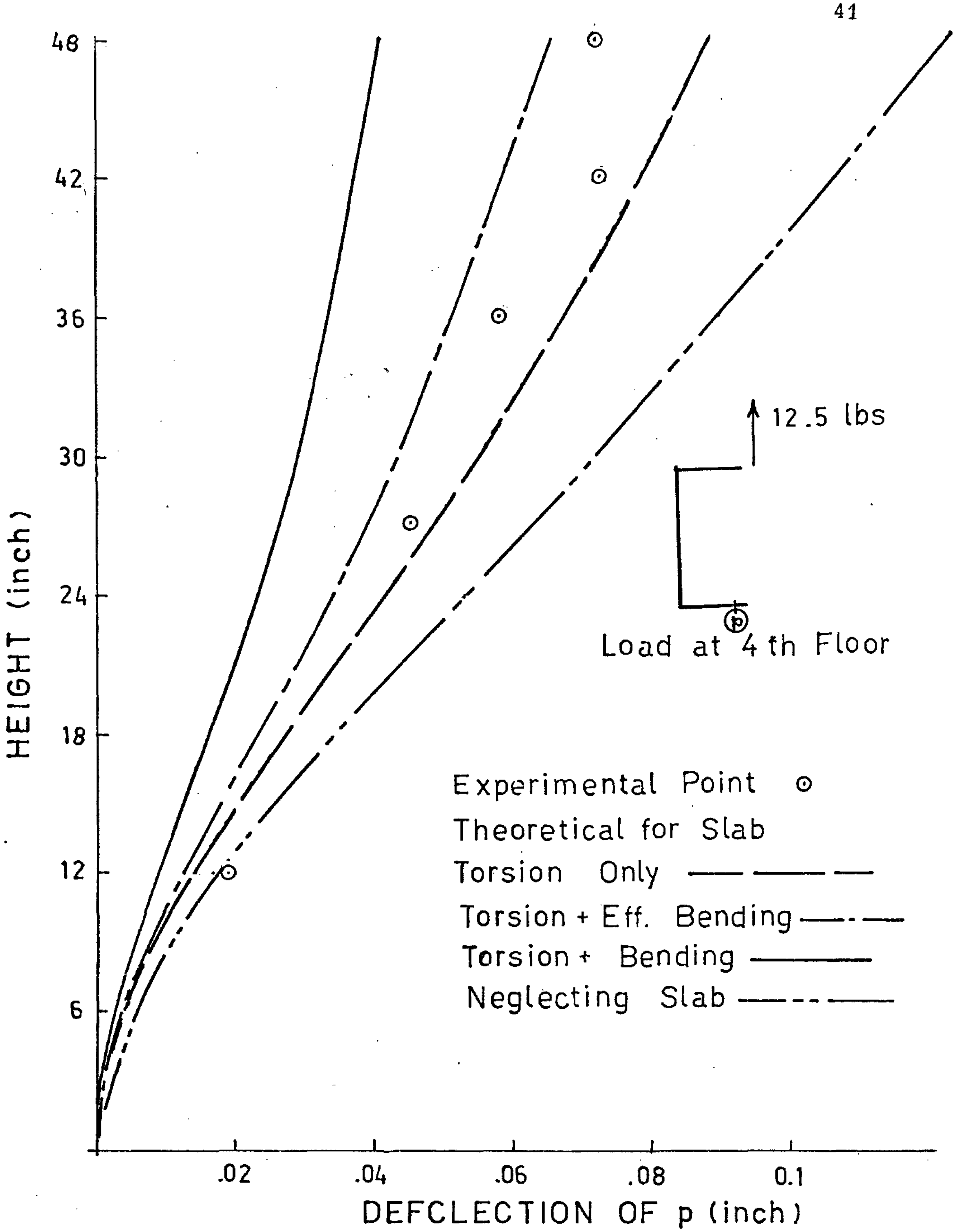
48
42
36
30
24
18
12
6
HEIGHT (inch)
.02
.04
.06
.08
0.1
DEFCLECTION OF p (inch)
12.5 lbs
p
Load at 4 th Floor
Experimental Point
Theoretical for Slab
Torsion Only
Torsion + Eff. Bending
Torsion + Bending
Neglecting Slab

FIG. 2.6.11

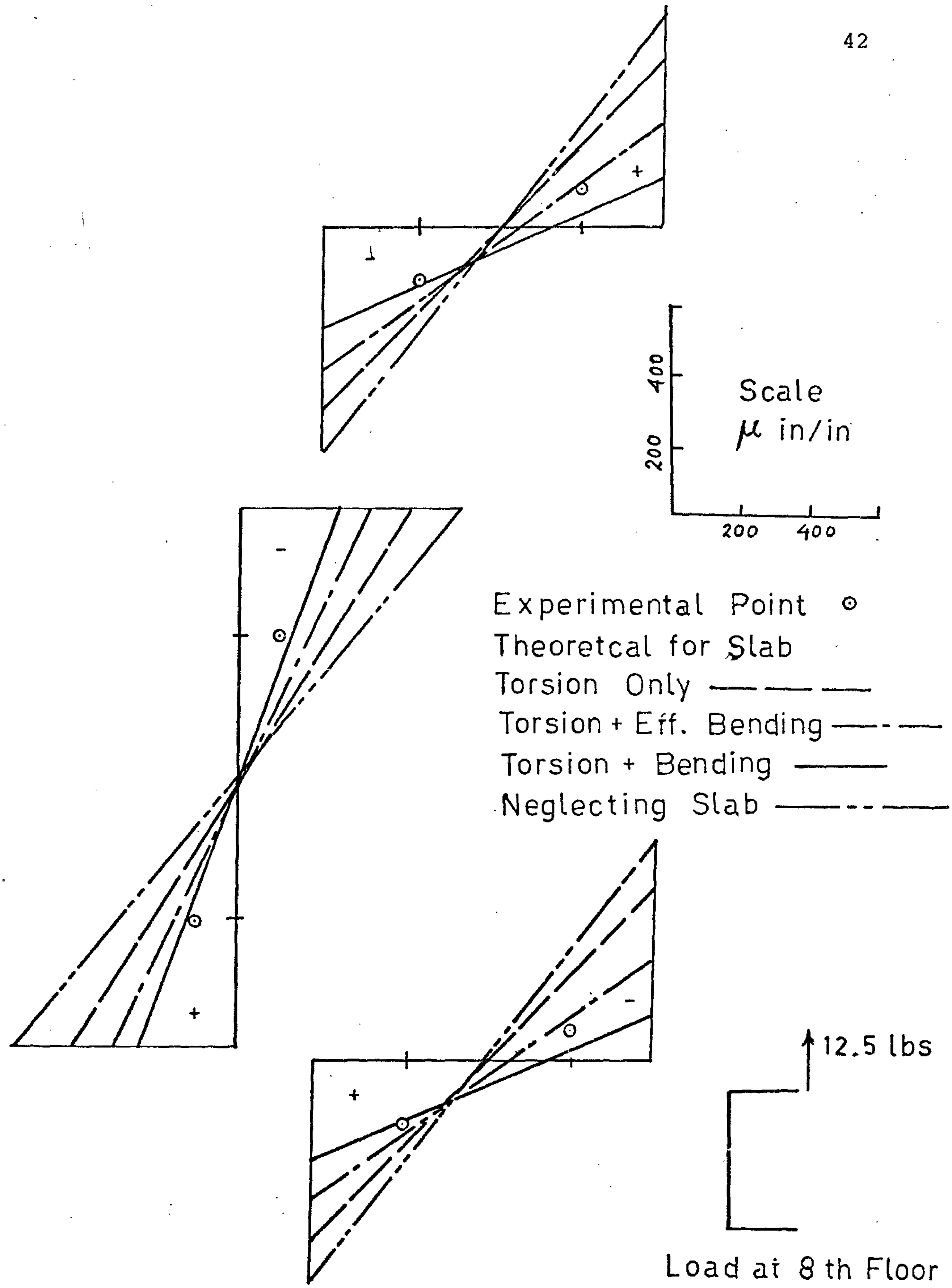

STRAIN DISTRIBUTION AT LEVEL A

FIG. 2.6.12

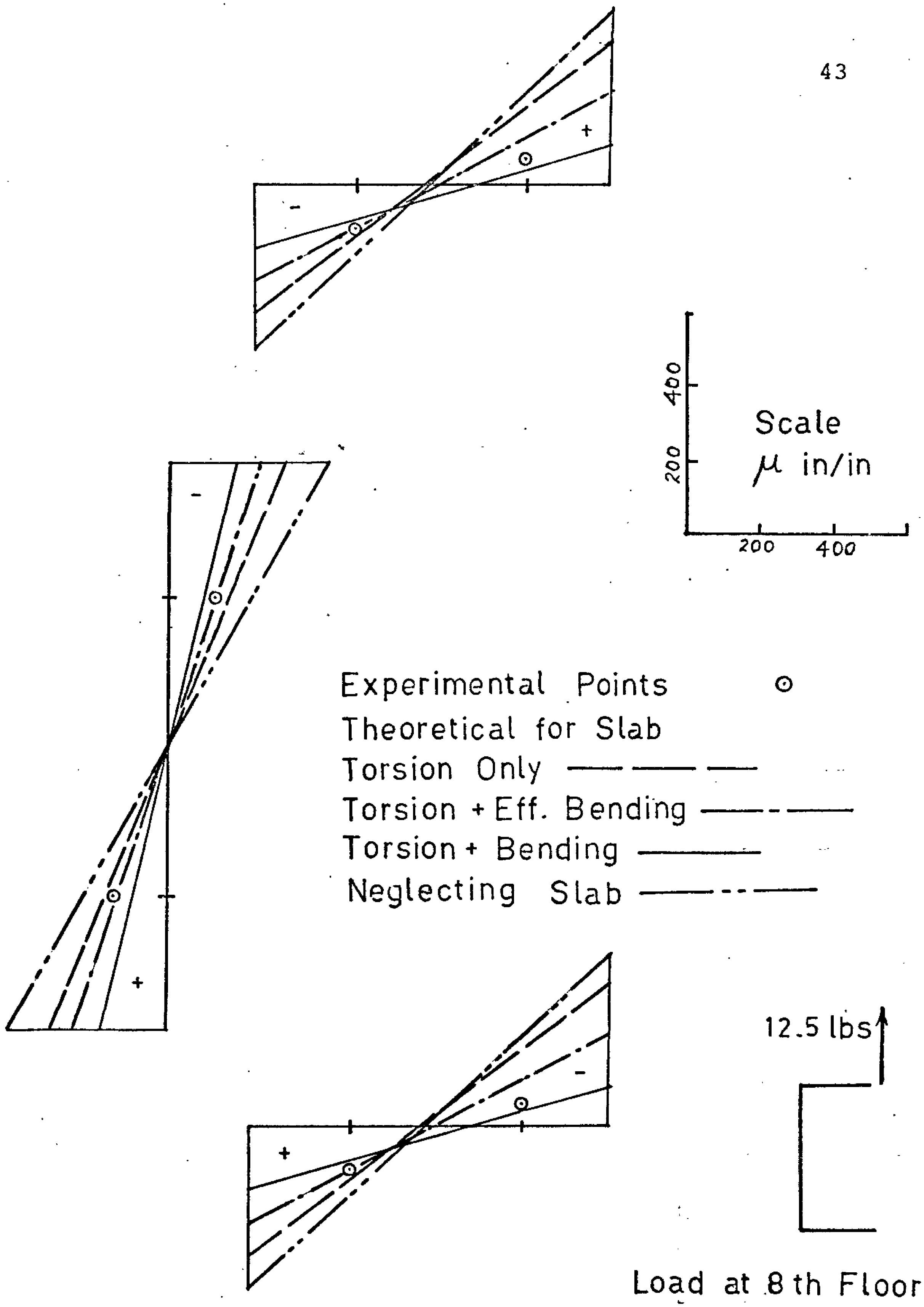

STRAIN DISTRIBUTION AT LEVEL B

FIG. 2.6.13

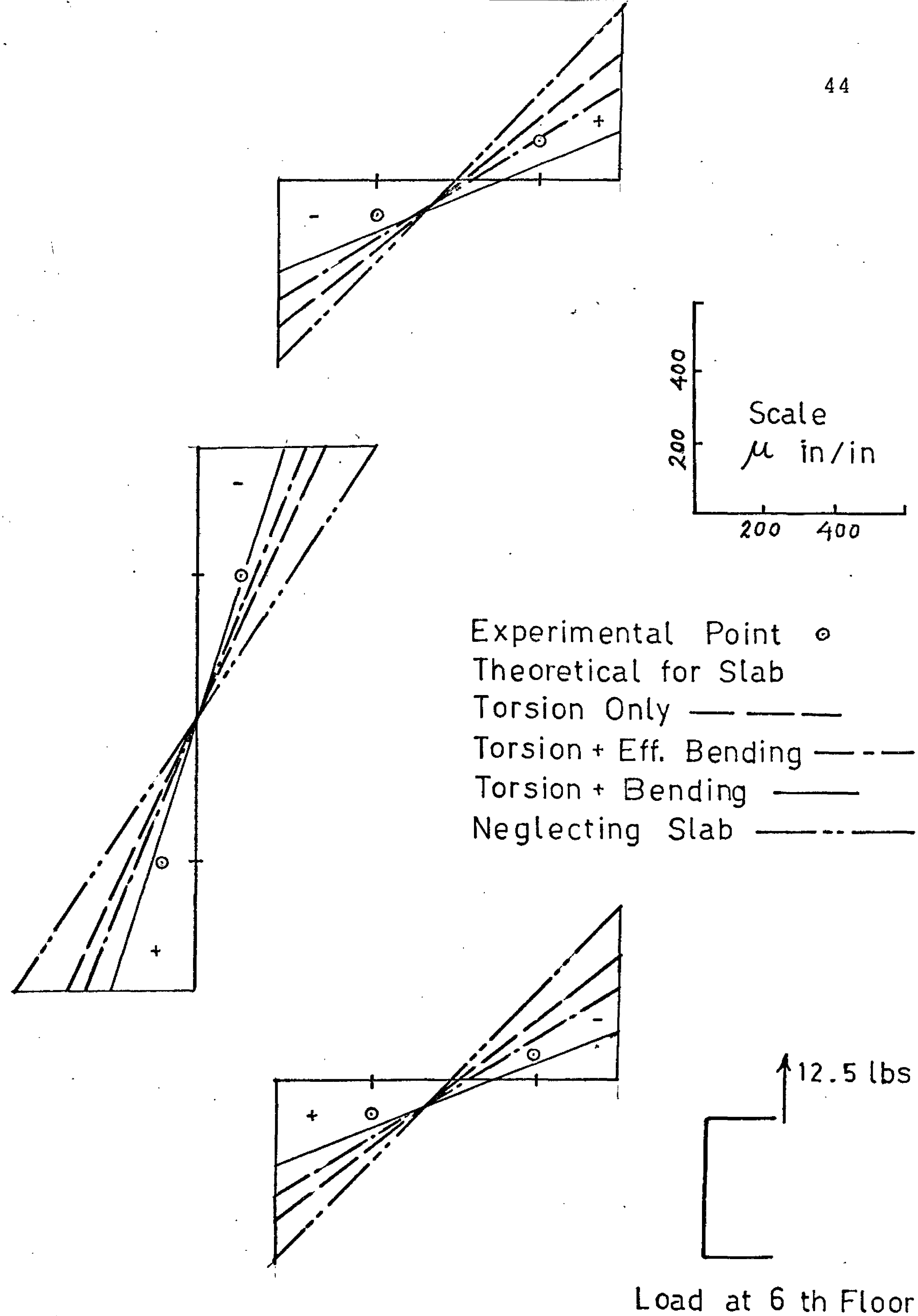

STRAIN DISTRIBUTION AT LEVEL A

FIG. 2.6.14

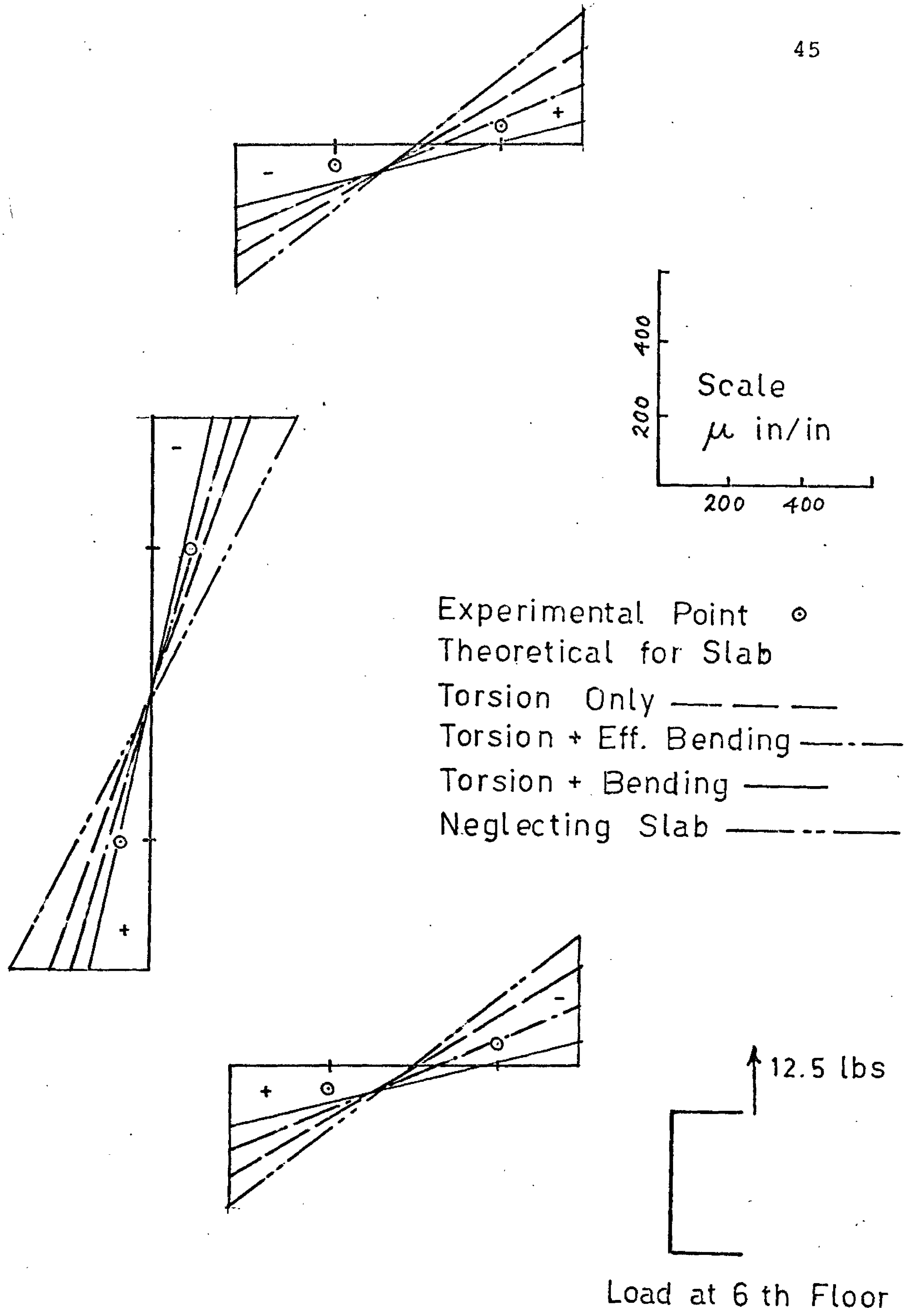

STRAIN DISTRIBUTION AT LEVEL B

FIG. 2.6.15

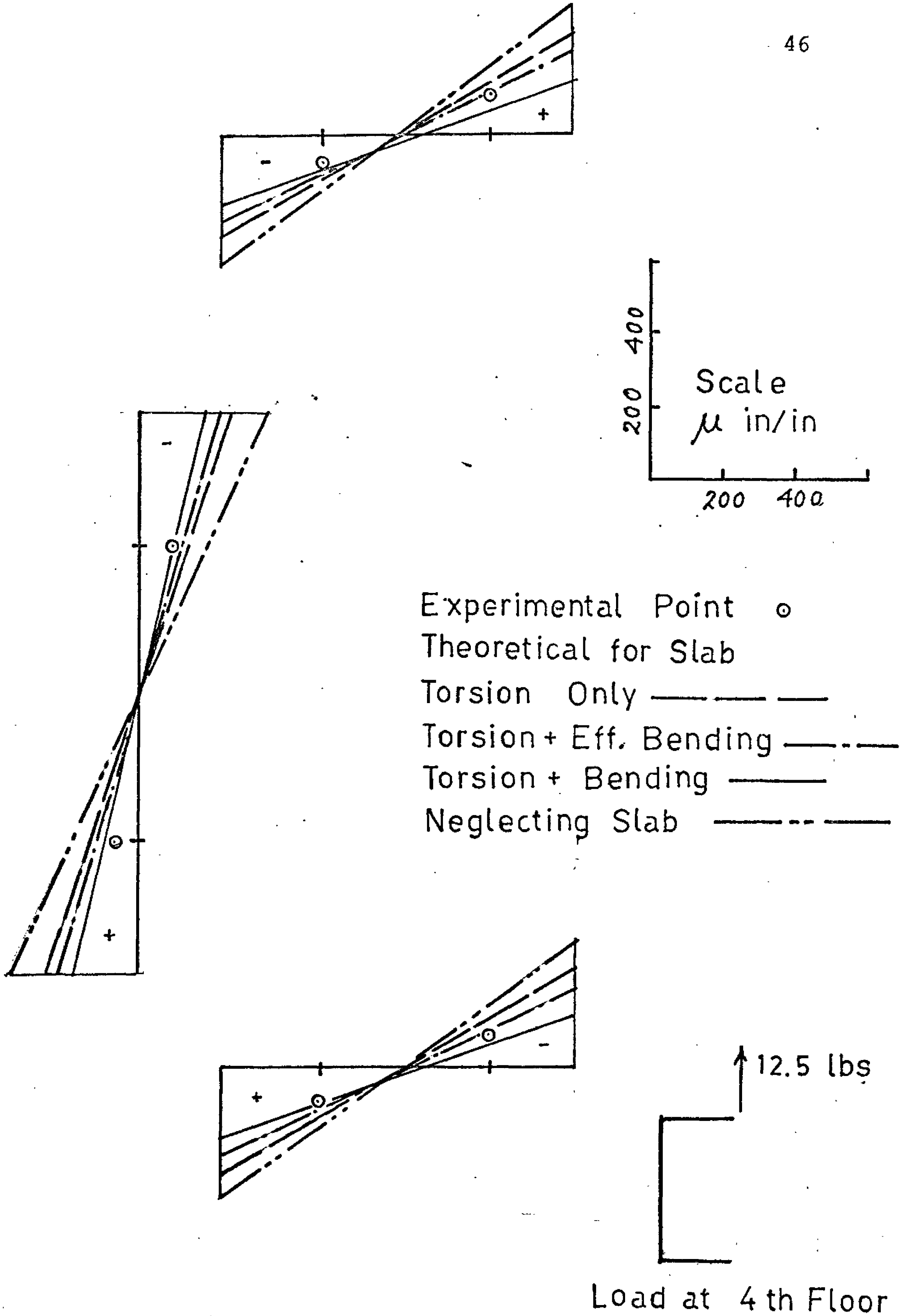

STRAIN DISTRIBUTION AT LEVEL A

FIG. 2.6.16

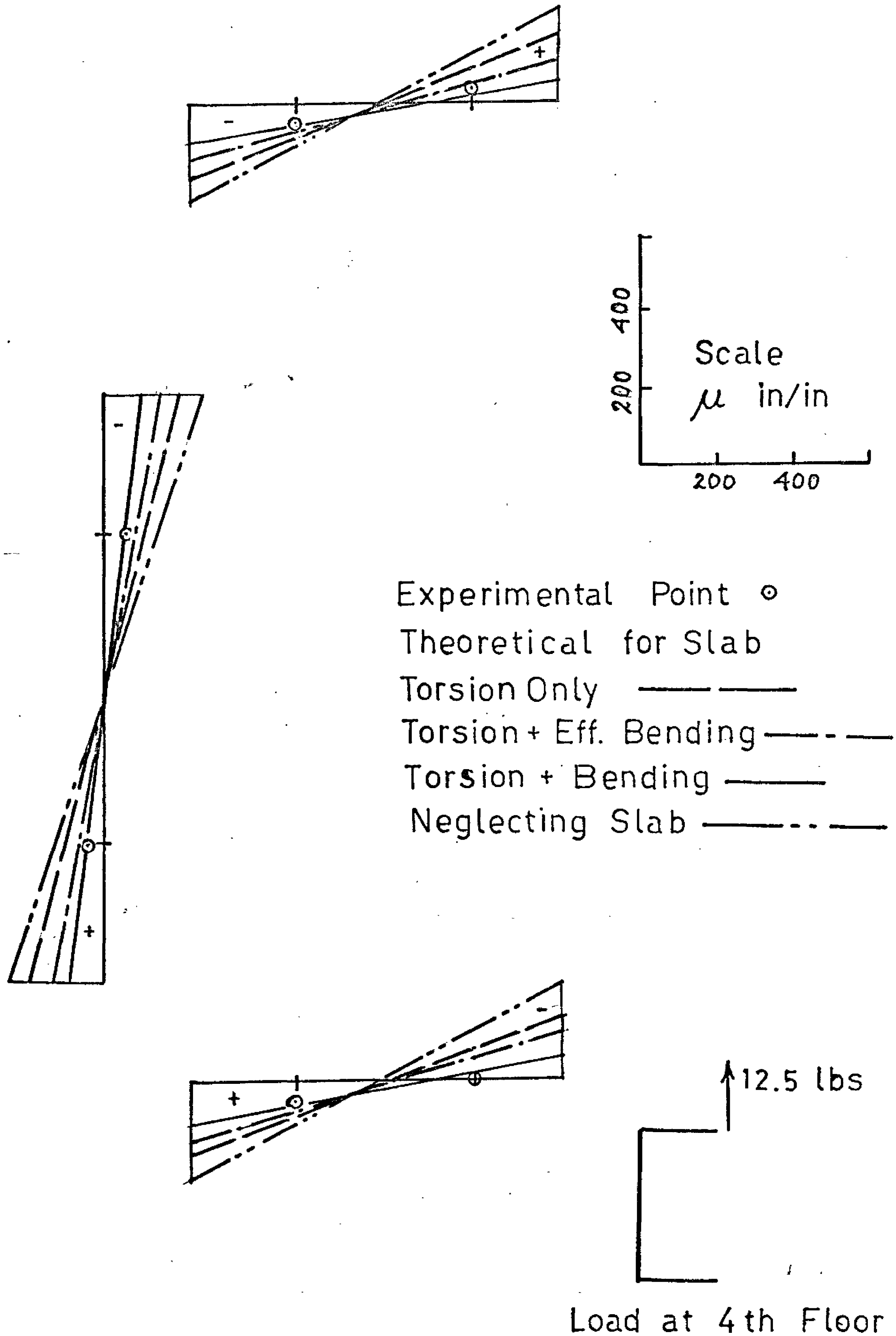

STRAIN DISTRIBUTION AT LEVEL B

FIG. 2.6.17

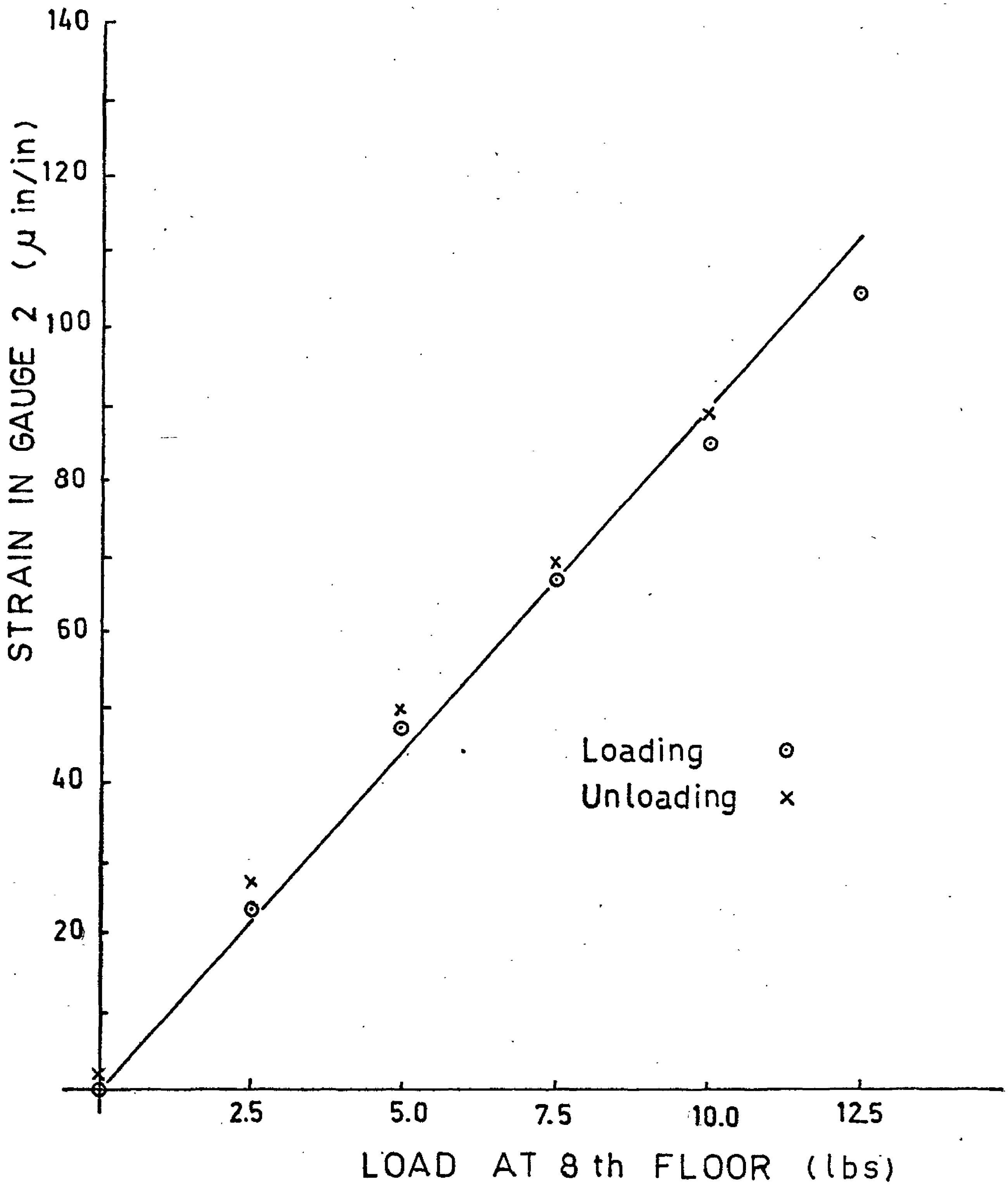

LOAD vs. STRAIN DIAGRAM FOR MODEL WITH FLOORS

FIG. 2.6.18

$$K = \frac{1}{1 + \left(\frac{t_s}{t_b}\right)^3 \frac{h}{2d}} \qquad (2.6.2)$$

Where t_s and t_b are thicknes of slab and beam flange respectively. The procedure of obtaining K is by a moment distribution scheme as shown in fig. 2.6.2.

If the ratio t_s/t_b is very small, the value of K is unity and the total flexural stiffness of the slab is effective. On the other hand if t_s/t_b is large, there will be large local bending of the flange which will violate the hypothesis of non deformable section of Vlasov. Therefore in order to use Vlasov's theory, the expression of K is valid only for $t_s/t_b < 3$.

For the model structure the value of K is 0.2545 and the displacement/rotation plots are found to have reasonable agreement with the experiment.

The strain distribution are plotted in fig. 2.6.12 to 2.6.17 and found to have reasonable agreement with the experiment.

CHAPTER III

DYNAMIC STUDY OF SHEAR WALL WITH FLOORS

3.1 Summary

In this chapter, the same shear wall structure treated in Chapter 2 is analysed, for dynamic loading. The 'Matrix Transfer' method is used in the analysis. A dynamic test was carried out to determine natural frequencies. The strain distribution at resonance was also determined. The experimental values are compared with the theoretical predictions.

3.2 Matrix Transfer Method

As in static case, field transfer matrix $[F_i]$ relates the state vector $\{z\}$ of two subpoints in ith field. The point transfer matrix $[P_i]$ relates the state vector $\{z\}$ of two subpoints in ith point. The application of the method is the same in the dynamic case except the external loading is replaced by inertial forces which appear in the point transfer matrix $[P_i]$. Consideration of equation for vibration is necessary for obtaining field transfer matrix $[F_i]$. The relation between state vectors can be expressed as

$$\{z_i^-\} = [F_i]\{z_{i-1}^+\} \tag{3.2.1}$$

$$\{z_i^+\} = [P_i]\{z_i^-\} \tag{3.2.2}$$

Where $i = 1,2,\ldots n$

From these relations, the state vectors at inner points can be eliminated and the relation between state vectors of extreme points $(0)_+$ and $(n)_+$ can be expressed as:

$$\{z_n^+\} = [A]\{z_o^+\} \qquad (3.2.3)$$

Where [A] is the combined transfer matrix and is defined as

$$[A] = [P_n][F_n]\ldots[P_2][F_2][P_1][F_1] \qquad (3.2.3a)$$

Substituting boundary conditions in the boundary state vectors namely $\{z_n^+\}$ and $\{z_o^+\}$ in eq. 3.2.3, a set of homogeneous linear simultaneous equations are obtained. They can be expressed in matrix form as

$$[R]\{X\} = 0 \qquad (3.2.4)$$

Where {X} is a vector formed by collecting non zero terms of state vector $\{z_o^+\}$. The matrix [R] is obtained from matrix [A] depending on boundary condition.

For non trivial solution, the determinant of R must vanish. Thus

$$|R| = 0 \qquad (3.2.5)$$

The eq. 3.2.5 is the condition to determine natural frequency of vibration of the structure.

3.3 Theoretical Analysis

The state vector is the same as used in Chapter 2. Fig. 2.3.1 and Fig. 2.3.2 are refered to for the simplified model and the illustration of notations.

3.3.1 Field Transfer Matrix

The field transfer matrix for a thin walled beam of length ℓ is determined from the solution of differential equation of free vibation. For mono-symmetric section, the equations are obtained by substituting $a_y = 0$ in the eq. A.5 (Appendix A). The first and the third equations are uncoupled and represent independent extensional vibration and flexural vibration in x-direction. The remaining equations representing coupled torsional and flexural vibration in y-direction are:

$$E\, I_x\, v^{IV} + \rho\, A\, \ddot{v} - \rho\, I_x\, \ddot{v}'' - \rho\, A\, a_x\, \ddot{\theta} = 0 \tag{3.3.1a}$$

$$E\, I_\omega\, \theta^{IV} - GJ\theta'' + \rho\, I_p \ddot{\theta} - \rho\, I_\omega\, \ddot{\theta}'' - \rho\, A\, a_x\, \ddot{v} = 0 \tag{3.3.1b}$$

Assuming periodic solution of the form

$$\begin{Bmatrix} v \\ \theta \end{Bmatrix} = \begin{Bmatrix} y \\ \phi \end{Bmatrix} e^{iwt} \tag{3.3.2a}$$

and substituting eq. 3.3.2 in eq. 3.3.1, there is obtained

$$E\, I_x\, y^{IV} - w^2\, \rho\, A\, y + w^2\, \rho\, I_x\, y'' + w^2\, \rho\, A\, a_x\, \phi = 0 \tag{3.3.3a}$$

$$E\, I_\omega\, \phi^{IV} - GJ\phi'' - w^2\, \rho\, I_p\, \phi + w^2\, \rho\, I_\omega\, \phi'' + w^2\, \rho\, A\, a_x\, y = 0 \tag{3.3.3b}$$

Expressing in terms of y from eq. 3.3.3a there is obtained

$$\phi = B_1\, y^{IV} + B_2\, y'' + B_3\, y \tag{3.3.4}$$

Where

$$B_1 = -E\, I_x/(w^2\, \rho\, A\, a_x);$$

$$B_2 = -I_x/(A\, a_x)\, ; \quad B_3 = 1/a_x$$

Eliminating ϕ from eq. 3.3.3b using eq. 3.3.4, there is obtained

$$B_4\, y^{VIII} + B_5\, y^{VI} + B_6\, y^{IV} + B_7\, y'' + B_8\, y = 0 \tag{3.3.5}$$

Where

$$\left.\begin{aligned}
B_4 &= - E^2\ I_\omega\ I_x \\
B_5 &= E\ GJ\ I_x - 2w^2\ \rho\ E\ I_\omega\ I_x \\
B_6 &= w^2\ \rho\ (E\ I_\omega\ A + E\ I_p\ I_x + GJ\ I_x) - w^4 \rho^2\ I_\omega\ I_x \\
B_7 &= - w^2\ \rho\ GJA + w^4 \rho^2 (I_p\ I_x + I_\omega\ A) \\
B_8 &= w^4 \rho^2\ (-I_p\ A + A^2\ a_x^2)
\end{aligned}\right\} \quad (3.3.5a$$

Assuming solution of the form

$$y = c\ e^{mZ}$$

The characteristic equation is

$$B_4 m^8 + B_5 m^6 + B_6 m^4 + B_7 m^2 + B_8 = 0 \qquad (3.3.6)$$

Let the eight roots of this polynomial are

$$m_1,\ m_2,\ m_3,\ \ldots\ldots\ m_8.$$

The solution can then be expressed as

$$v(z) = e^{iwt} \sum_{i=1}^{8} K_i\ e^{m_i z}$$

$$v'(z) = e^{iwt} \sum_{i=1}^{8} K_i\ m_i\ e^{m_i z}$$

$$M(z) = E\ I_x\ v'' = e^{iwt} \left(\sum_{i=1}^{8} K_i\ m_i^2\ e^{m_i z} \right) E I_x$$

$$V(z) = - E\ I_x\ v''' = - e^{iwt}\ E\ I_x \sum_{i=1}^{8} K_i\ m_i^3\ e^{m_i z}$$

$$\theta(z) = e^{iwt} \sum_{i=1}^{8} (B_i m_i^4 + B_2\ m_i^2 + B_3) K_i\ e^{m_i z}$$

$$\theta'(z) = e^{iwt} \sum_{i=1}^{8} (B_1 m_i^5 + B_2 m_i^3 + B_3 m_i) K_i\ e^{m_i z}$$

$$B(z) = -E\ I_\omega \theta'' = -e^{iwt}\ EI_\omega \sum_{i=1}^{8} (B_i m_i^6 + B_2 m_i^4 + B_3 m_i^2)$$

$$\times\ K_i\ e^{m_i z}$$

$$H(z) = -E\, I_\omega \theta''' + GJ\theta'$$

$$= e^{iwt} \sum_{i=1}^{8} \{-E\, I_\omega\, B_i m_i^7 + (-E\, I_\omega\, B_2 + GJB_1) m_i^5$$

$$+ (-E\, I_\omega\, B_3 + GJB_2) m_i^3 + GJB_3 m_i\}\, e^{m_i z}$$

Where K_1, K_2, ... K_8 are the constants to be determined from boundary conditions.

The above equations can be expressed in matrix form as

$$\{Z(z)\} = [C][D(z)\lrcorner]\{K\}\, e^{iwt} \qquad (3.3.8)$$

Where Z(z) is the state vector at a distance z from the origin and defined as

$$Z(z) = \begin{Bmatrix} V(z) \\ v'(z) \\ M(z) \\ V(z) \\ \theta(z) \\ \theta'(z) \\ B(z) \\ H(z) \end{Bmatrix} \qquad (3.3.8a)$$

[C] is a 8 x 8 square matrix with elements as follows

$$c(1,i) = 1$$

$$c(2,i) = m_i$$

$$c(3,i) = E\, I_x\, m_i^2$$

$$c(4,i) = -\, E\, I_x\, m_i^3$$

$$c(5,i) = B_1\, m_i^4 + B_2\, m_i^2 + B_3$$

$$c(6,i) = B_1\, m_i^5 + B_2\, m_i^3 + B_3\, m_i$$

$$c(7,i) = -\, E\, I_\omega\, (B_1 m_i^6 + B_2\, m_i^4 + B_3 m_i^2)$$

$$c(8,i) = -E I_\omega B_1 m_i^7 + (-E I_\omega B_2 + GJB_1) m_i^5 + (-E I_\omega B_3 + GJB_2) m_i^3 + GJB_3 m_i$$

where $i = 1,2, \ldots 8$

$[D(z)]$ is a 8 x 8 diagonal matrix with diagonal elements as

$$d(i,i) = e^{m_i z}, \text{ where } i=1,2\ldots8$$

$\{K\}$ is a column matrix consisting of constants K_i $i=1,2\ldots8$

The boundary conditions at the base $z = 0$ are

$$v = v(0),\ v' = v'(0),\ M = M(0),\ V = V(0)$$

$$\theta = \theta(0),\ \theta' = \theta'(0),\ B = B(0),\ H = H(0)$$

Substituting these conditions in eq. 3.3.8, there is obtained

$$\{Z(0)\} = [C][I]\{K\} e^{iwt} \tag{3.3.9}$$

The constants can be determined by matrix inversion in eq. 3.3.9

$$\{K\} = [C]^{-1}\{Z(0)\} e^{-iwt} \tag{3.3.9a}$$

The boundary conditions at $z = \ell$ are

$$v = v(\ell),\ v' = v'(\ell),\ M = M(\ell),\ V = V(\ell)$$

$$\theta = \theta(\ell),\ \theta' = \theta'(\ell),\ B = B(\ell),\ H = H(\ell)$$

Substituting these conditions in eq. 3.3.8 and using eq. 3.3.9 to eliminate $\{K\}$

$$\{Z(\ell)\} = [C][D(\ell)][C]^{-1}\{z(0)\} \tag{3.3.10}$$

The field transfer matrix is a 8 x 8 square matrix obtained from matrix multiplication

$$[F] = [C][D(\ell)][C]^{-1} \tag{3.3.11}$$

3.3.2 Point Transfer Matrix

The displacement of the center of gravity of the slab is shown in Fig. 3.3.1a. The inertia forces due to motion of the slab is shown in Figs. 3.3.1b to 3.3.1d. Stiffening action of the slab to contribute bimoment is shown in Fig. 3.3.1e.

Consideration of equilibrium of the slab element yields the following equations.

$$\left.\begin{aligned} V_+ &= V_- + m\ddot{v} + am\ddot{\theta} \\ H_+ &= H_- + J_m\ddot{\theta} + am\ddot{v} + a^2m\ddot{\theta} \\ M_+ &= M_- + J_x\ddot{\psi} = M_- + J_x\ddot{v}' + aJ_x\ddot{\theta}' \\ B_+ &= B_- - B_s = B_- - D\theta' \end{aligned}\right\} \qquad (3.3.12)$$

Notations used in the above eqs. are

- a Distance between shear center of the section and the center of gravity of the slab
- m Mass of the slab
- J_m Polar mass moment of inertia of the slab about an axis through the center of gravity.
- J_x Mass moment of inertion of the slab about an axis parallel to x and passing through the center of gravity
- D Bimoment contribution factor defined in eq. 2.3.12

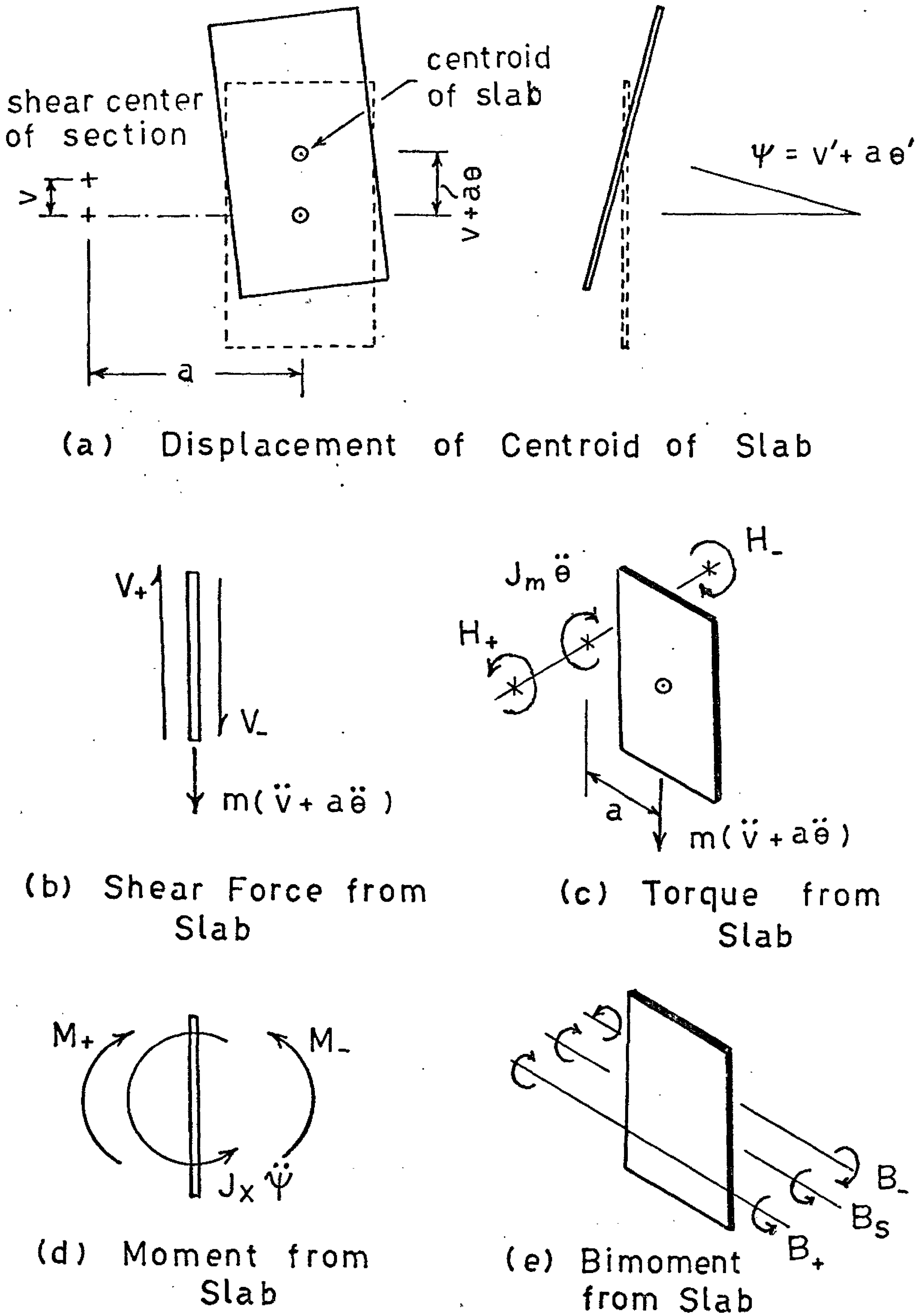

(a) Displacement of Centroid of Slab

(b) Shear Force from Slab

(c) Torque from Slab

(d) Moment from Slab

(e) Bimoment from Slab

FIG. 3.3.1

For a periodic vibration of frequency w

$$\begin{Bmatrix} v(z,t) \\ v'(z,t) \\ \theta(z,t) \\ \theta'(z,t) \end{Bmatrix} = \begin{Bmatrix} y(z) \\ y'(z) \\ \phi(z) \\ \phi'(z) \end{Bmatrix} e^{iwt}$$

Differentiating twice with respect to time

$$\begin{Bmatrix} v^{\cdot\cdot}(z,t) \\ v'^{\cdot\cdot}(z,t) \\ \theta^{\cdot\cdot}(z,t) \\ \theta'^{\cdot\cdot}(z,t) \end{Bmatrix} = -w^2 \begin{Bmatrix} v(z,t) \\ v'(z,t) \\ \theta(z,t) \\ \theta'(z,t) \end{Bmatrix} \tag{3.3.13}$$

Substituting in eq. 3.3.12, there is obtained

$$\left.\begin{aligned} V_+ &= V_- - w^2 mv - w^2 am\theta \\ H_+ &= H_- - w^2 amv - w^2 (J_m + a^2 m)\theta \\ M_+ &= M_- - w^2 J_x v' - w^2 aJ_x \theta' \\ B_+ &= B_- - D\theta' \end{aligned}\right\} \tag{3.3.14}$$

Compatibility conditions give

$$\left.\begin{aligned} v_+ &= v_- \\ v'_+ &= v'_- \\ \theta_+ &= \theta_- \\ \theta'_+ &= \theta'_- \end{aligned}\right\} \tag{3.3.15}$$

Point transfer matrix [P] can there be formed from eq. 3.3.14 and eq. 3.3.15 as

$$[P] = \begin{bmatrix} 1 & 0 & 0 & 0 & 0 & 0 & 0 & 0 \\ 0 & 1 & 0 & 0 & 0 & 0 & 0 & 0 \\ 0 & p_{32} & 1 & 0 & 0 & p_{36} & 0 & 0 \\ p_{41} & 0 & 0 & 1 & p_{45} & 0 & 0 & 0 \\ 0 & 0 & 0 & 0 & 1 & 0 & 0 & 0 \\ 0 & 0 & 0 & 0 & 0 & 1 & 0 & 0 \\ 0 & 0 & 0 & 0 & 0 & p_{76} & 1 & 0 \\ p_{81} & 0 & 0 & 0 & p_{85} & 0 & 0 & 1 \end{bmatrix} \qquad (3.3.16)$$

The elements of matrix are

$$p_{32} = -w^2J_x \text{ , } p_{36} = -w^2aJ_x$$
$$p_{41} = -w^2m \text{ , } p_{45} = -w^2am$$
$$p_{76} = -D \text{ , } p_{81} = -w^2am$$
$$p_{85} = -w^2(J_m + a^2m)$$

3.3.3 Boundary Conditions

The boundary conditions for the shear wall fixed at base and free at top can be written as

$$\{z_o^+\} = \begin{Bmatrix} 0 \\ 0 \\ M_o^+ \\ V_o^+ \\ 0 \\ 0 \\ B_o^+ \\ H_o^+ \end{Bmatrix} \quad \text{and} \quad \{z_8^+\} = \begin{Bmatrix} v_8^+ \\ v_8'^+ \\ 0 \\ 0 \\ \theta_8^+ \\ \theta_8'^+ \\ 0 \\ 0 \end{Bmatrix}$$

Substituting these conditions in eq. 3.2.3, there is obtained

$$\begin{Bmatrix} v_8^+ \\ v_8'^+ \\ 0 \\ 0 \\ \theta_8^+ \\ \theta_8'^+ \\ 0 \\ 0 \end{Bmatrix} = \begin{bmatrix} A \end{bmatrix} \begin{Bmatrix} 0 \\ 0 \\ M_o^+ \\ V_o^+ \\ 0 \\ 0 \\ B_o^+ \\ H_o^+ \end{Bmatrix} \tag{3.3.17}$$

Re-arrangement of terms of the above eq. yields

$$[R]\{X\} = 0 \tag{3.3.18}$$

Where

$$[R] = \begin{bmatrix} a_{33} & a_{34} & a_{37} & a_{38} \\ a_{43} & a_{44} & a_{47} & a_{48} \\ a_{73} & a_{74} & a_{77} & a_{78} \\ a_{83} & a_{84} & a_{87} & a_{88} \end{bmatrix}$$

Here 'a' denotes elemnets of matrix [A].

$$\{X\} = \begin{Bmatrix} M_o^+ \\ V_o^+ \\ B_o^+ \\ H_o^+ \end{Bmatrix}$$

The condition to determine the natural freqeuncies is

$$|R| = 0 \tag{3.3.19}$$

After determining the natural frequencies, the relative values of the elements in vector $\{X\}$ can be determined. The mode shape of the structure follows by back substitution of the vector $\{X\}$.

3.4 Computer Program

A computer program based on the above analysis has been written. The input data are the geometric and elastic properties of the shear wall structure. The trial frequency w is increased from an initial value and $|R|$ (eq. 3.3.19) is calculated. If $|R| \neq 0$ another value of w is tried. The same procedure is repeated until $|R|$ is reasonably small to be considered as zero. The next higher frequency is then determined following the same scheme. These natural frequencies obtained are then used as inputs in a second program to determine associated mode shapes.

The flow chart for the first program is shown in fig. 3.4.1 and the computer program is included in Appendix B.

3.5 Experiment

A dynamic experiment was carried out on the model (Fig. 2.1.1). The model was fixed on the shaking table and subjected to lateral vibration of known amplitude while the frequency is gradually swept from an initial value upwards. In all the dynamic tests, the shaking table was subjected

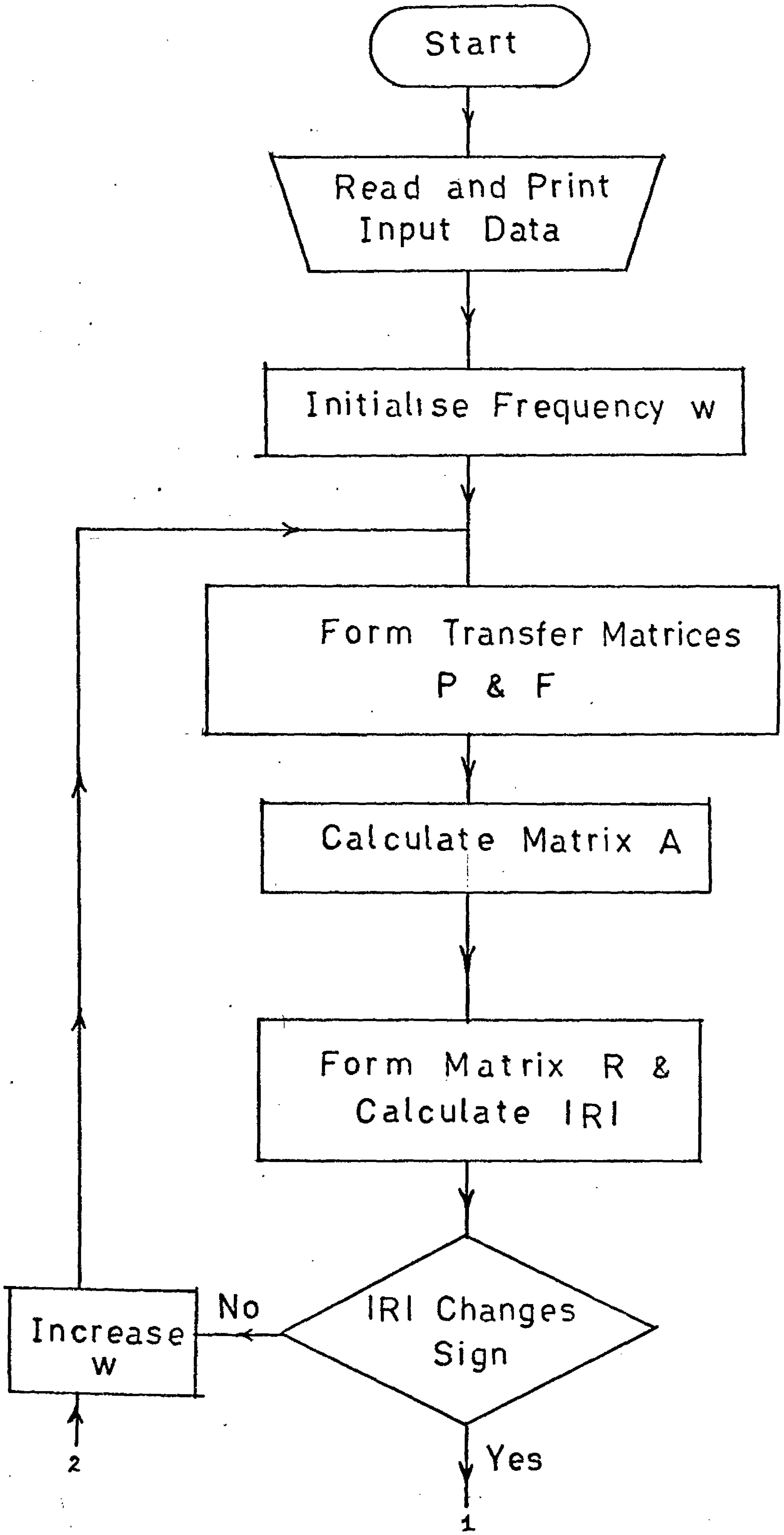
Start
Read and Print Input Data
Initialise Frequency w
Form Transfer Matrices P & F
Calculate Matrix A
Form Matrix R & Calculate |R|
|R| Changes Sign
No
Yes
Increase w
2
1

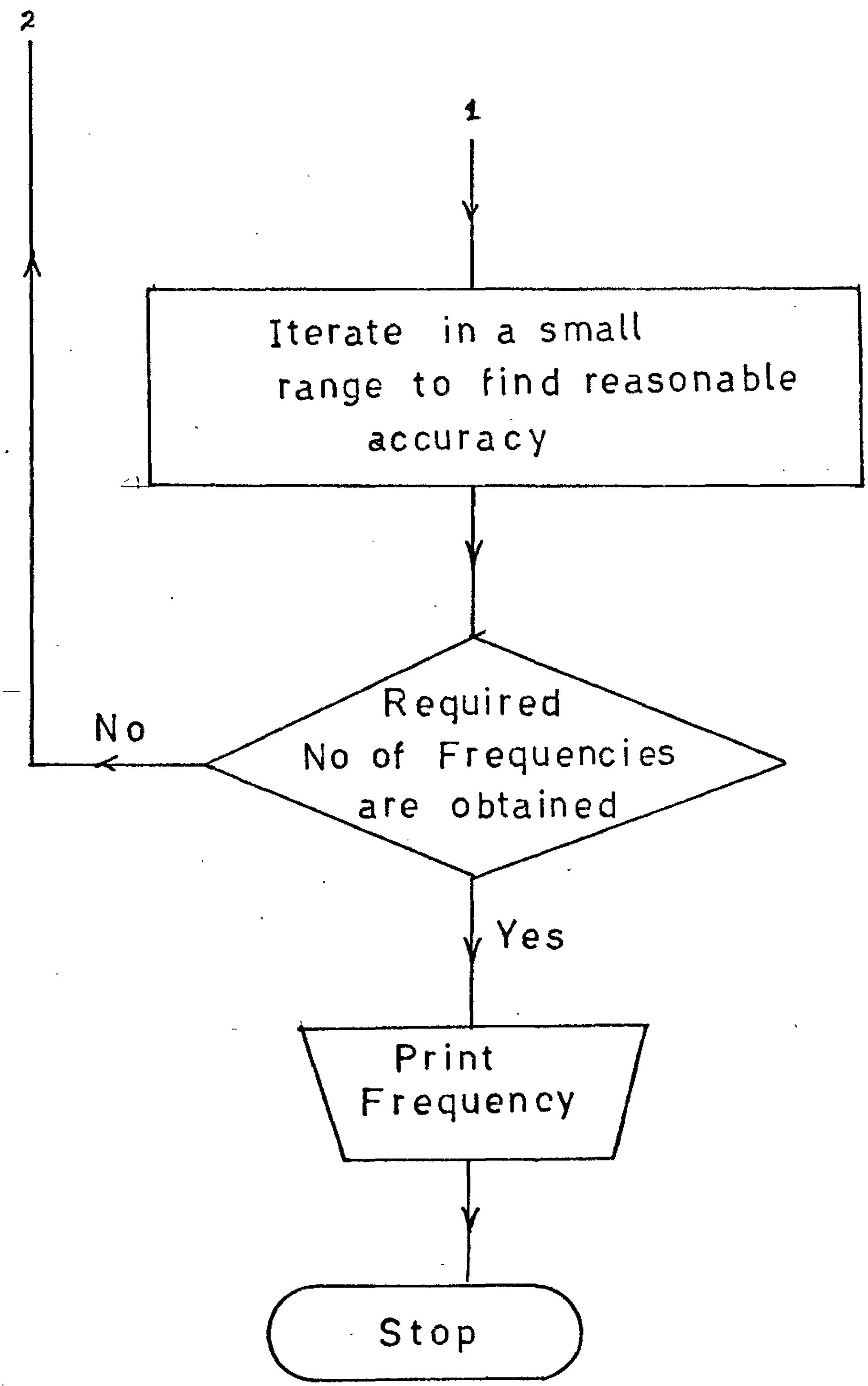

FLOW CHART

FIG. 3.4.1

to a constant displacement of 0.005 inch from 10 cps to 44 cps. After cross over frequency of 44 cps it was subjected to constant acceleration of 0.5 g. The response of the accelerometers fixed at different points of the model was studied. The experimental set up is shown in fig. 3.5.1 to 3.5.3. The output from the accelerometers was viewed in an oscilloscope. The RMS response of the accelerometers were plotted in a XY recorder. D.C. voltage proportional to RMS acceleration was fed in X ordinate and Y ordinate was adjusted in a suitable time scale. The arrangement of instruments is shown in fig. 3.5.4. arked increase in response is noticed in the frequency response plots (Fig. 3.6.1 to 3.6.4) at the resonant frequencies. For locating the resonant peak more accurately, the frequency was manually changed around each resonance zone and the response was monitored on a RMS voltmeter. The strains at resonance were determined from plotting outputs from the strain gauges in the Visicorder. The arrangement of instrument used is shown in fig. 3.5.5. Relative strain distirubtion is drawn from these plots and shown in fig. 3.6.7 to fig. 3.6.10.

The following is a list of different instruments used in the experiment.

The dynamic testing set-up consists of

A. Sweep Oscillator SD104A-5D

Make: Spectal Dynamic Corporation

Fig. 3.5.1
EXPERIMENTAL SET UP FOR DYNAMIC TEST

Fig. 3.5.2
MODEL FIXED ON THE SHAKING TABLE

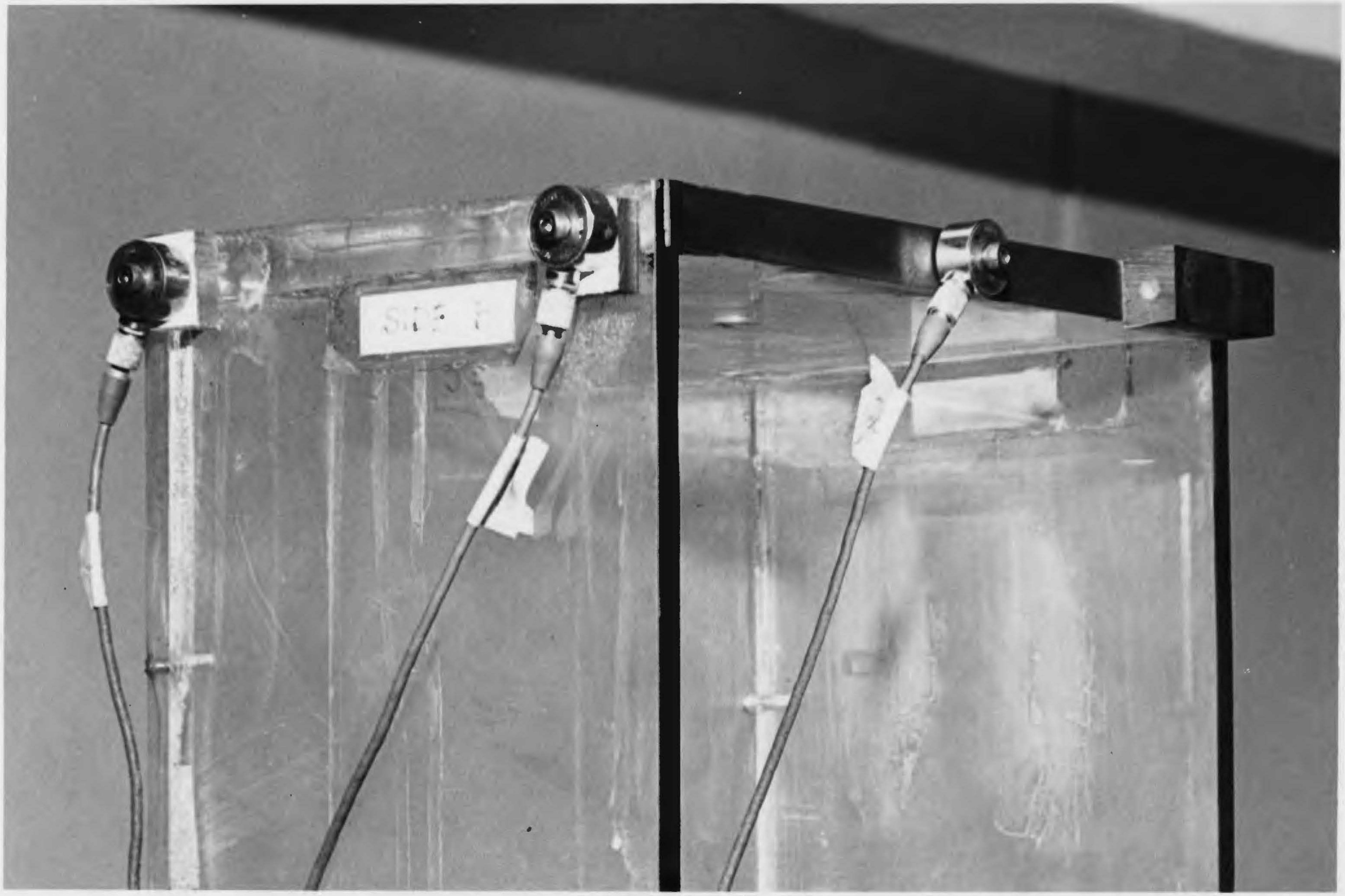

Fig. 3.5.3

ACCELEROMETERS ATTACHED TO THE MODEL

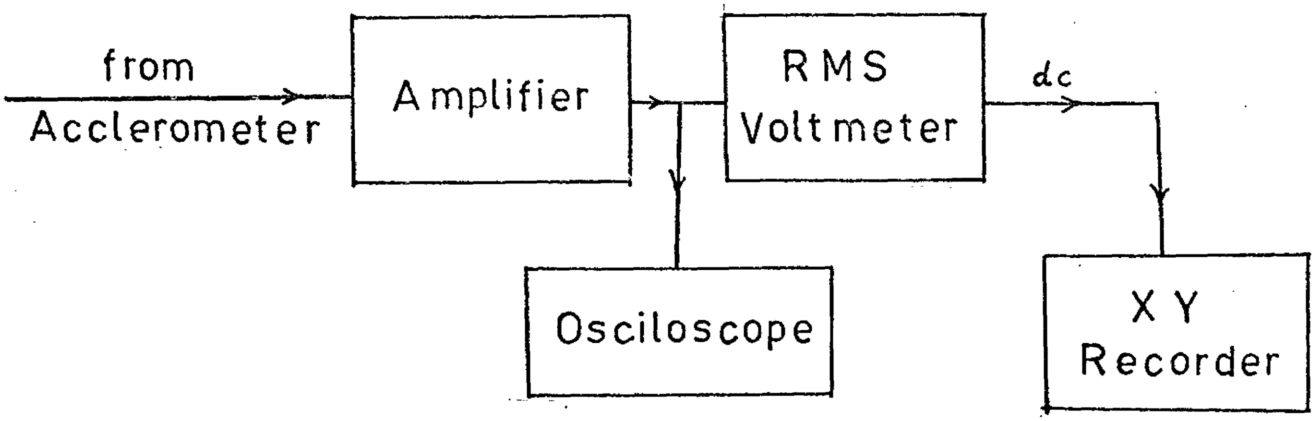

ARRANGEMENT FOR RESONANCE SEARCH

FIG. 3.5.4

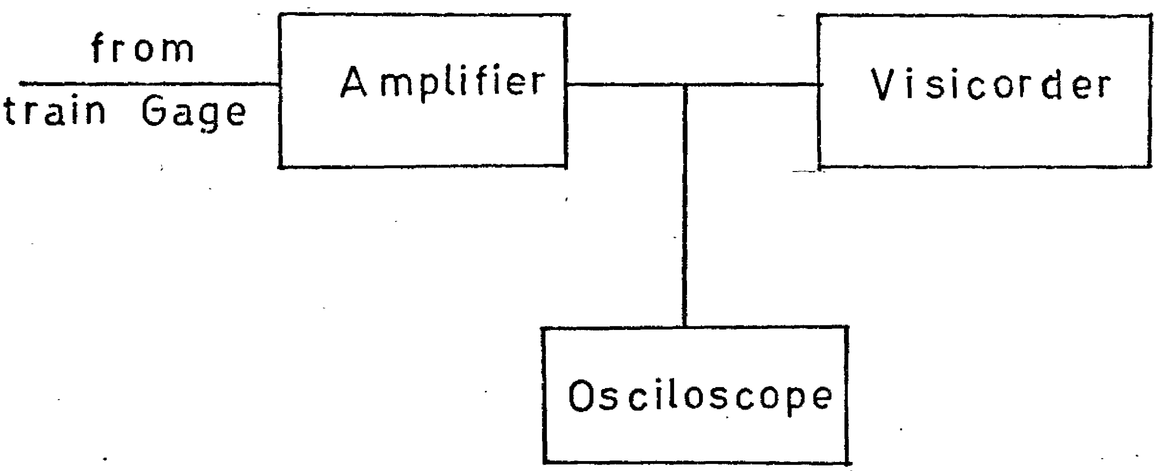

ARRANGEMENT FOR MEASURING STRAINS

FIG. 3.5.5

B. Amplitude Servo/Monitor SD105A

Make: Spectal Dynamic Corporation.

D. Accelerometer source follower SFA-100

Make: Ling Electronics

E. Accelerometer Normalizing Amplifier ANA-101

Make: Ling Electronics

F. Power Amplifier CP-5/6

Make: Ling Electronics

G. Shaker B 290

Make: Ling Electronics

H. Vibraglide Sliptable SINGCO 30-30

Make: Marshall Research and Dvelopment Corporation

For monitoring and plotting the response the following instruments were employed.

I. Dual Beam Oscilloscope

Make: Tectronix Inc.

J. Accelerometer

K. Laboratory amplifier 2616B

Make: Endevco Corporation

L. D.C. Amplifier, High Gain Type 1-165

Make: Endevco Corporation

M. Bridge Amplifier

Make: Ellis Associates

N. RMS Voltmeter

Make: Hewlett Packard

O. Visicorder (2 channels)

Make: Honeywell Controls Ltd.

P. Digital Counter

Make: Hewlet Packard.

3.6 Results and Discussions

The frequency response plots as obtained from the dynamic test for the accelerometers located at different positions are shown in fig. 3.6.1 to 3.6.4. The figures near the peaks are the experimental resonant frequencies. Average of all the experimental frequencies together with the theoretical frequencies for different consideration of floor slabs are shown in table 3.6.1.

It can be seen that for the first and third modes the experimental freq. lies between the theoretical predicted value when the torsional restraining effect of the slab is considered and the theoretical predicted value when both the torsional and effective bending restraining effect of the slab is considered. The difference between the theoretical and experimental values is about 5%.

In the second mode, the experimental value is 16% lower than the theoretical calculated value. Since the second mode is a bending predominant mode, in this case, the larger difference may be caused be neglecting shear deformation in the mathematical model. The importance of considering shear deformation for bending predominant mode was noted by Tso (29).

NO. FREQ.	THEORETICAL FREQUENCY (cps)				EXPERIMENTAL FREQUENCY (cps)
	Floor -less Structure	Torsion Only of Slab	Torsion + Eff. Bending of Slab	Torsion + Bending of Slab	
1	16.5	14.5	16.8	20.8	15.9
2	65.6	56.7	57.8	60.9	48.7
3	93.9	71.8	76.5	89.0	72.9

COMPARISON OF FREQUENCIES

TABLE 3.6.1

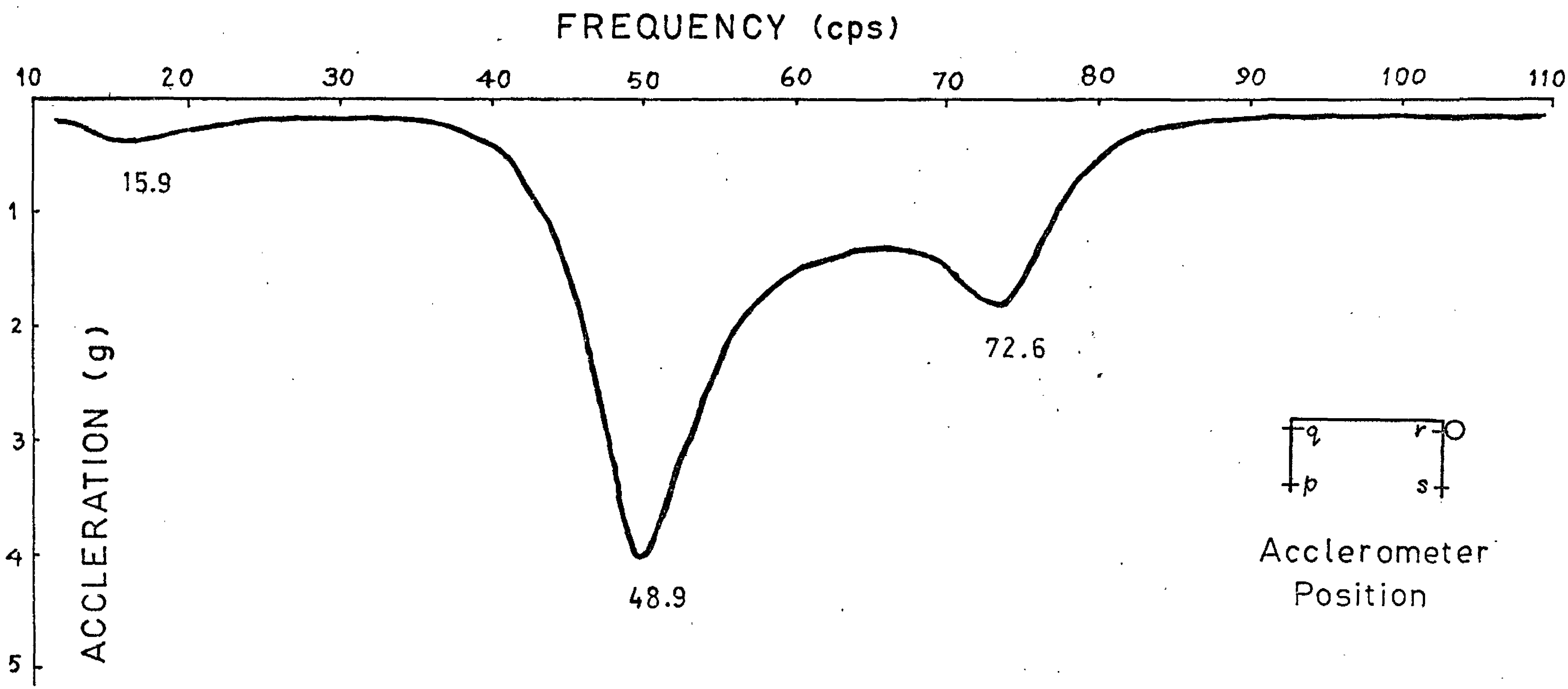

FREQUENCY RESPONSE PLOT

FIG. 3.6.1

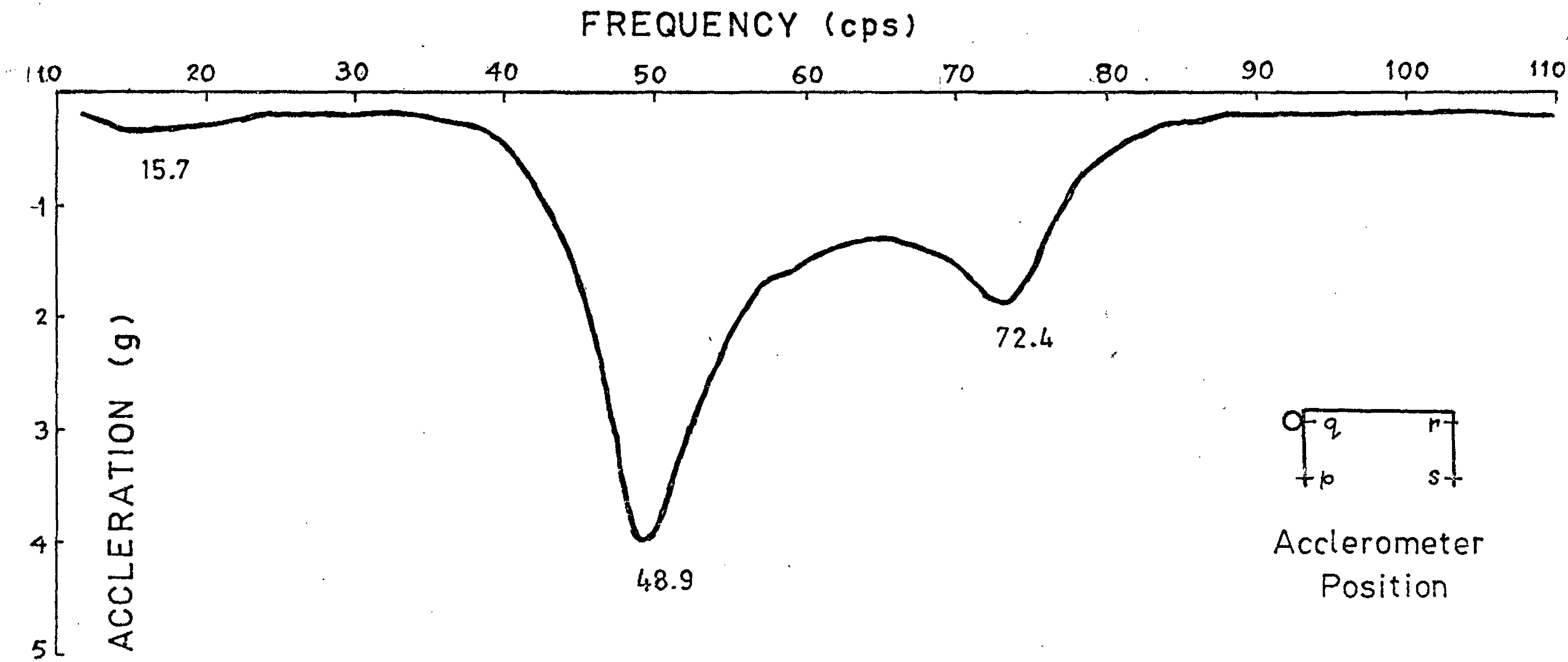

FREQUENCY RESPONSE PLOT

FIG. 3.6.2

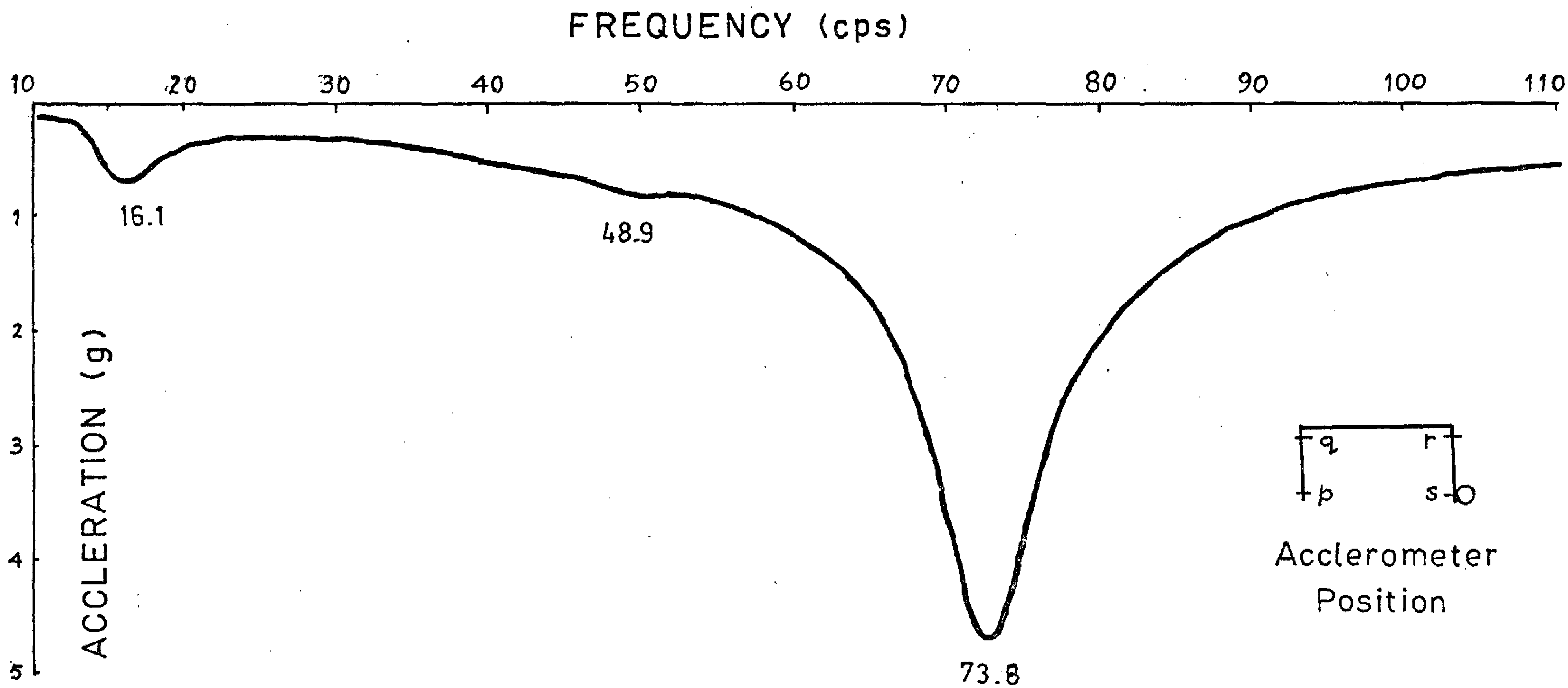

FREQUENCY RESPONSE PLOT

FIG 3.6.3

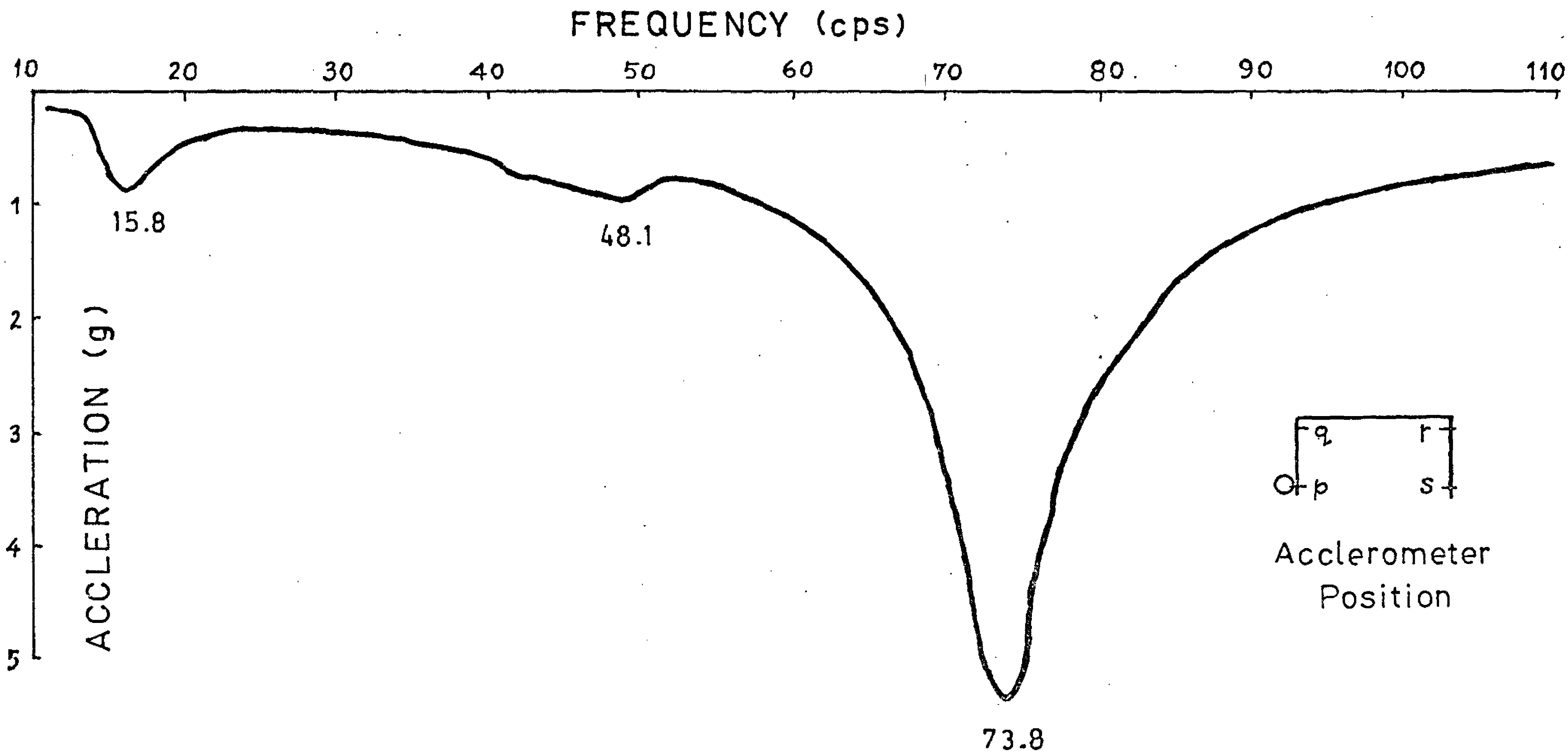

FREQUENCY RSPONSE PLOT

FIG. 3.6.4

FIG. 3.6.5

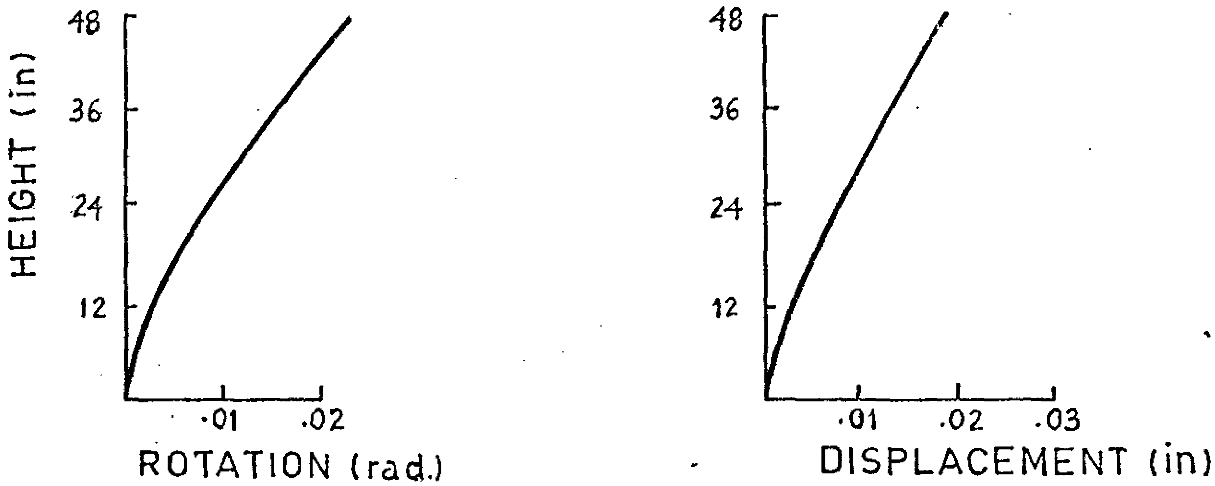

(a) MODE SHAPE FOR FIRST FREQ.

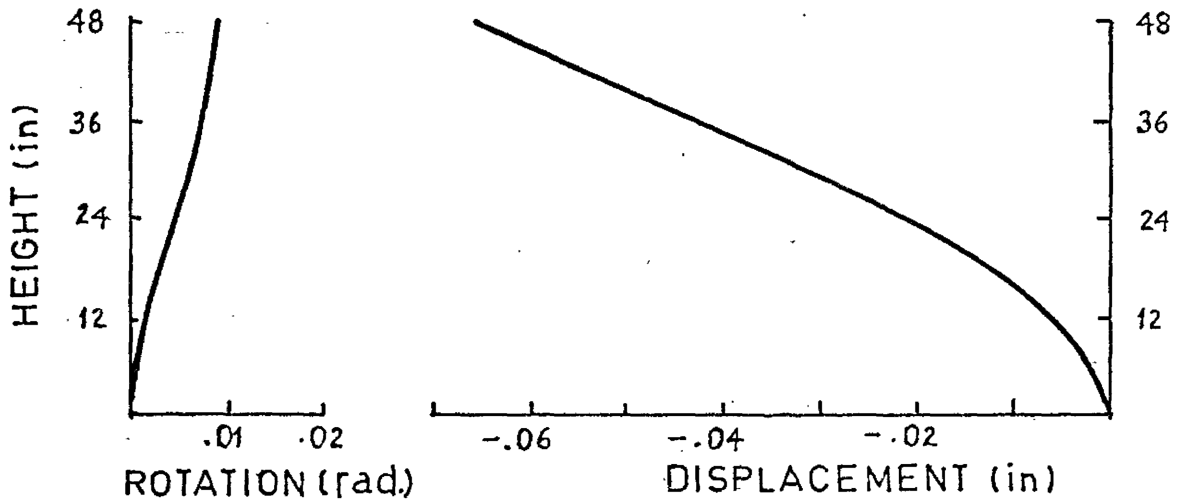

(b) MODE SHAPE FOR SECOND FREQ.

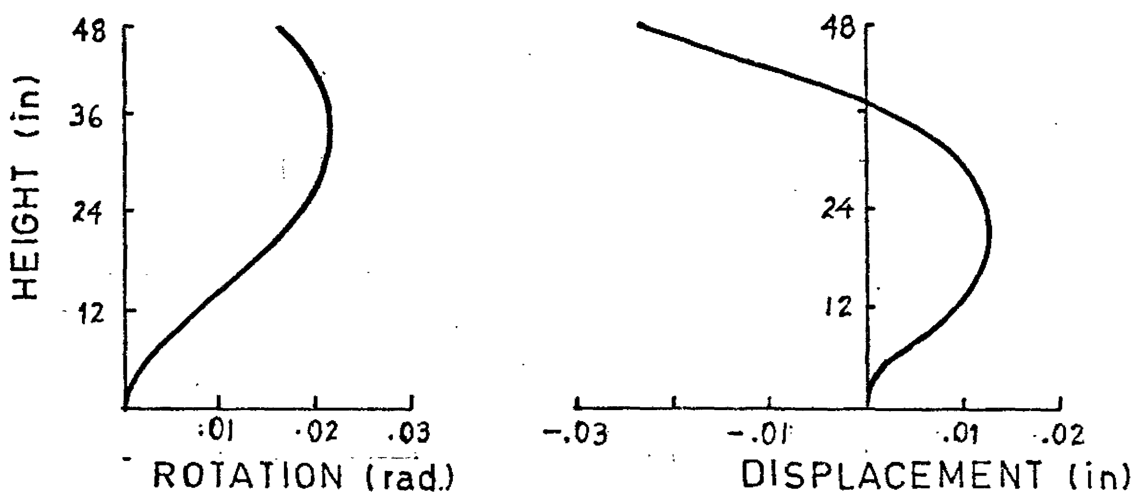

(c) MODE SHAPE FOR THIRD FREQ.

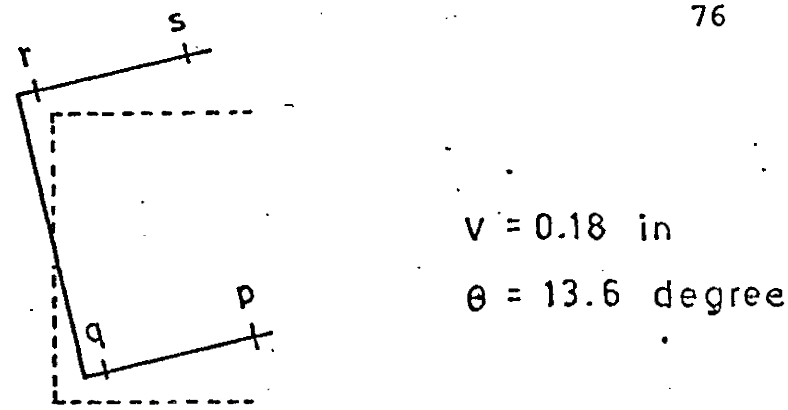

(a) FIRST MODE

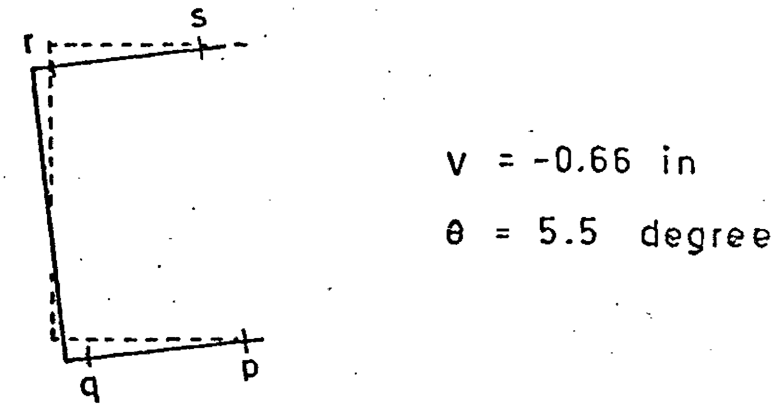

(b) SECOND MODE

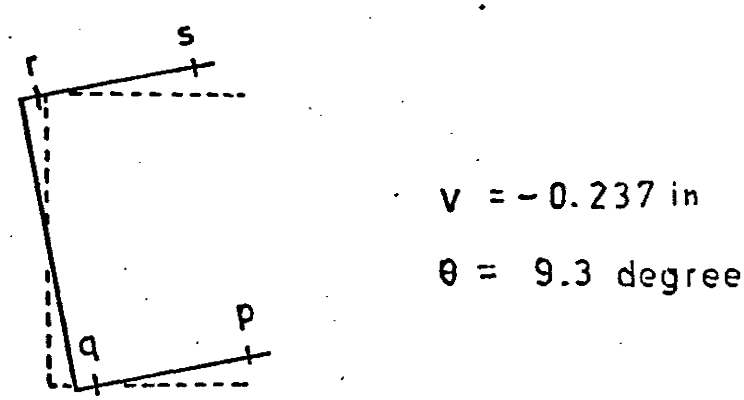

(c) THIRD MODE

RELATIVE ROTATION & DISPLACEMENT
AT 8TH. FLOOR
FIG. 3.6.6

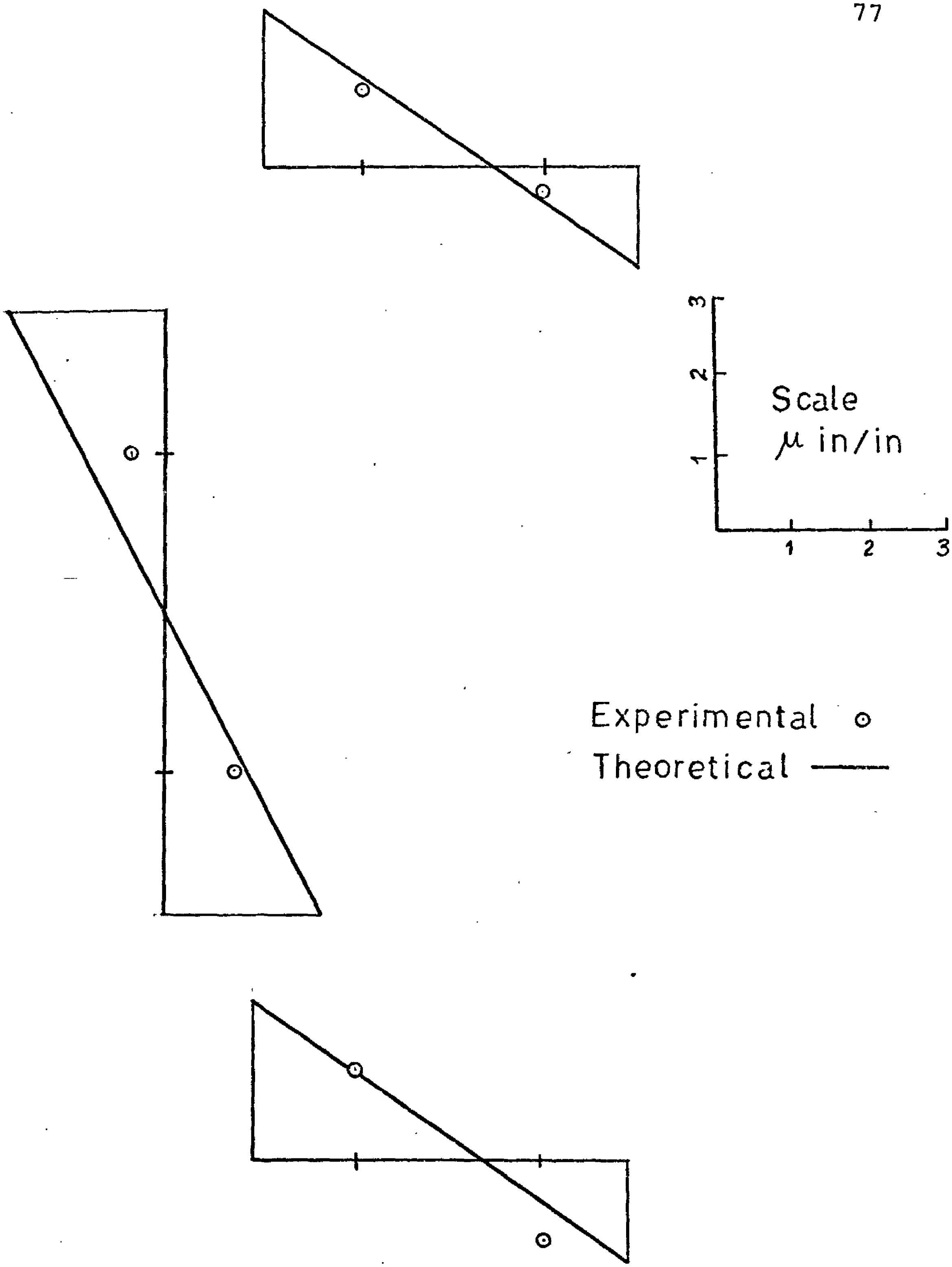

RELATIVE STRAIN DISTRIBUTION AT LEVEL A
AT FIRST FREQUENCY

FIG. 3.6.7

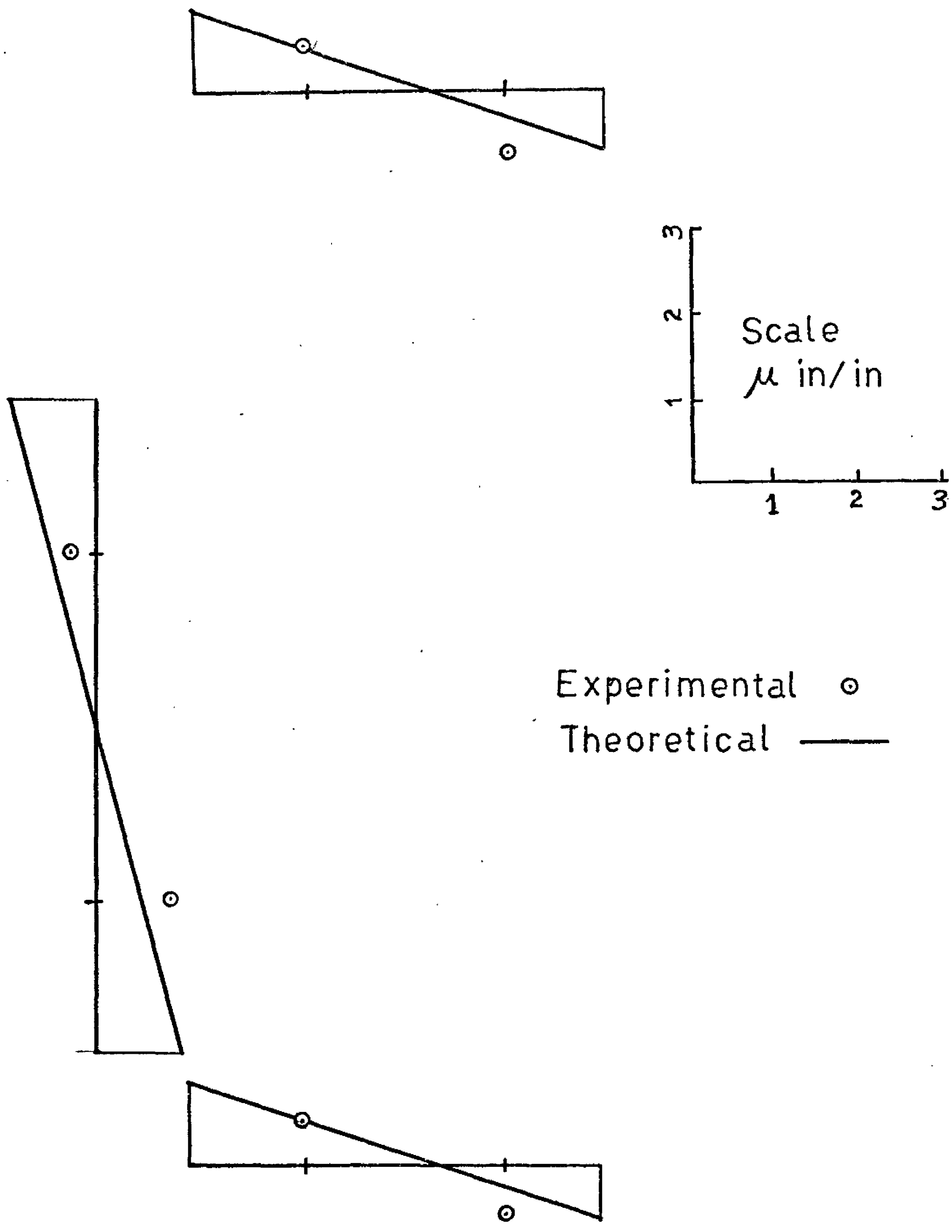

RELATIVE STRAIN DISTRIBUTION AT LEVEL B
AT FIRST FREQUENCY

FIG. 3.6.8

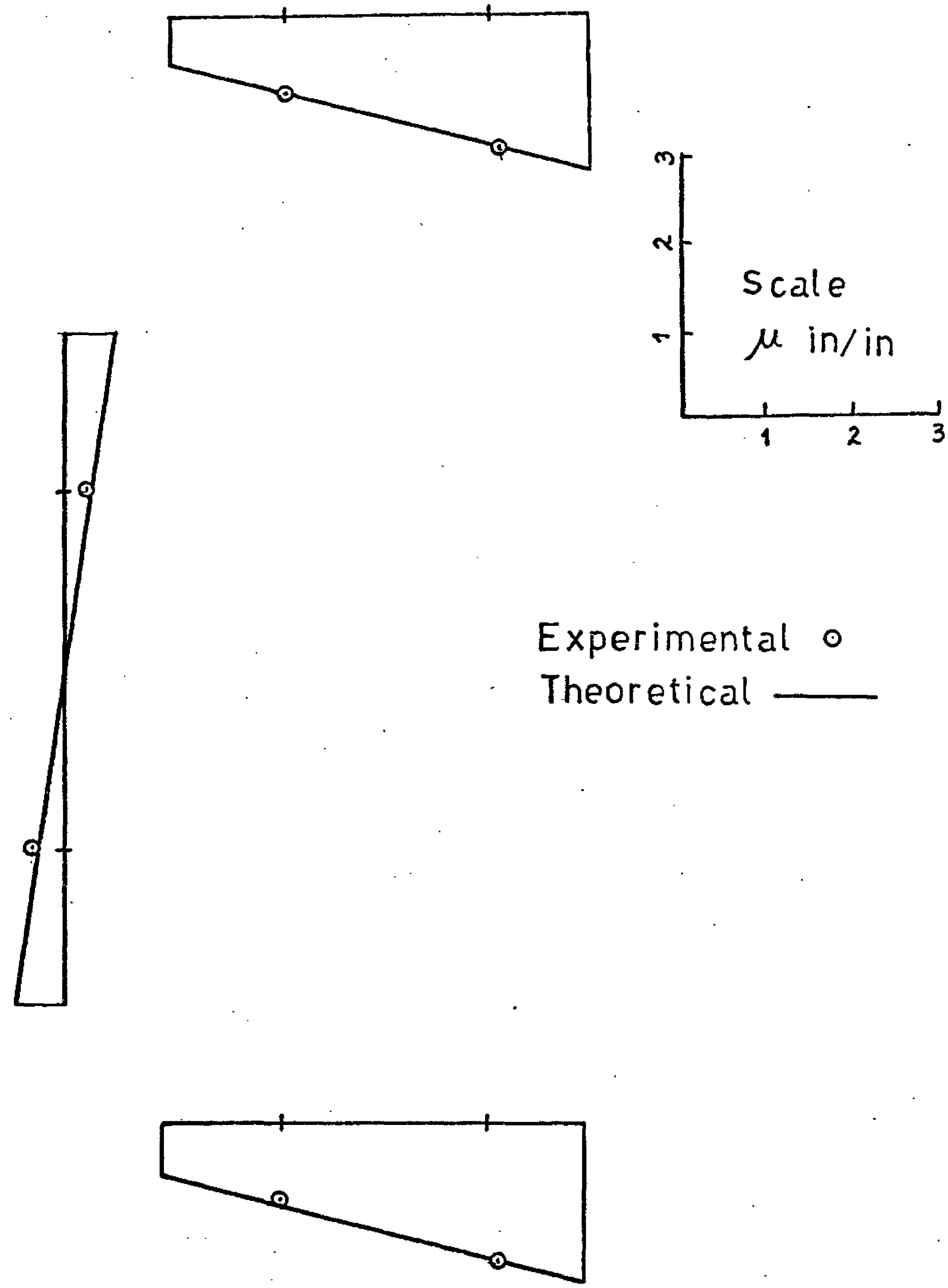

RELATIVE STRAIN DISTRIBUTION AT LEVEL A
AT SECOND FREQUENCY

FIG. 3.6.9

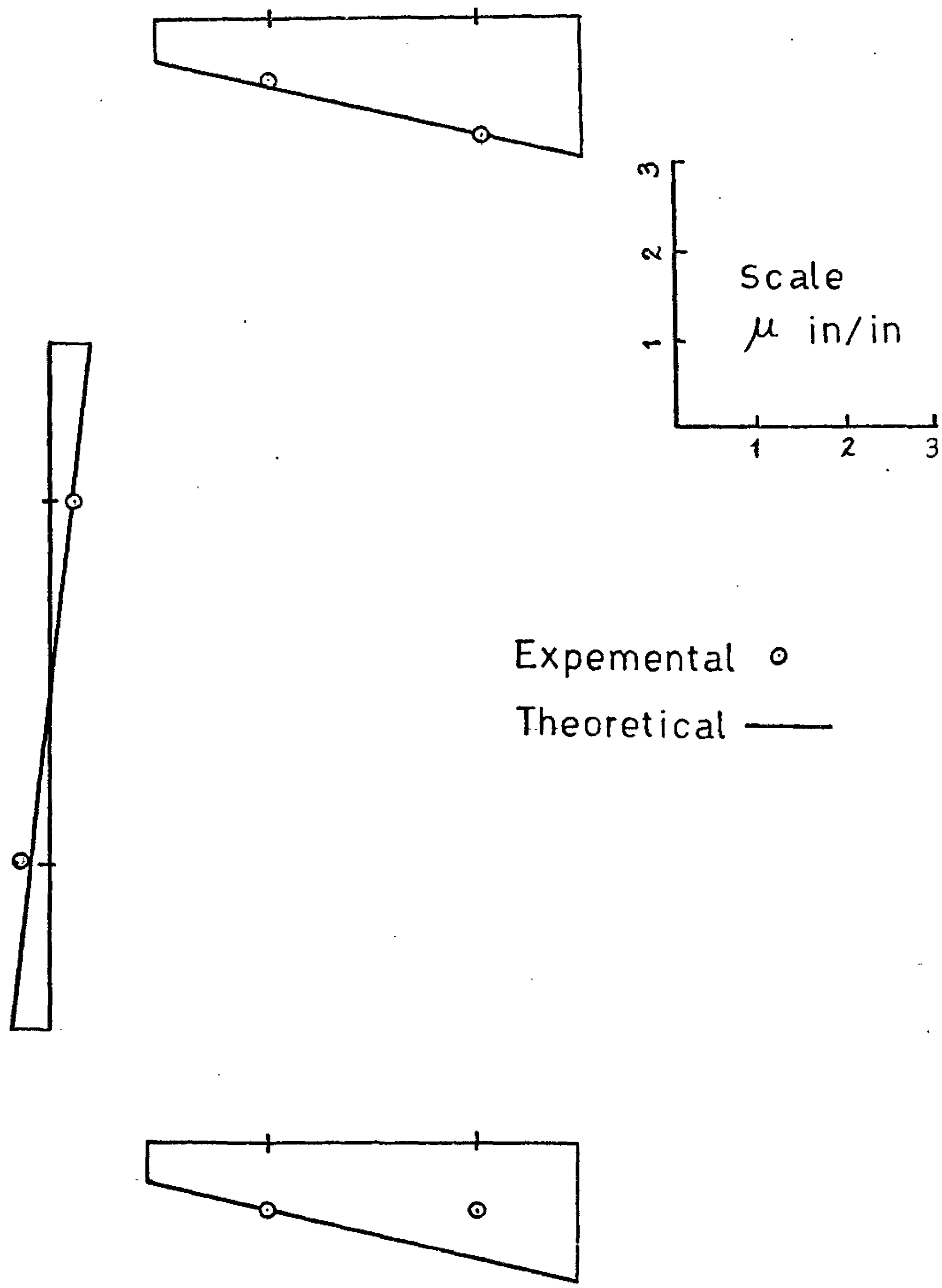

RELATIVE STRAIN DISTRIBUTION AT LEVEL B
AT SECOND FREQUENCY

FIG. 3.6.10

The associated mode shapes of the structure for first three modes obtained theoretically are plotted in fig. 3.6.5. It shows from these plots that the first mode consists of torsion predominant displacement and the second mode consists of bending predominant displacements.

It is also noted that in first mode displacement and rotation are in phase. In second mode they are out of phase. In third mode they are in phase in lower part of the structure but out of phase in top part.

The displacements and rotations at the top of the structure for different modes are plotted in fig. 3.6.6 The values of v and θ written on the figure are the values of mode shapes curve (Fig. 3.6.5) at 48 inch levels are relative values only. In other words the values for the first mode does not have any relation with that for the second or the third mode.

It is seen from the frequency response plots (fig. 3.6.1 to fig. 3.6.4) that at any resonant frequency, the response varies depending on the position of the accelerometer. For example in the third resonance the accelerometers mounted at points q and r show lower response than that mounted at points p and s. In the second resonance, the accelerometers mounted at points q and r shows higher response than that mounted at points p and s. In the first resonance, the response of accelerometers mounted at p and s shows higher response than that mounted at q and r. These type of behaviour is due to the in phase or out of phase nature of displacements and rotations in different modes and can be explained from fig. 3.6.6. It is seen from the plot that points p and s undergo maximum translational displacement due to combined action of v and θ in the third and the first mode. Whereas points q and r undergo maximum translational displacement in second mode only.

The relative strain distribution at level A and level B (refer fig. 2.5.2 for level A and B) at the first and the second resonace are plotted (Fig. 3.6.7 to Fig. 3.6.10). Theoretical distribution are drawn from the calculated mode shapes. Since the mode shapes are defined by relative values only the theoretical strain diagram is made to pass through one experimental point. A reasonable agreement between the theory and experiment is shown in these plots.

CHAPTER IV

STATIC FORMULATION OF NON PLANAR COUPLED SHEAR WALL

4.1 Summary

In this chapter, the nonplanar coupled shear wall is analysed using the continuum approach. Differential equations are developed for such wall subjected to lateral forces and torques distributed along the height. Special configurations of shear walls are shown and the modification on differential equations and solution is indicated. The experimental study was performed on a small scale plexiglas model consisting of two angles connected by beams at equal spacing (Fig. 4.4.1). The model was subjected to a force and a torque at the top storey and strains and deflections are measured. The experimental results are then compared with the theoretical predictions.

4.2 Theoretical Analysis

Consider two nonplanar piers which are connected by floor beams at equal spacing (Fig. 4.2.1). In the analysis the center of the connecting beam O is taken as the reference point. The differential equations are derived in terms of the displacement variables of point O, namely u, v and θ. The external forces and torques are also refered to the same point O. The theory is based on two assumptions:

(i) The deformation of the connecting beams due to bending in horizontal plane is restricted.

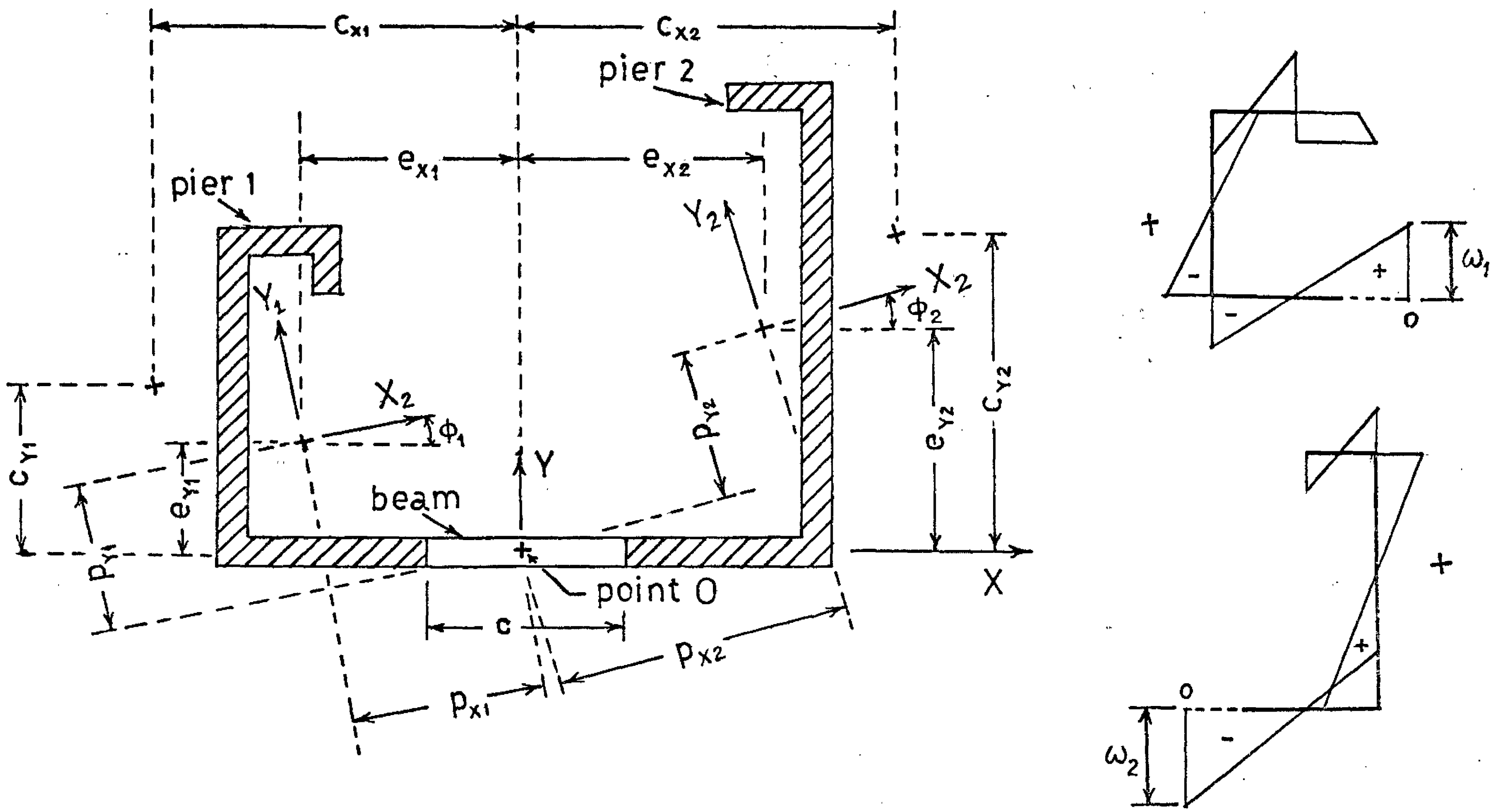

GEOMETRY OF COUPLED SHEAR WALL

FIG. 4.2.1

(ii) Points of contraflexure for the connecting beams due to bending in vertical plane are taken to be at the center.

In addition to the above assumptions, Vlasov's theory is taken to be valied for individual section constituting the coupled wall.

Using the continuum approach, the connecting beams are replaced by independently acting laminae of appropriate stiffness (Fig. 4.2.2a).

4.2.1 Notations Used

The notations used in the present analysis are listed below and illustrated in fig. 4.2.1.

X_1, Y_1	Orthogonal principal axes for pier 1
u_1, v_1, θ_1	Generalised displacements of the shear center of pier 1.
X, Y, Z	Orthogonal global axes with origin at point O. X is parallel to the length of the beam.
$\bar{X}_1, \bar{Y}_1$	Orthogonal axes parallel to X and Y and passing through centroid of pier 1 (Fig. 4.2.4).
u, v, θ	Generalised global displacements of point O.
$e_{X1} e_{Y1}$	Co-ordinates of the centroid of pier 1 refered to global axes.
$c_{X1} c_{Y1}$	Co-ordinate of the shear center of pier 1 refered to global axes.
p_{x1}, p_{x2}	Distances of the centroid of pier 1 from point O measured parallel to X_1, Y_1 axes.
q_{X1}, q_{X2}	Distances of the shear center of pier 1 from point O measured parallel to X_1, Y_1 axes.
ϕ_1	Angle between X_1 and X axes.
ω_1	Sectoral ordinate of pier 1 at the point O refered to shear center of the same pier.

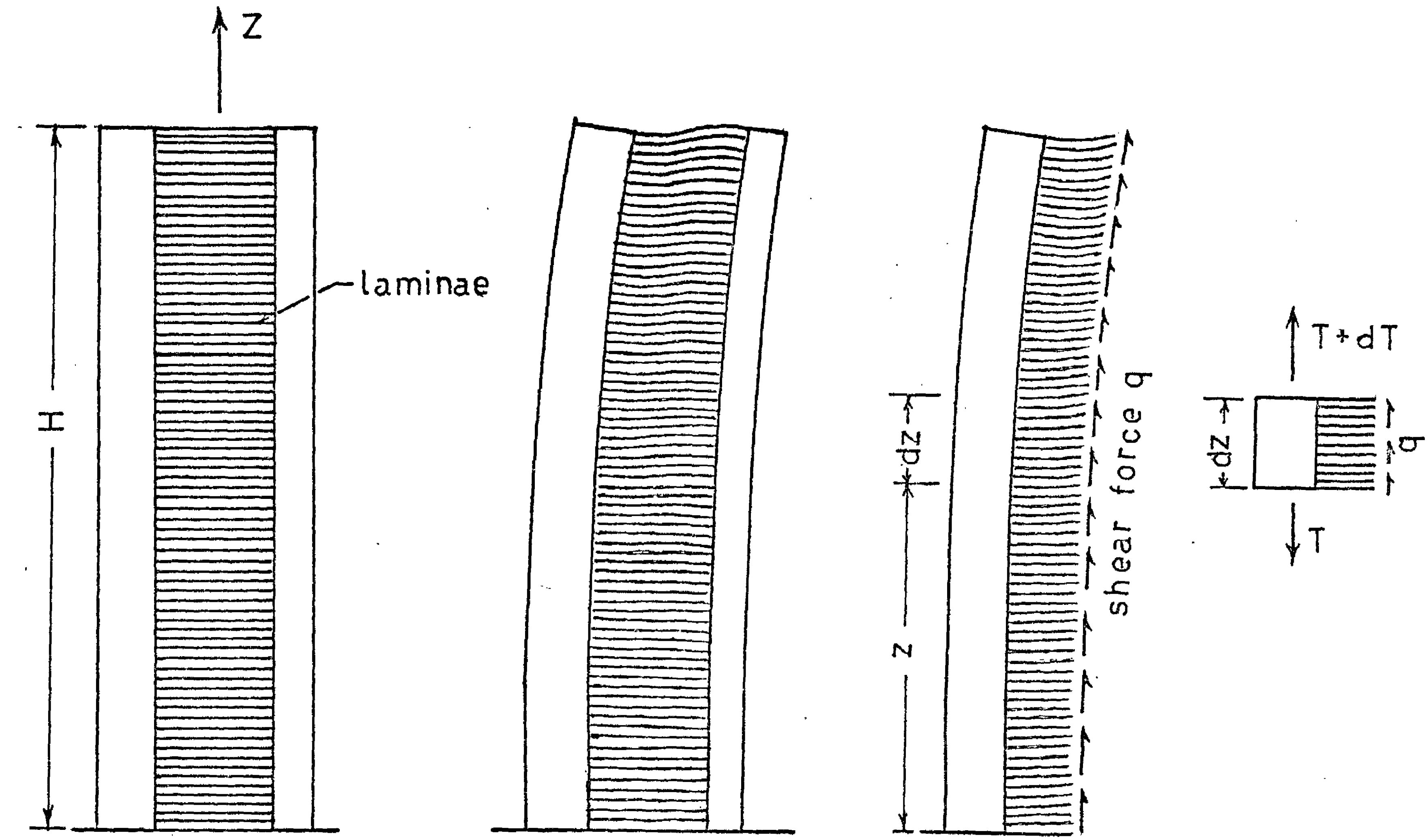

(a) Replaced Structure (b) Deformed Structure (c) Shear Force & Axial Force

FIG. 4.2.2

I_{X1}, I_{Y1}	Moment of inertia of pier 1 about X_1, Y_1 axes.
S_{X1}, S_{Y1}	Moment of inertia of pier 1 about $\overline{X}_1$ and $\overline{Y}_1$ axes (Fig. 4.2.4).
S_{XY1}	Product moment of inertia of pier 1 about axes parallel to X,Y and passing through centroid i.e. $\overline{X}_1$,$\overline{Y}_1$ axes respectively.
$I_{\omega 1}$	Principal sectorial moment of inertia.
M_X	External moment about X axis
M_Y	External moment about Y axis
Q_t	External torque about point O.
I_b	Moment of inertia of the connecting beam
A_b	Area of the connecting beam
c	Clear span of connecting beam.
h	Storey height

Note:--The subscript 1 in the above notations are replaced by 2 for pier 2.

4.2.2. Geometric Relations

The global axes of the structure are X, Y and Z are the reference axes about which the displacements and forces are refered. The X axis is parallel to the longitudinal axis of the connecting beam. The principal axis of the piers are inclined at angles ϕ_1 and ϕ_2 to the X axis (Fig. 4.2.1). The Z axis is the vertical axis through point O.

The assumption (i) along with Vlasov's hypothesis of non deformable cross section leads to a rigid section of the coupled wall, for which the following geometric relation are valied for the transformation of displacement of the cross section from one reference point to another.

The Transfer matrices $[R_j]$ and $[T_j]$ can be defined as:

$$[R_j] = \begin{bmatrix} \mathrm{Cos}\ \phi_j & \mathrm{Sin}\ \phi_j & 0 \\ -\mathrm{Sin}\ \phi_j & \mathrm{Cos}\ \phi_j & 0 \\ 0 & 0 & 1 \end{bmatrix} \tag{4.2.1}$$

$$[T_j] = \begin{bmatrix} 1 & 0 & -c_{yi} \\ 0 & 1 & c_{xj} \\ 0 & 0 & 1 \end{bmatrix} \tag{4.2.2}$$

$$(j = 1,2)$$

The relatinn between the global displacement variables u, v and θ and the displacement variables of the piers are:

$$\begin{Bmatrix} u_j \\ v_j \\ \theta_j \end{Bmatrix} = [R_j]\,[T_j] \begin{Bmatrix} u \\ v \\ \theta \end{Bmatrix} \tag{4.2.3}$$

$$(j = 1,2)$$

Other geometric relations which relate the distances measured along the principal axes of the piers to the global directions are:

$$\begin{Bmatrix} p_{xj} \\ p_{yi} \end{Bmatrix} = \begin{bmatrix} \mathrm{Cos}\ \phi_j & \mathrm{Sin}\ \phi_j \\ -\mathrm{Sin}\ \phi_j & \mathrm{Cos}\ \phi_j \end{bmatrix} \begin{Bmatrix} e_{xj} \\ e_{yj} \end{Bmatrix} \tag{4.2.4}$$

$$\begin{Bmatrix} q_{xj} \\ q_{yj} \end{Bmatrix} \quad \begin{bmatrix} \mathrm{Cos}\ \phi_j & \mathrm{Sin}\ \phi_j \\ -\mathrm{Sin}\ \phi_j & \mathrm{Cos}\ \phi_j \end{bmatrix} \begin{Bmatrix} c_{xj} \\ c_{yj} \end{Bmatrix} \tag{4.2.5}$$

in which $j = 1,2$

4.2.3 Displacement Consideration

An imaginary cut is made along the center line of the laminae. Due to deflection of the piers, there is a relative displacement δ_1 to the left and the right of the cut as shown in fig. 4.2.3(a).

$$\delta_1 = u_2' p_{x2} - u_1' p_{x1} + v_2' p_{y2} - v_1' p_{y1} \\ -\theta_2' I_{\omega 2} + \theta_1' I_{\omega 1} \tag{4.2.6}$$

Using relations in eq. 4.2.3 and 4.2.4 this equation becomes:

$$\delta_1 = u'a + v'b + \theta'(\omega + d) \tag{4.2.7}$$

Where

$$a = e_{x2} - e_{x1}$$
$$b = e_{y2} - e_{y1}$$
$$\omega = \omega_1 - \omega_2$$
$$d = c_{x2}e_{y2} - c_{y2}e_{x2} + c_{y1}e_{x1} - c_{x1}e_{y1}$$

The shear force distribution q induced at the center of laminae produces compressive force on one pier and tensile force in the other. This axial force T in pier is related to q (Fig. 4.2.2c) as:

$$q = -\frac{dT}{dZ} \tag{4.2.8}$$

This axial force T produces axial deformation of the pier which decreases the relative displacement at center of laminae by δ_2.

$$\delta_2 = \int_0^Z \frac{1}{E}\left(\frac{1}{A_1} + \frac{1}{A_2}\right) T(\xi)\, d\xi \tag{4.2.9}$$

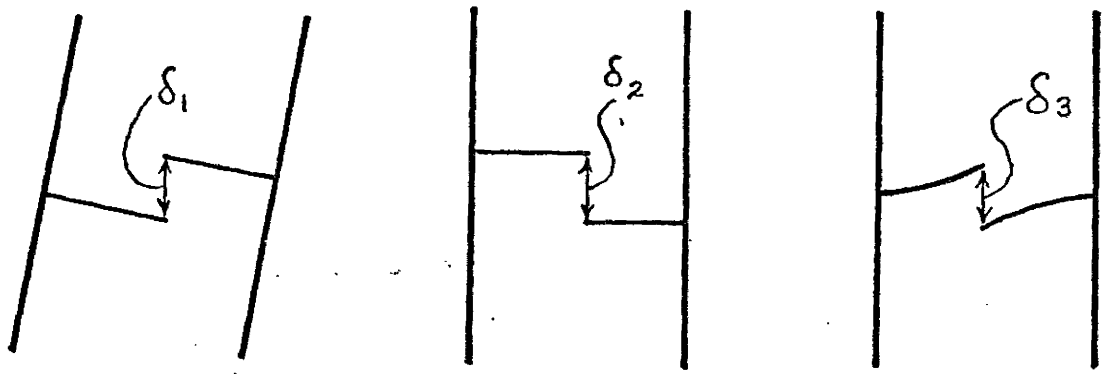

(a) Gap due to Deflection of Piers

(b) Gap due to Axial Deformation of Piers

(c) Gap due to Deformation of Laminas

FIG. 4.2.3

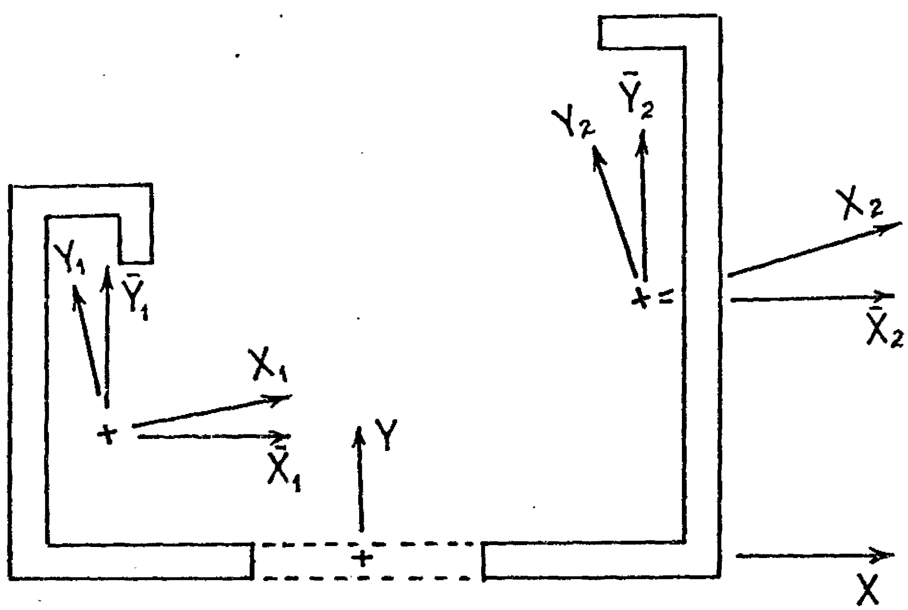

TRANSFORMATION OF MOMENT OF INERTIA

FIG. 4.2.4

Finally the force q will produce in the laminae a deformation δ_3 due to bending and shear.

$$\delta_3 = \frac{qc^3}{12EJ_b} \tag{4.2.10}$$

Where J_b is the equivalent moment of inertia of laminas taking into account shear deformation of beam.

$$J_b = \frac{I_b}{h\left(1 + \dfrac{12EI_b}{c^2GA_b}\right)} \tag{4.2.11}$$

To satisfy the condition of compatibility it is required

$$\delta_1 = \delta_2 + \delta_3$$

Substituting above expressions for δ_1, δ_2, and δ_3

$$u'a + v'b + \theta'(\omega+d) = \int_0^Z \frac{1}{E}\left(\frac{1}{A_1} + \frac{1}{A_2}\right)T(\xi)\, d\xi + \frac{qc^3}{12EJ_b} \tag{4.2.12(a)}$$

Differenting once

$$u''a + v''b + \theta''(\omega+d) = \frac{1}{E}\left(\frac{1}{A_1} + \frac{1}{A_2}\right) T + \frac{c^3}{12EJ_b}\frac{dq}{dZ} \tag{4.2.12}$$

4.2.4 Force Equilibrium Conditions

The internal moments acting on the different components of coupled shear wall are shown in fig. 4.2.5. These internal moments along with couple produced by axial force T balances the external moment. For equilibrium of moments about Y and X axis, the following expressions can be derived.

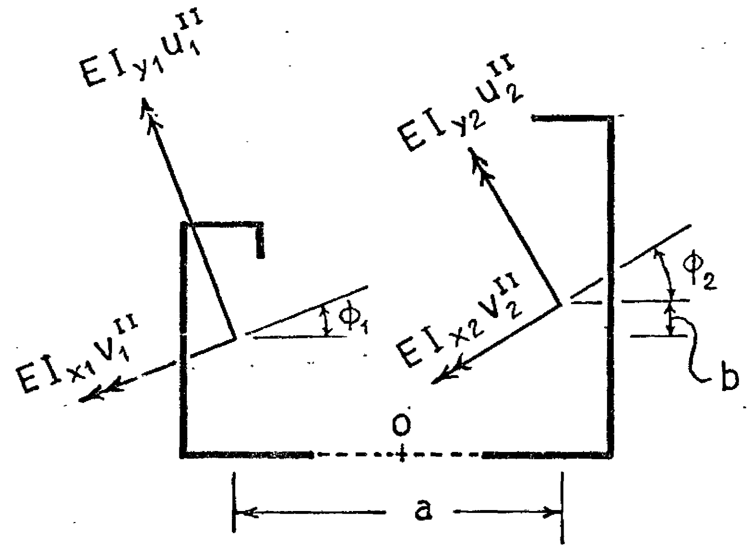

INTERNAL MOMENTS

FIG. 4.2.5

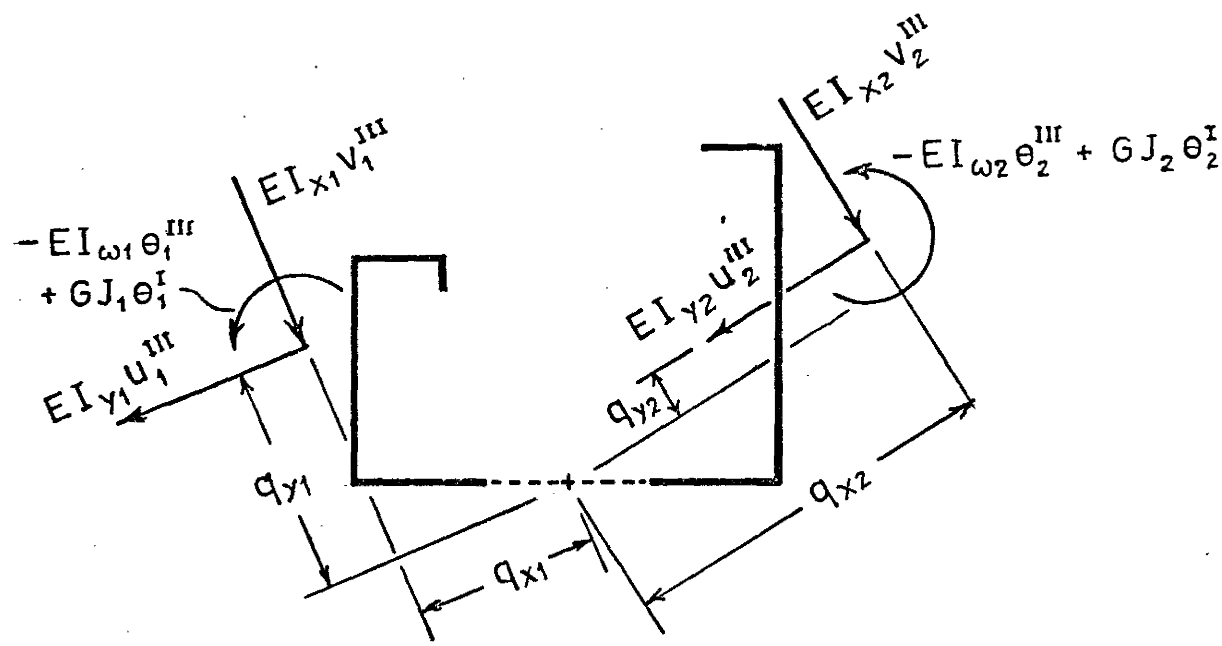

INTERNAL TORQUES & SHEAR FORCES

FIG. 4.2.6

$$EI_{y1}u_1'' \text{ Cos } \phi_1 - EI_{x1}v_1'' \text{ Sin } \phi_1 + EI_{y2}u_2'' \text{ Cos } \phi_2$$

$$-EI_{x2}v_2'' \text{ Sin } \phi_2 + Ta = M_y \tag{4.2.13}$$

$$EI_{y1}u_1'' \text{ Sin } \phi_1 + EI_{x1}v_1'' \text{ Cos } \phi_1 + EI_{y2}u_2'' \text{ Sin } \phi_2$$

$$+EI_{x2}v_2'' \text{ Cos } \phi_2 + Tb = M_x \tag{4.2.14}$$

The relations between the moment of inertia with reference to different axes (Fig. 4.2.4) are:

$$\left.\begin{aligned} S_{xj} &= I_{yj} \text{ Sin}^2 \phi_j + I_{xj} \text{ Cos}^2 \phi_j \\ S_{yj} &= I_{yj} \text{ Cos}^2 \phi_j + I_{xj} \text{ Sin}^2 \phi_j \\ S_{xyj} &= (I_{yj} - I_{xj}) \text{ Sin } \phi_j \text{ Cos } \phi_j \end{aligned}\right\} \tag{4.2.15}$$

in which $j = 1,2$

Using relations in eq. 4.2.3 and 4.2.15, the above equations are simplified as follows.

$$E\, S_y u'' + E_{xy} v'' - E\, S_{yc}\, \theta'' + Ta = M_y \tag{4.2.16}$$

$$E\, S_{xy} u'' + E\, S_x v'' + E\, S_{xc}\, \theta'' + Tb = M_x \tag{4.2.17}$$

Where

$$\left.\begin{aligned} S_y &= S_{y1} + S_{y2} \\ S_x &= S_{x1} + S_{x2} \\ S_{xy} &= S_{xy1} + S_{xy2} \\ S_{yc} &= c_{y1}\, S_{y1} + c_{y2}\, S_{y2} - c_{x1}\, S_{xy1} - c_{x2}\, S_{xy2} \\ S_{xc} &= c_{x1}\, S_{x1} + C_{x2}\, S_{x2} - c_{y1}\, S_{xy1} - c_{y2}\, S_{xy2} \end{aligned}\right\} \tag{4.2.18}$$

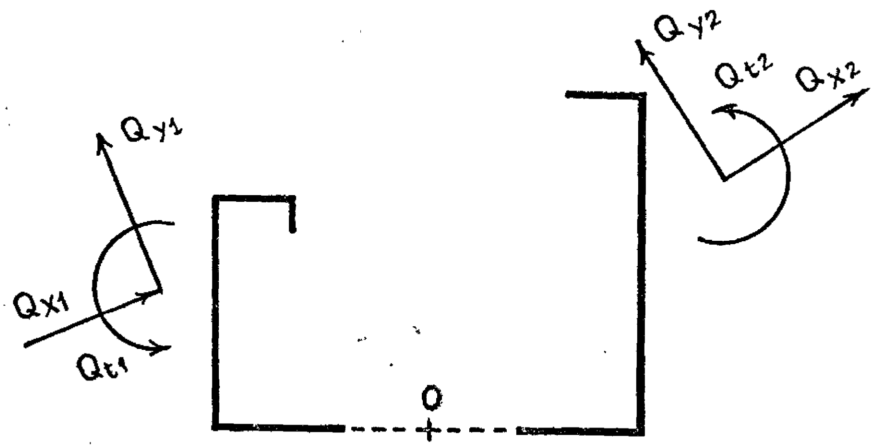

TORQUES & SHEAR FORCES DUE TO BEAM SHEAR q

FIG. 4.2.7

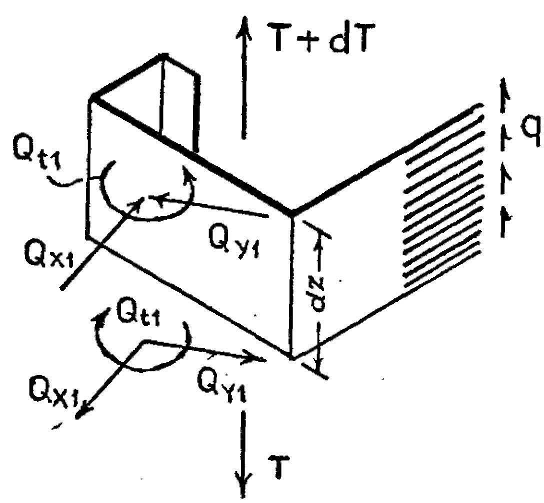

FORCES ACTING ON AN ELEMENT

FIG. 4.2.8

The internal torques and shear forces acting on different components of coupled shear wall are shown in fig. 4.2.6. Let $\overline{Q}_t$ be the resultant torque of all these forces about point O. Therefore:

$$Q_t = - EI_{x1}v_1'''q_{x1} + EI_{y1}u_1'''q_{y1} - EI_{x2}v_2'''q_{x2}$$

$$+ EI_{y2}u_2'''q_{y2} - E(I_{\omega 1} + I_{\omega 2})\theta''' + G(J_1 + J_2)\theta' \qquad (4.2.19)$$

Using relations in eq. 4.2.3 and 4.2.15 the above equation is simplified as follows:

$$\overline{Q}_t = E\,S_{yc}u''' - E\,S_{xc}v''' - EI_{\omega}\theta''' + GJ\theta' \qquad (4.2.20)$$

Where

$$\left.\begin{aligned} I_{\omega} &= I_{\omega 1} + I_{\omega 2} + c_{x1}^2\, I_{x1} + c_{x2}^2\, I_{x2} + c_{y1}^2\, I_{y1} \\ &\quad + c_{y2}^2\, I_{y2} - 2c_{x1}c_{y1}I_{xy1} - 2c_{x2}c_{y2}I_{xy2} \\ J &= J_1 + J_2 \end{aligned}\right\} \qquad (4.2.21)$$

Additional shear forces Q_{x1}, Q_{y1}, Q_{x2} and Q_{y2} and torques Q_{t1} and Q_{t2} develop in the section due to the shear force q in the laminae (Fig. 4.2.7). These forces can be expressed in terms of q from consideration of equilibrium of an element as shown in fig. 4.2.8. Thus,

$$\left.\begin{aligned} Q_{x1} &= - qp_{x1} \;; \quad Q_{y2} = - qp_{y1}; \\ Q_{x2} &= qp_{x2} \;; \quad Q_{y2} = qp_{y2} \\ Q_{t1} &= q\omega_1 \;; \quad Q_{t2} = - q\omega_2 \end{aligned}\right\} \qquad (4.2.22)$$

The resultant torque $\bar{\bar{Q}}_t$ about the point O then becomes

$$\bar{\bar{Q}}_t = Q_{t1} + Q_{t2} - Q_{x1}\, q_{y1} + Q_{y1}\, q_{x1} - Q_{x2}\, q_{y2} + Q_{y2}\, q_{x2} \qquad (4.2.23)$$

Using relations in eq. 4.2.4, eq. 4.2.5 and eq. 4.2.22, the above equation is simplified as follows:

$$\bar{\bar{Q}}_t = q(\omega+d) = -(\omega+d)\,\frac{dT}{dZ} \qquad (4.2.24)$$

Equilibrium of torque about O gives the internal torque $\bar{Q}_t$ together with torque due to shear force $\bar{\bar{Q}}_t$ must balance the external torque Q_t. Thus

$$\bar{Q}_t + \bar{\bar{Q}}_t = Q_t$$

or

$$-E\, S_{xc} v''' + E\, S_{yc} u''' - EI_{\omega}\, \theta''' + GJ\theta' - (\omega+d)\,\frac{dT}{dZ} = Q_t \qquad (4.2.25)$$

4.2.5 Differential Equations

The compatibility condition (eq. 4.2.12) and the three force equilibrium condition in eq. 4.2.16, eq. 4.2.17 and eq. 4.2.25 are four equations relating the unknown of the problem u, v, θ and T. In the following paragraphs, simplification is made to reduce the four coupled equations to a single equation in θ. From eq. 4.2.16 and 4.2.17 the following expressions are obtained by algebraic elimination.

$$u'' = C_1\theta'' + C_2\, T + C_3\, M_y + C_4\, M_x \qquad (4.2.26)$$

$$v'' = C_5\theta'' + C_6\, T + C_7\, M_y + C_8\, M_x \qquad (4.2.27)$$

Where

$$\left.\begin{aligned}
SS_{xy} &= S_x\ S_y - S_{xy}^2\ ; \\
C_1 &= (S_{xy}\ S_{xc} + S_x\ S_{yc})/SS_{xy}; \\
C_2 &= -(a\ S_x - b\ S_{xy})/E\ SS_{xy}; \\
C_3 &= S_x/E\ SS_{xy}\ ;\ C_4 = -\ S_{xy}/E\ SS_{xy}; \\
C_5 &= -(S_y\ S_{xc} + S_{xy}\ S_{yc})/SS_{xy}; \\
C_6 &= -(b\ S_y - a\ S_{xy})/E\ SS_{xy}; \\
C_7 &= -\ S_{xy}/E\ SS_{xy};\quad C_8 = Sy/E\ SS_{xy}
\end{aligned}\right\} \qquad (4.2.28)$$

Differenciating eq. 4.2.26 and eq. 4.2.27 and substituting in eq. 4.2.25,

$$-q = \frac{dT}{dZ} = -\ \frac{E\overline{I}_\omega}{r_1}\ \theta''' + \frac{GJ}{r_1}\ \theta' + C_9\ M_y' + C_{10}\ M_x' + C_{11}\ Q_t \qquad (4.2.29)$$

Where

$$\overline{I}_\omega = I_\omega - (S_y\ S_{xc}^2 + S_x\ S_{xc}^2)/SS_{xy}$$

$$r_1 = \omega + d - S_{xc}(b\ S_y - a\ S_{xy})/SS_{xy}$$

$$+\ S_{yc}\ (a\ S_x - b\ S_{xy})/SS_{xy}$$

$$C_9 = (S_{xy}\ S_{xc} + S_x\ S_{yc})/SS_{xy}\ r_1$$

$$C_{10} = -(S_y\ S_{xc} + S_{xy}\ S_{yc})/SS_{xy}\ r_1$$

$$C_{11} = -\ 1/r_1$$

Substituting eq. 4.2.26 and eq. 4.2.27 in eq. 4.2.12,

$$Er_2\ \theta'' - \frac{1}{A}\ T + C_{12}\ M_y + C_{13}\ M_x + \gamma\ \frac{d^2T}{dZ^2} = 0 \qquad (4.2.30)$$

Where

$$r_2 = \omega + d + a(S_{xy}\ S_{xc} + S_x S_{yc})/SS_{xy}$$

$$-b(S_y\ S_{xc} + S_{xy}\ S_{yc})/SS_{xy}$$

$$1/A = 1/A_1 + 1/A_2 + a(a\ S_x - b\ S_{xy})/SS_{xy} + + b(b\ S_y - a\ S_{xy})/SS_{xy}$$

$$\begin{aligned} C_{12} &= (a\ S_x - b\ S_{xy})/SS_{xy} \\ C_{13} &= (b\ S_y - a\ S_{xy})/SS_{xy} \\ \gamma &= c^3/12J_b \end{aligned} \qquad (4.2.31)$$

Differentiating eq. 4.2.31 once

$$E\Gamma_2\theta''' - \frac{1}{A}\frac{dT}{dZ} + C_{12}\ M'_y + C_{13}\ M'_x + \gamma\frac{d^3T}{dZ^3} = 0 \qquad (4.2.32)$$

Eliminating $\frac{dT}{dZ}$ and $\frac{d^3T}{dZ^3}$ using eq. 4.2.29 the following fifth order differential equation in θ is obtained.

$$\beta_1\theta^V - \beta_2\theta''' + \beta_3\ \theta' = C_{14}\ M'_y + C_{15}\ M'_x + C_9\ M'''_y + C_{10}\ M'''_x + C_{16}\ Q_t - Q''_t \qquad (4.2.33)$$

Where

$$\left.\begin{aligned} \beta_1 &= E\overline{I}_\omega \\ \beta_2 &= \frac{EI_\omega}{A\gamma} + GJ + \frac{E\Gamma_1\Gamma_2}{\gamma} \\ \beta_3 &= GJ/A\gamma\ ;\ C_{16} = 1/A\gamma \\ C_{14} &= \frac{C_{12}\Gamma_1}{\gamma} - \frac{C_9}{A\gamma} \\ C_{15} &= \frac{C_{13}\Gamma_1}{\gamma} - \frac{C_{10}}{\gamma} \end{aligned}\right\} \qquad (4.2.34)$$

The Eq. 4.2.33 along with eq. 4.2.26, eq. 4.2.27 and eq. 4.2.29 are the final equations used in the analysis.

4.2.5 Boundary Conditions

For no rotation and displacement at base

$$\theta(0) = 0 \tag{4.2.41(a)}$$

$$u(0) = 0 \tag{4.2.41(b)}$$

$$v(0) = 0 \tag{4.2.41(c)}$$

For no slope and warping at base

$$\theta'(0) = 0 \tag{4.2.42(a)}$$

$$u'(0) = 0 \tag{4.2.42(b)}$$

$$v'(0) = 0 \tag{4.2.42(c)}$$

For no moment and bi moment at top

$$\theta''(H) = 0 \tag{4.2.43(a)}$$

$$u''(H) = 0 \tag{4.2.43(b)}$$

$$v''(H) = 0 \tag{4.2.43(c)}$$

Substituting eq. 4.2.42 in eq. 4.2.12a the following condition is obtained at Z = 0.

$$q(0) = - \left.\frac{dT}{dZ}\right|_{Z=0} = 0$$

Using eq. 4.2.29

$$\underline{\left(\frac{E\bar{I}_{\omega}}{r_1}\theta''' - \frac{GJ}{r_1}\theta' - C_9 M_y' - C_{10} M_x' - C_{11} Q_t\right)}\Bigg|_{Z=0} = 0 \tag{4.2.44}$$

Axial force T can be expressed in terms of q by the following relation

$$T = \int_{Z}^{H} q(\xi)\, d\xi \tag{4.2.45}$$

From which at Z = H, T = 0 (4.2.46)

Substituting eq. 4.2.43 and 4.2.46 in eq. 4.2.12

$$\left.\frac{dq}{dZ}\right|_{Z=H} = - \left.\frac{d^2T}{dZ^2}\right|_{Z=H} = 0 \tag{4.2.47}$$

Differentiating expression in eq. 4.2.29 and using in eq. 4.2.47

$$\left(\frac{E\bar{I}_\omega}{r_1}\theta^{IV} - \frac{GJ}{r_1}\theta'' - C_9 M_y'' - C_{10} M_x'' - C_{11} Q_t'\right)\Bigg|_{x=H} = 0 \tag{4.2.48}$$

The solution of the differential equation subjected to the above boundary conditions are the complete solution to the problem.

4.2.7 Solution

The solution of the differential equation (eq. 4.2.33) will consist the complimentary solution θ_C and a particular integral θ_P. Thus

$$\theta = \theta_C + \theta_P$$

The complimentary part θ_C will satisfy the following equation

$$\beta_1 \theta^V - \beta_2 \theta''' + \beta_3 \theta' = 0 \tag{4.2.50}$$

Assuming solution of the form $\theta_C = Ke^{mZ}$ the following characteristic equation is obtained.

$$\beta_1 m^5 - \beta_2 m^3 + \beta_3 m = 0 \tag{4.2.51}$$

The roots are: $m_1 = 0$

$$m_2, m_3 = \pm\sqrt{\frac{\beta_2 + \sqrt{\beta_2^2 - 4\beta_1\beta_3}}{2\beta_1}}$$

$$m_4,\ m_5 = \pm\sqrt{\frac{\beta_2 - \sqrt{\beta_2^2 - 4\beta_1\beta_3}}{2\beta_1}}$$

In the above expressions β_1, β_2 and β_3 are positive. It can be shown that

$$\beta_2^2 > 4\beta_1\beta_3$$

Therefore all roots are real.

Defining

$$\alpha_1 = |m_2| = |m_3|$$
$$\alpha_2 = |m_4| = |m_5|$$

The solution is of the following form.

$$\theta_C = \kappa_1 + \kappa_2 \operatorname{Cosh}\alpha_1 Z + \kappa_3 \operatorname{Sinh}\alpha_1 Z + \kappa_4 \operatorname{Cosh}\alpha_2 Z + \kappa_5 \operatorname{Sinh}\alpha_2 Z \qquad (4.2.52)$$

The particular integral θ_P depends on loading.

Case-I, Concentrated load W_x, W_y and torque W_t at top. The loads are acting in the +ve directions and refered to the center line of beams. For such loading

$$M_y = W_x(H-Z)$$
$$M_x = W_y(H-Z)$$
$$Q_t = W_t$$

Particular integral for this case is:

$$\theta_P = K_P\, Z$$

Where

$$K_p = -(C_{14} W_x + C_{15} W_y - C_{16} W_t) \qquad (4.2.53)$$

Case-II, Uniformly distributed load w_x, w_y and torque w_t acting though out the height. The loads are acting in the positive directions and refered to the center line of beams. For such loading:

$$M_y = w_x (H-Z)^2/2$$
$$M_x = w_y (H-Z)^2/2$$
$$Q_t = w_t \, Z$$

Particular integral for this case is:

$$\theta_p = K_{p1} Z^2 + K_{p2} Z$$

Where

$$K_{p1} = (C_{14} w_x + C_{15} w_y - C_{16} w_t)/2\beta_3$$
$$K_{p2} = -H(C_{14} w_x + C_{15} w_y - C_{16} w_t)/\beta_3 \qquad (4.2.54)$$

The constants κ_1, κ_2, κ_3, κ_4, κ_5 (eq. 4.2.52) are determined from the boundary condition in eq. 4.2.41(a), eq. 4.2.42(a), eq. 4.2.43(a), eq. 4.2.44 and eq. 4.2.48.

After obtaining complete solution for θ, the expression for shear force q is determined from eq. 4.2.29. The expression for axial force T is determined from direct integration of the expression for q subjected to boundary condition as in eq. 4.2.46.

The expression of displacements u and v are determined from direct integration of the expressions in eq. 4.2.26 and eq. 4.2.27 subjected to boundary condition as in eq. 4.2.41(b), eq. 4.2.41(c), eq. 4.2.42(b) and eq. 4.2.42(c).

The displacement of the individual piers u_j, v_j and θ_j (where j = 1,2) are determined from the relation in eq. 4.2.3. The average moment and bimoment of the indivdual piers are determined from the following relations.

$$M_{yj} = EI_{yj}\, u_j'' ,\quad M_{xj} = EI_{xj} v''$$

$$B_j = - EI_{\omega j}\, \theta_j'' \tag{4.2.55}$$

where j = 1,2

4.2.8 Special Configurations

For a mono symmetric configuration of piers as shown in Case-A (fig. 4.2.11) b = 0; $S_{xy} = 0$; $S_{xc} = 0$. Substituting these conditions in the governing equations (eq. 4.2.12, eq. 4.2.16, eq. 4.2.17 and eq. 4.2.25) they are reduced to

$$u''a + \theta''(\omega + d) = \frac{1}{E}\left(\frac{1}{A_1} + \frac{1}{A_2}\right)T + \frac{c^3}{12J_bE}\frac{dq}{dZ} \tag{4.2.56}$$

$$E\,S_y u'' + E\,S_{yc}\,\theta'' + Ta = M_y \tag{4.2.57}$$

$$E\,S_x v'' = M_x \tag{4.2.58}$$

$$E\,S_{yc} u''' - EI_\omega\,\theta''' + GJ\theta' - (\omega + d)\frac{dT}{dZ} = Q_t \tag{4.2.59}$$

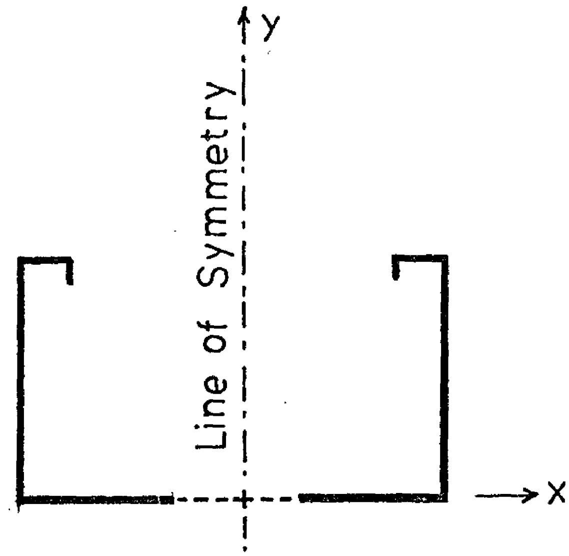

$b = 0$
$S_{xy} = 0$
$S_{xc} = 0$

CASE - A

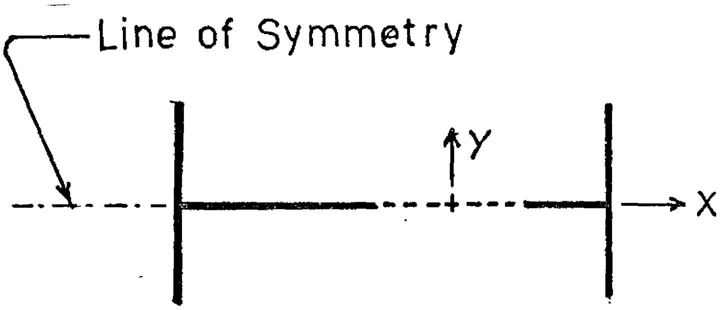

$b = 0$
$S_{xy} = 0$
$S_{yc} = 0$
$\omega + d = 0$
$I_{\omega 1} = I_{\omega 2} = 0$

CASE - B

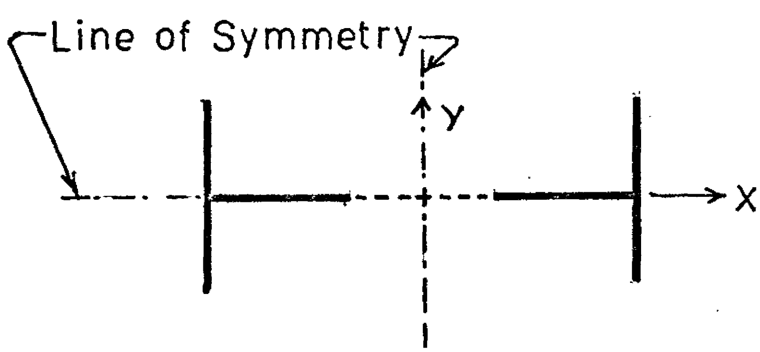

$b = 0$
$S_{xy} = 0$
$S_{xc} = 0$
$S_{yc} = 0$
$\omega + d = 0$
$I_{\omega 1} = I_{\omega 2} = 0$

CASE - C

FIG. 4.2.11

The eq. 4.2.58 is uncoupled and represents independent bending of the structure about the X axis. The other equations can be combined in a single differential equation in θ and solved following the same scheme as before.

For a mono symmetric configuration of piers as in Case-B (fig. 4.2.11) $b = 0$, $S_{xy} = 0$, $S_{xc} = 0$; $(\omega+d) = 0$. Substituting these conditions the governing equations (eq. 4.2.12, eq. 4.2.16, eq. 4.2.17 and eq. 4.2.25) they are reduced to.

$$u''a = \frac{1}{E}\left(\frac{1}{A_1} + \frac{1}{A_2}\right)T + \frac{c^3}{12EJ_b}\frac{dq}{dz} \tag{4.2.60}$$

$$E\,S_y\,u'' + T\,a = M_y \tag{4.2.61}$$

$$E\,S_x\,v''' + E\,S_{xc}\,\theta'' = M_x \tag{4.2.62}$$

$$-E\,S_{xc}\,v''' - EI_\omega\,\theta''' + GJ\,\theta' = Q_t \tag{4.2.63}$$

In the above equations u and T are coupled in the first two equations. In the last two equations v and θ are coupled but independent of u and T. The first two equations (eq. 4.2.60 and eq. 4.2.61) represent plane coupled case for bending about y axis but the bending about x axis and rotation are coupled in the other two equations.

For a symmetric configuration of piers as shown in Case-C (fig. 4.2.11) $b = 0$, $I_{xy} = 0$, $I_{xc} = 0$; $I_{yc} = 0$; $(\omega+d) = 0$. Substituting these conditions in the governing equations (eq. 4.2.12, eq. 4.2.16, eq. 4.2.17 and eq. 4.2.25), they are reduced to:

$$u'' a = \frac{1}{E}\left(\frac{1}{A_1} + \frac{1}{A_2}\right)T + \frac{c^3}{12EJ_b}\frac{dq}{dz} \tag{4.2.64}$$

$$E S_{yc} u'' + T a = M_y \tag{4.2.65}$$

$$E S_x v'' = M_x \tag{4.2.66}$$

$$-EI_\omega\theta''' + GJ\theta' = Q_t \tag{4.2.67}$$

The first two equations (eq. 4.2.64 and eq. 4.2.65) represent the plane coupled case for bending about y axis. The other two equations (eq. 4.2.66 and eq. 4.2.67) are uncoupled representing independent rotation and bending about x axis. It should be noted that though the individual piers do not have any sectorial moment of inertia, the group has an equivalent I_ω as defined in eq. 4.2.21. In this case

$$I_\omega = C_{x1}^2 I_{x1} + C_{x2}^2 I_{x2} \tag{4.2.68}$$

Therefore, the torsional resistance of the combined structure is substantially larger than the sum of individual resistance.

4.2.9 Effect of Neglecting Axial Deformation of Piers

Gluck (22) assumed the axial deformation of piers to be very small and neglected it in his analysis. It is of interest to indicate the present analysis is reducible to the equation given by Gluck.

If axial deformation of piers is neglected, $\delta_2 = 0$ (eq. 4.2.9). For which the compatibility equation (eq. 4.2.12a) is reduced to,

$$u' \, a + v' \, b + \theta' \, (\omega + d) = \frac{c^3}{12 E J_b} q \qquad (4.2.69)$$

Differentiating eq. 4.2.16 and eq. 4.2.17 and using eq. 4.2.8

$$E \, S_y \, u''' + S_{xy} \, v''' - E \, S_{yc} \, \theta''' - aq = M_y' \qquad (4.2.70)$$

$$E \, S_{xy} \, u''' + E \, S_x \, v''' + E \, S_{xc} \, \theta''' - bq = M_x' \qquad (4.2.71)$$

Using eq. 4.2.8, eq. 4.2.25 becomes

$$-E \, S_{xc} \, v''' + E \, S_{yc} \, u''' - EI_\omega \theta''' + GJ\theta' + (\omega + d) q = Q_t \qquad (4.2.72)$$

Eliminating eq. q from eq. 4.2.70, eq. 4.2.71 and eq. 4.2.72 by the help of eq. 4.2.69 and expressing in matrix form:

$$- \begin{bmatrix} E \, S_y & E \, S_{xy} & -E \, S_{yc} \\ E \, S_{xy} & E \, S_x & E \, S_{xc} \\ -E \, S_{yc} & E \, S_{xc} & E \, I_\omega \end{bmatrix} \begin{Bmatrix} u''' \\ v''' \\ \theta''' \end{Bmatrix}$$

$$+ \begin{bmatrix} 0 & 0 & 0 \\ 0 & 0 & 0 \\ 0 & 0 & GJ \end{bmatrix} \begin{Bmatrix} u' \\ v' \\ \theta' \end{Bmatrix}$$

$$+ \frac{12EJ_b}{c^3} \begin{bmatrix} a^2 & ab & a(\omega+d) \\ ab & b^2 & b(\omega+d) \\ a(\omega+d) & b(\omega+d) & (\omega+d)^2 \end{bmatrix} \begin{Bmatrix} u' \\ v' \\ \theta' \end{Bmatrix} = \begin{Bmatrix} -M'_y \\ -M'_x \\ Q_t \end{Bmatrix} \quad (4.2.73)$$

This equation is same as Gluck (22) except the factor d which is omitted. The error has been noted and suggested by Biswas and Tso (24).

4.3 Computer Program

A computer program based on the analysis has been written. This program covers the general configuration and the special configuration in Case-A (Fig. 4.2.11). subjected to concentrated force and/or torque at top. The input data are the geometric and elastic properties of the shear wall. The program determines the value of constants $\kappa_1, \kappa_2, \ldots \kappa_5$ (eq. 4.2.52) by solving a set of linear simultaneous equation obtained from the boundary conditions. The output consists of the generalised displacement of reference point O, shear force in the connecting beams and bending moment of the individual piers at chosen levels. The computer program is included in Appendix B.

4.4 Experiment

An experiment was done on a small scale model (fig. 4.4.1). It consisted of two equal angles connected by floor beams at equal spacing. The model was made from plexiglas sheet. It was loaded by a concentrated force at the top by hanging weights over a pulley system (Fig. 4.4.2). A

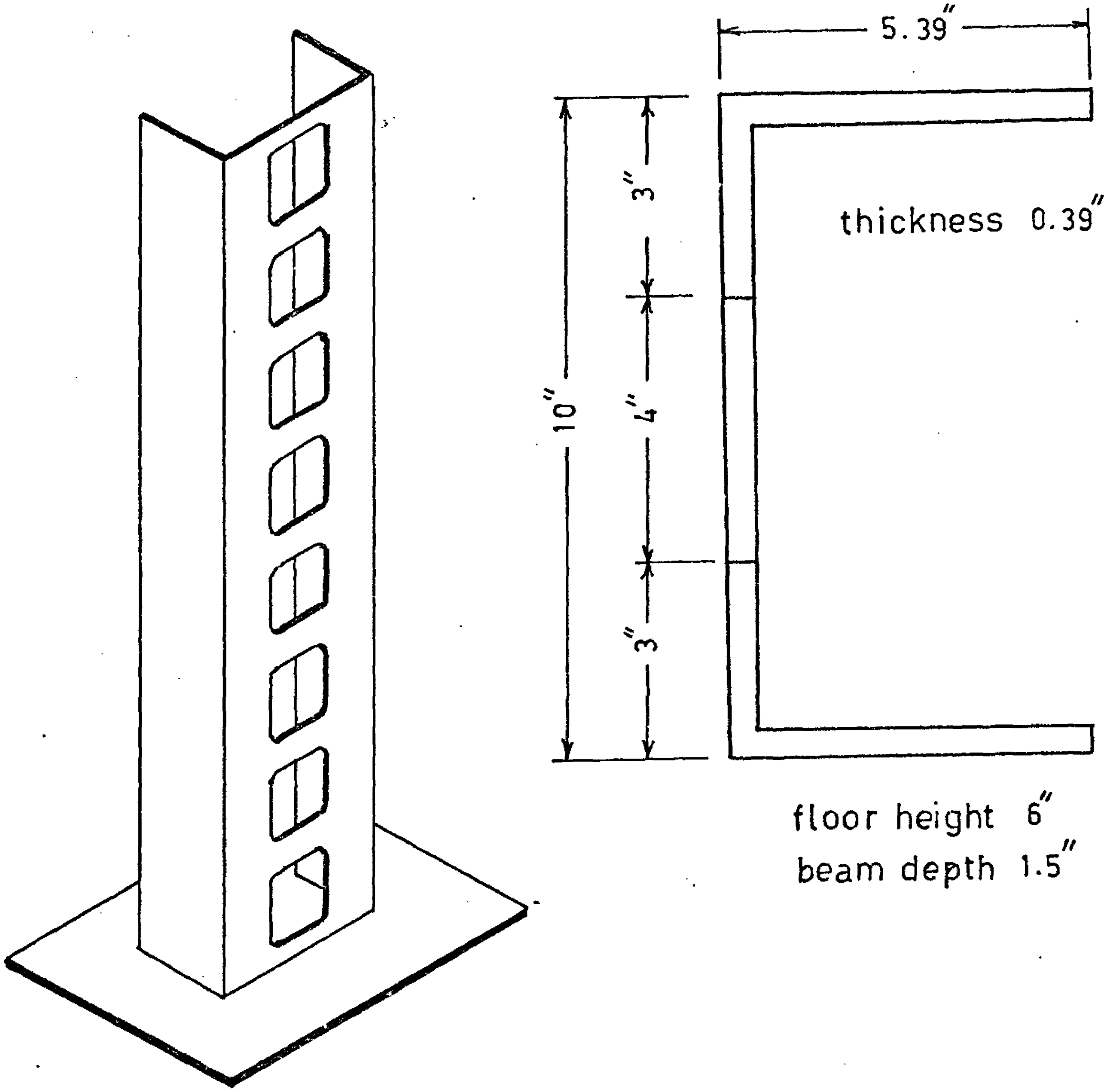

TEST MODEL

FIG. 4.4.1

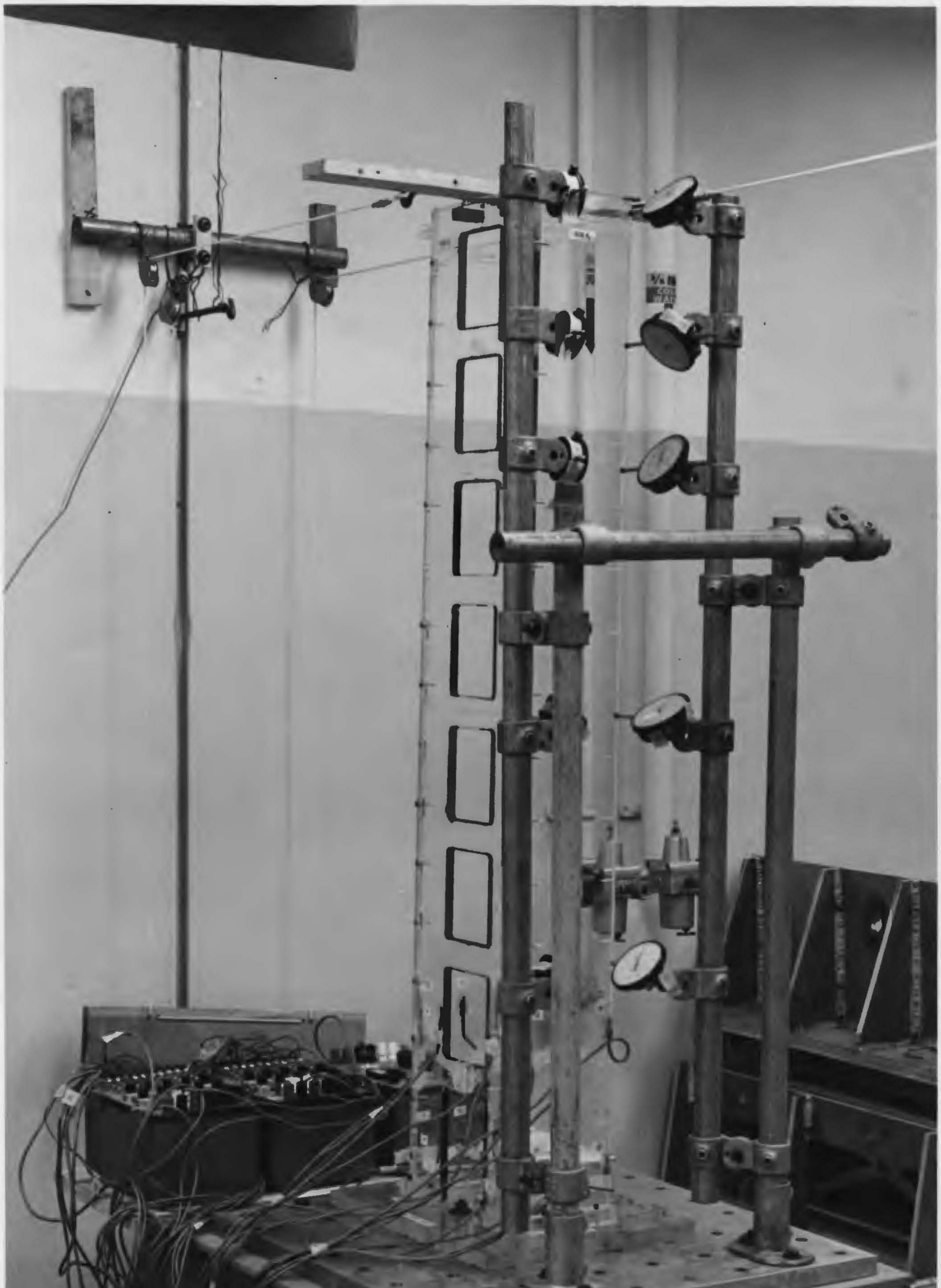

Fig. 4.4.2

EXPERIMENTAL SET UP

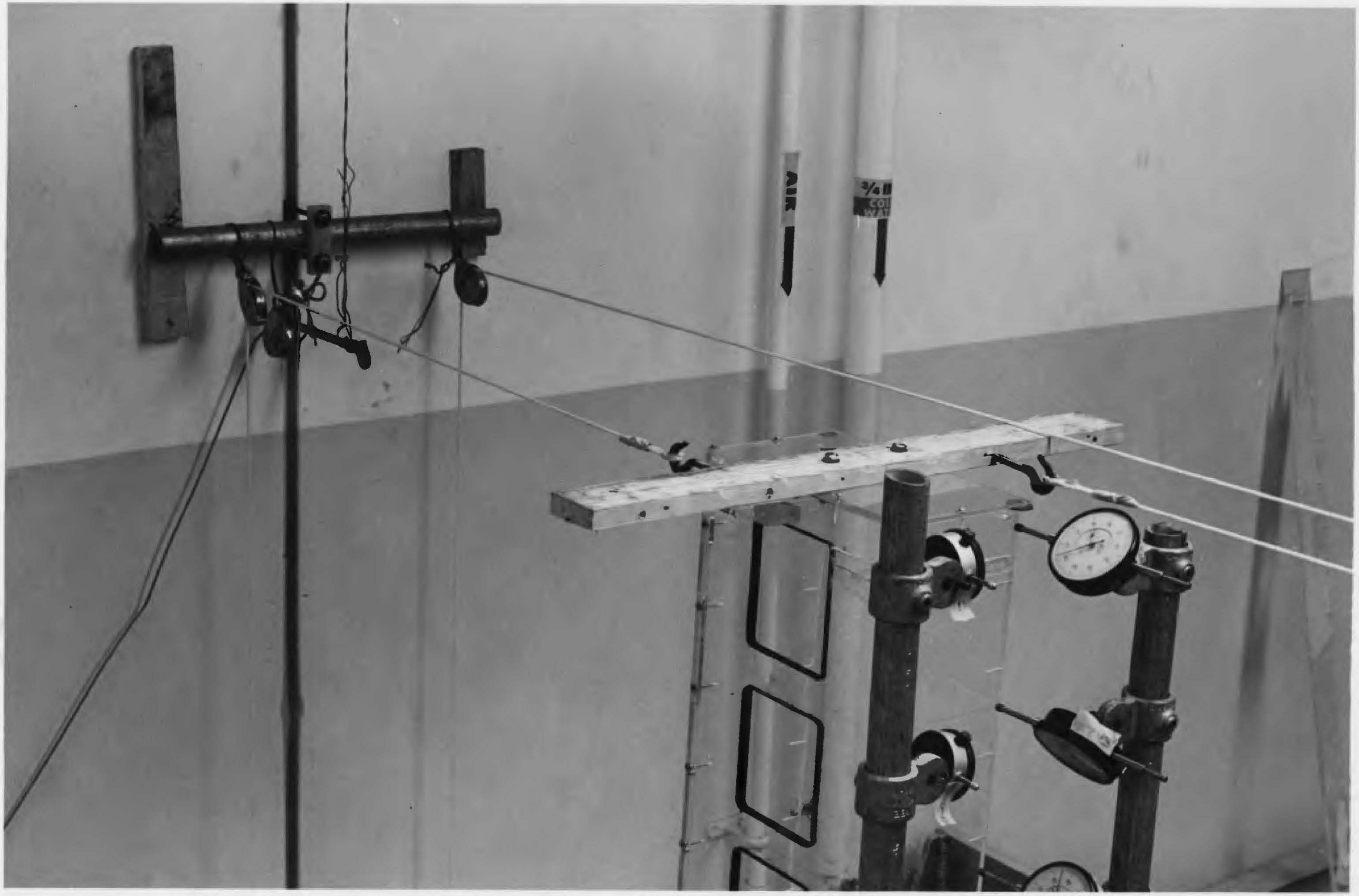

Fig. 4.4.3

TORQUE APPLYING DEVICE

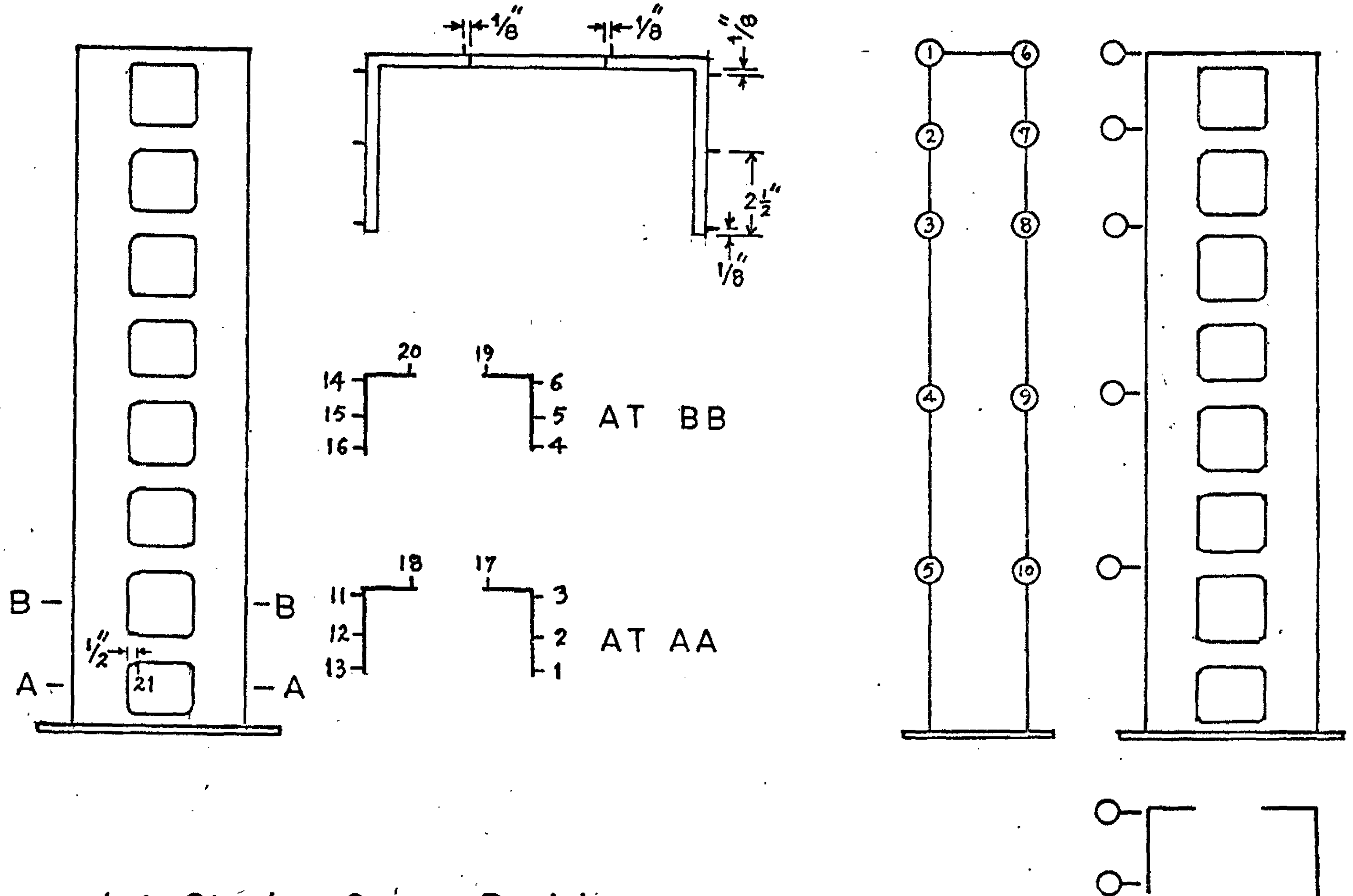

(a) Strain Gauge Positions

(b) Dial Gauge Positions

FIG. 4.4.4

second loading configuration consists of a torque applied at top of the same structure. This was done by applying two equal but opposite forces as shown in fig. 4.4.3. Strain gauges and dial gauges were fixed at different points of the model (Fig. 4.4.4) and readings were taken at every increment of loading. Strain gauge and dial gauge readings are tabulated in Appendix-C. The same set of instruments used for static test of model with floor (Chapter 2) was used.

4.5 Results and Discussion

The linearity of the test structure is checked in fig. 4.8.10.. The rotation and displacement of the model subjected to concentrated load and torque at top are plotted in fig. 4.5.1 to fig. 4.5.4. The moment in pier 1 in the principal directions and distributed shear force q in the connecting beam are plotted in fig. 4.5.5. From the moment diagram, the theoretical strains at different points in level AA and BB (Fig. 4.4.4) are determined. The strain distribution thus obtained together with the experimental strains are plotted in Fig. 4.5.6 to 4.5.9.

The experimental results of rotation and displacement compared reasonably well with the theory except for the case of displacement measured due to an applied torque as shown in fig. 4.5.3. The probable reason for difference in fig. 4.5.3 may be due to the imperfection of the torque applying device. It is conceivable that some lateral load may develop in addition to the applied torque during the test.

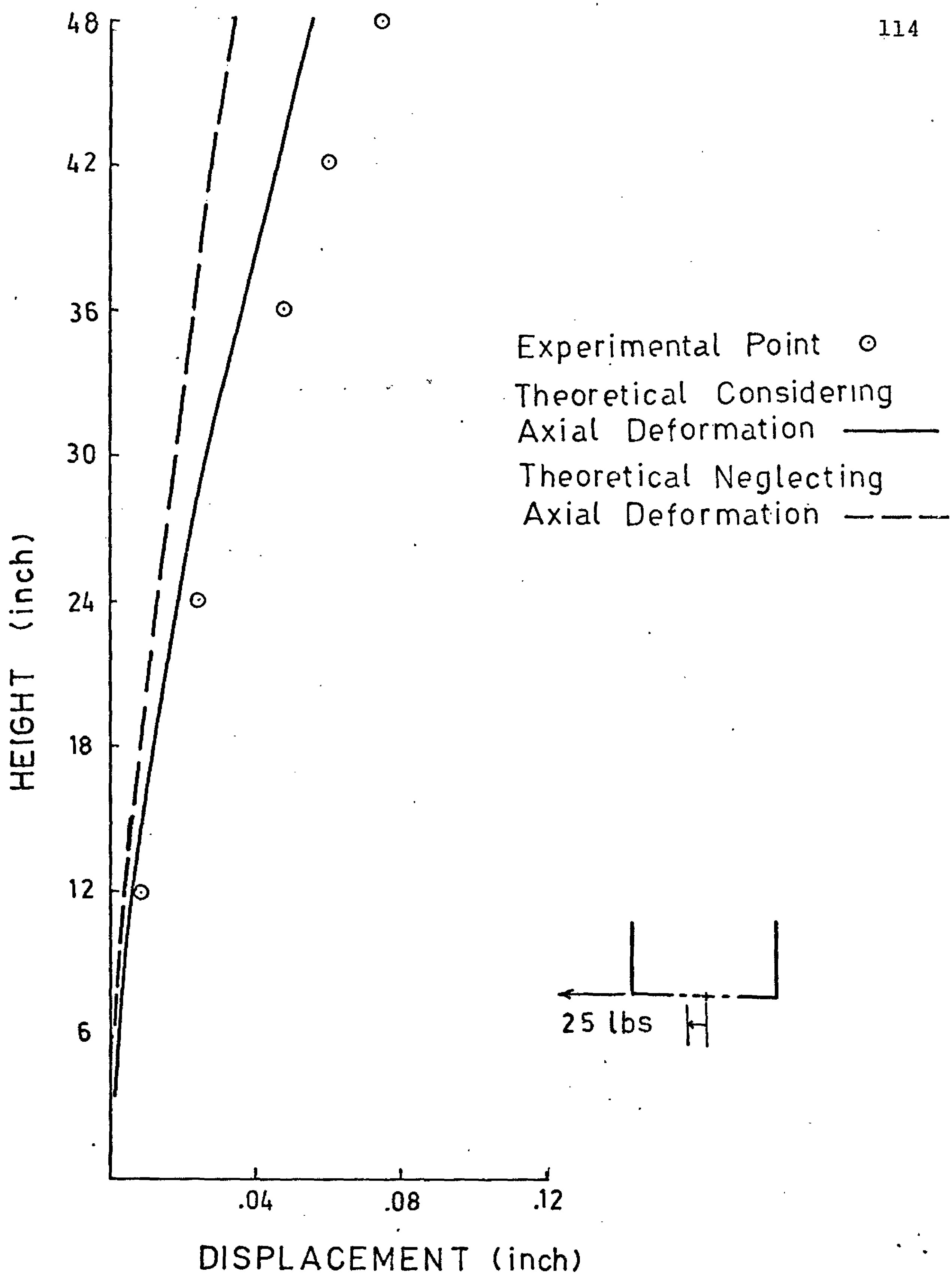
48
42
36
30
24
18
12
6
HEIGHT (inch)
.04
.08
.12
DISPLACEMENT (inch)
Experimental Point
Theoretical Considering Axial Deformation
Theoretical Neglecting Axial Deformation
25 lbs

FIG. 4.5.1

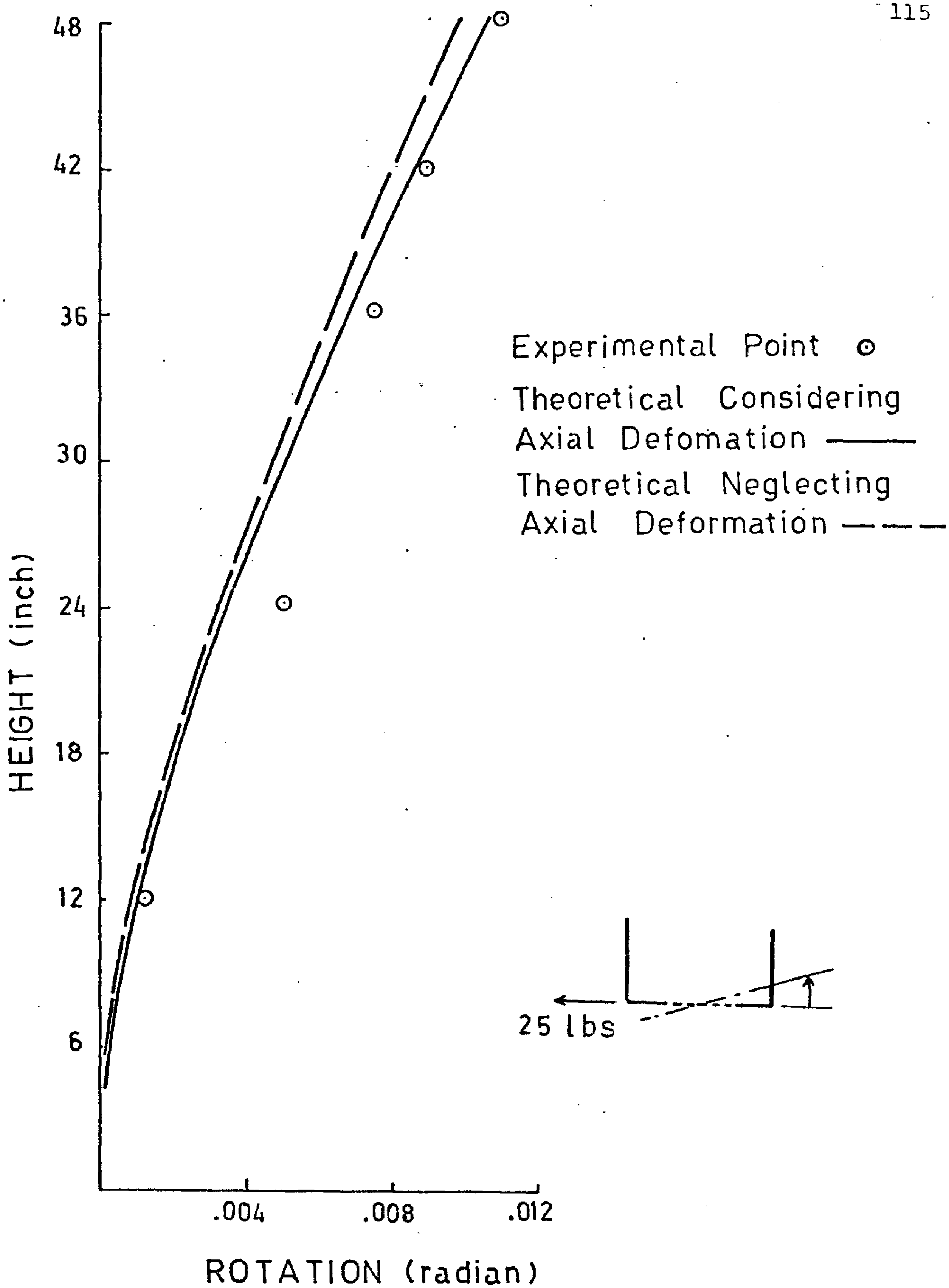

48
42
36
30
24
18
12
6
HEIGHT (inch)
.004
.008
.012
ROTATION (radian)
Experimental Point
Theoretical Considering
Axial Defomation
Theoretical Neglecting
Axial Deformation
25 lbs

FIG. 4.5.2

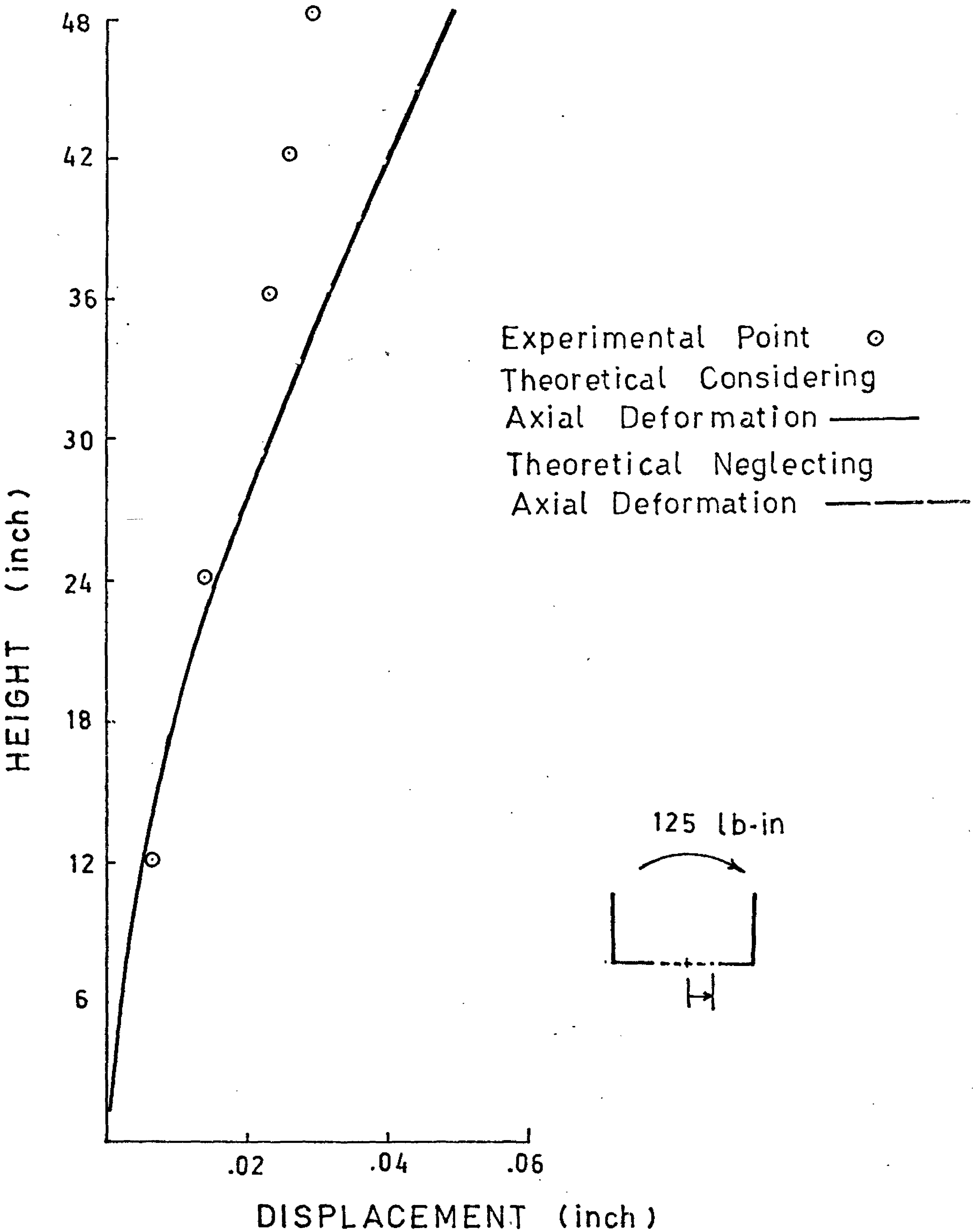
48
42
36
30
24
18
12
6
HEIGHT (inch)
.02
.04
.06
DISPLACEMENT (inch)
Experimental Point
Theoretical Considering Axial Deformation
Theoretical Neglecting Axial Deformation
125 lb-in

FIG. 4.5.3

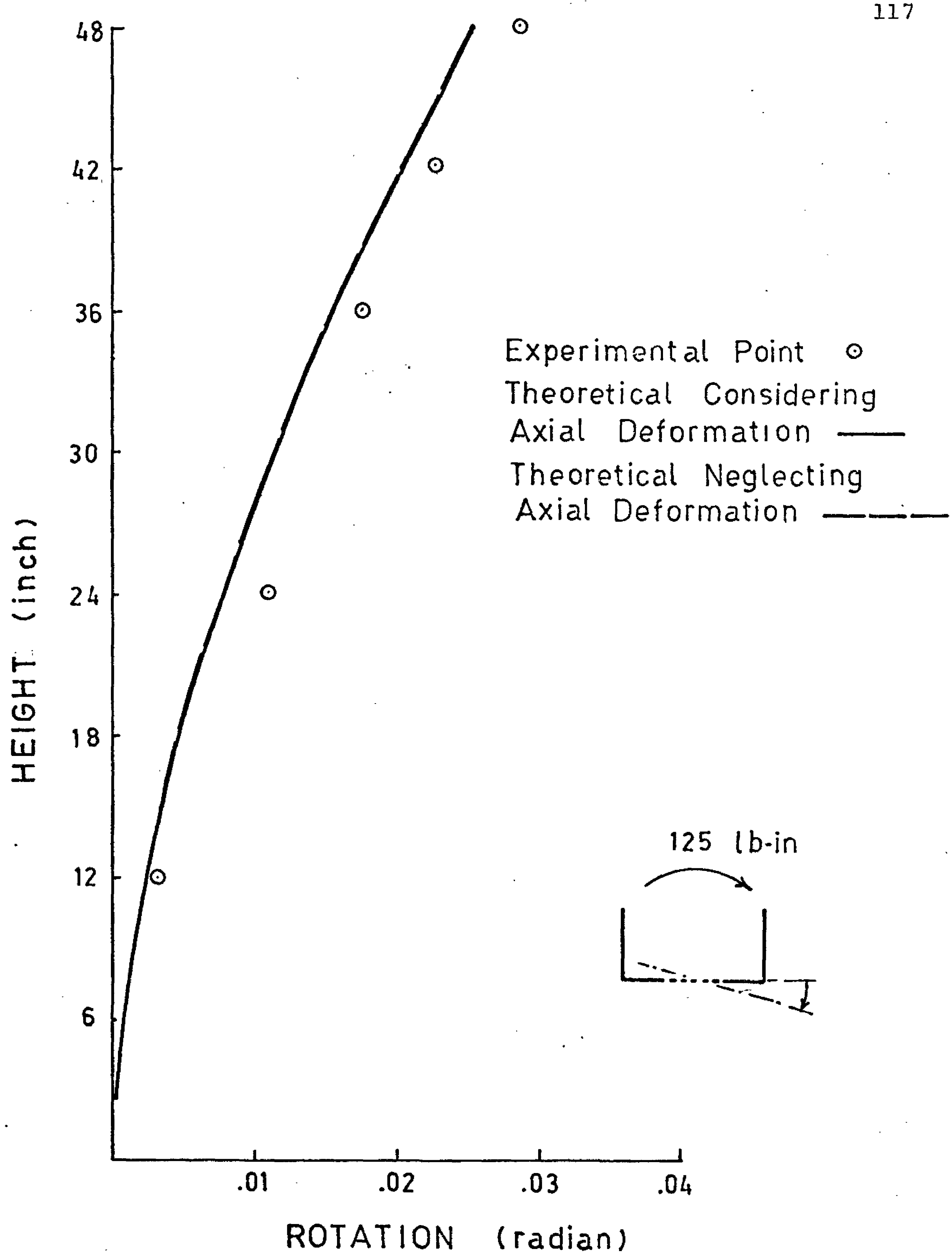

48
42
36
30
24
18
12
6
HEIGHT (inch)
.01
.02
.03
.04
ROTATION (radian)
Experimental Point
Theoretical Considering Axial Deformation
Theoretical Neglecting Axial Deformation
125 lb-in

FIG. 4.5.4

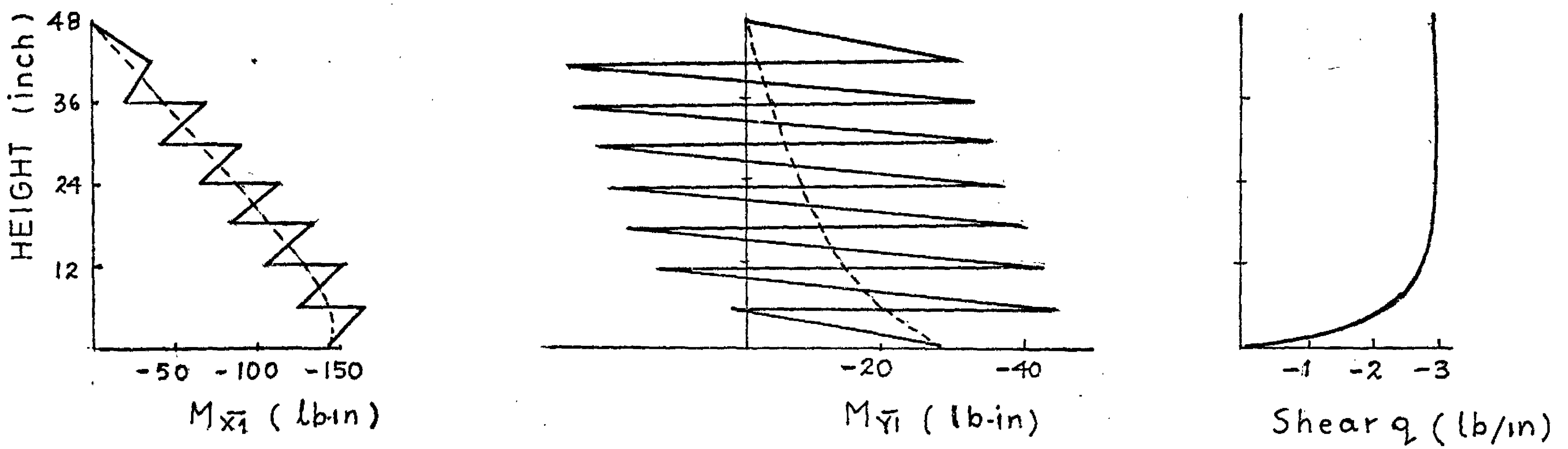

DUE TO CONCENTRATED FORCE 25 lbs AT TOP

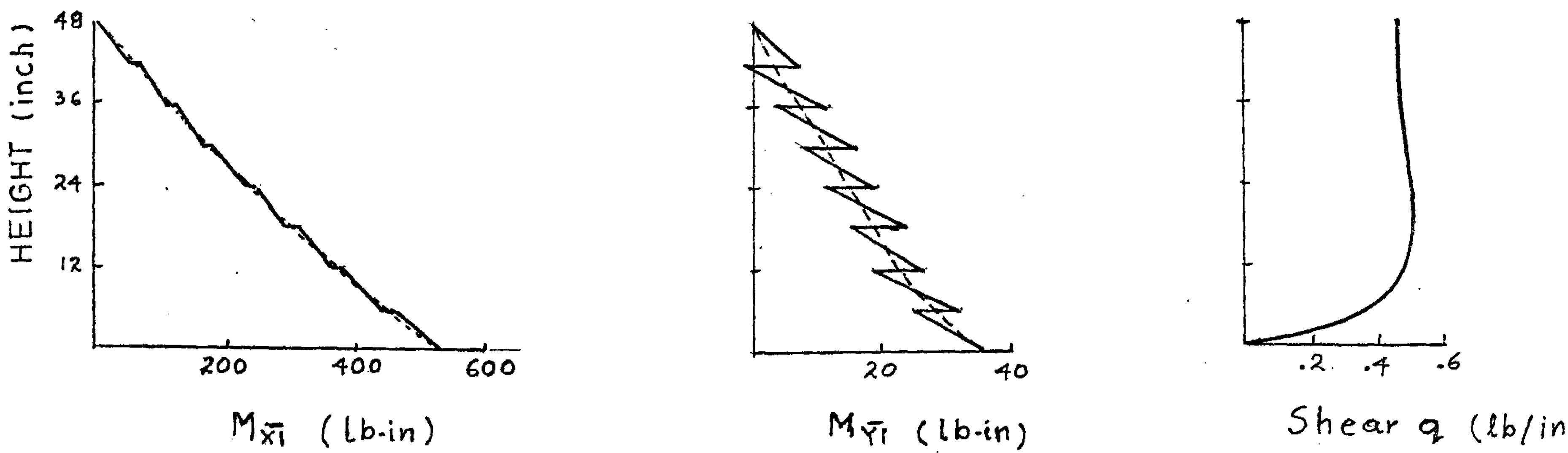

DUE TO CONCENTRATED TORQUE 125 lb-in AT TOP

FIG. 4.5.5

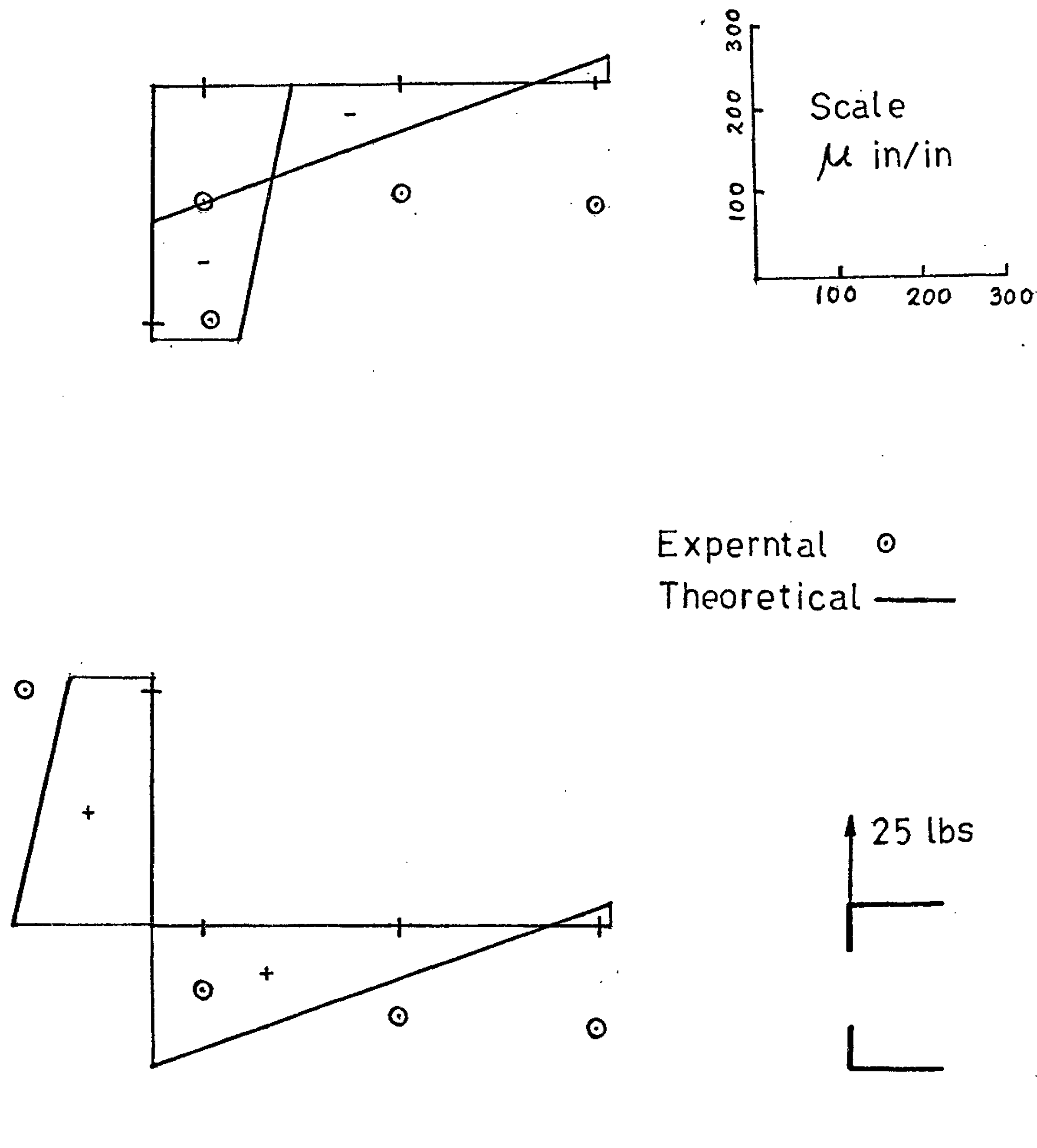

STRAIN DISTRIBUTION AT LEVEL AA

FIG. 4.5.6

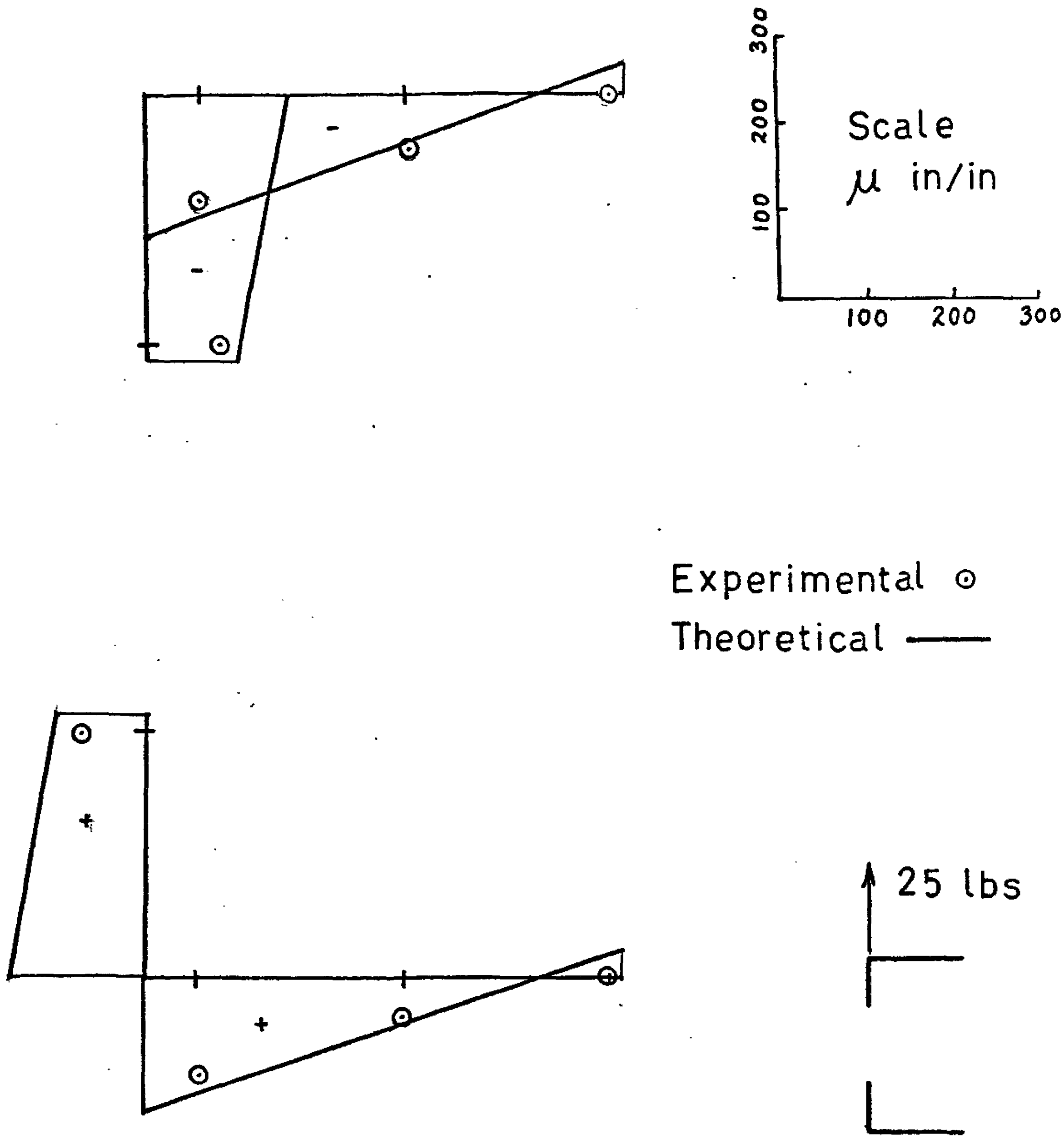

STRAIN DISTRIBUTION AT LEVEL BB

FIG. 4.5.7

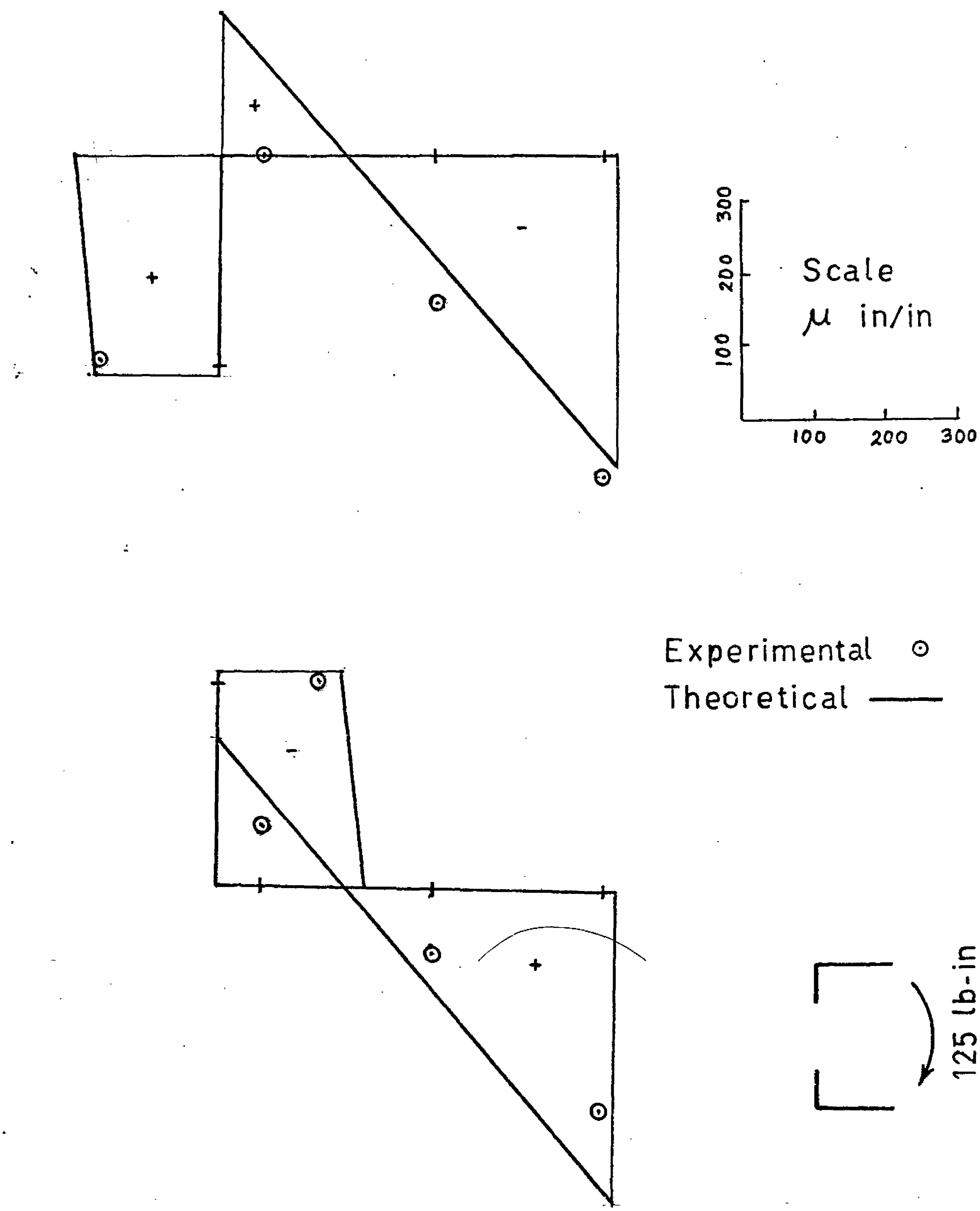

STRAIN DISTRIBUTION AT LEVEL AA

FIG. 4.5.8

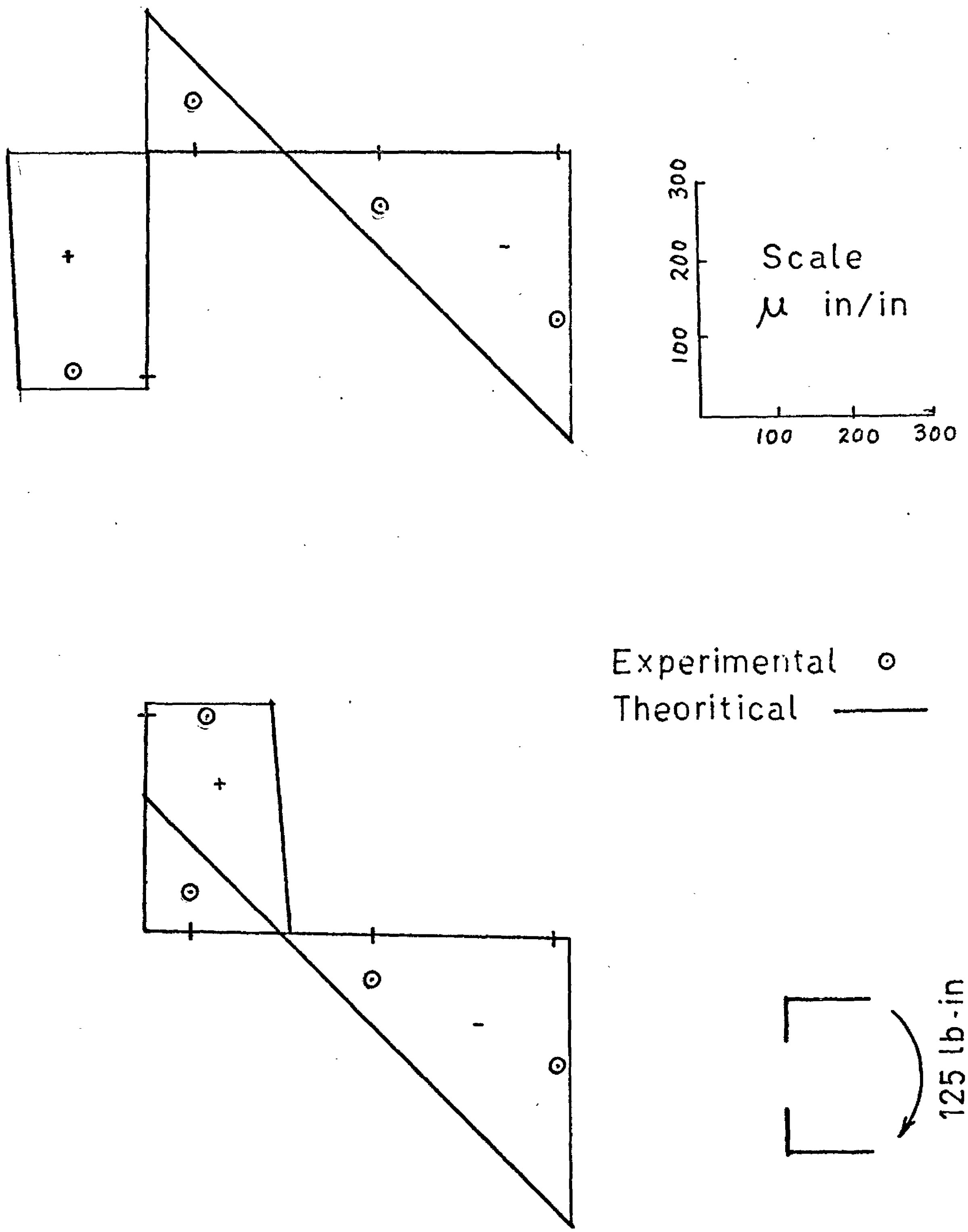

STRAIN DISTRIBUTION AT LEVEL BB

FIG. 4.8.9

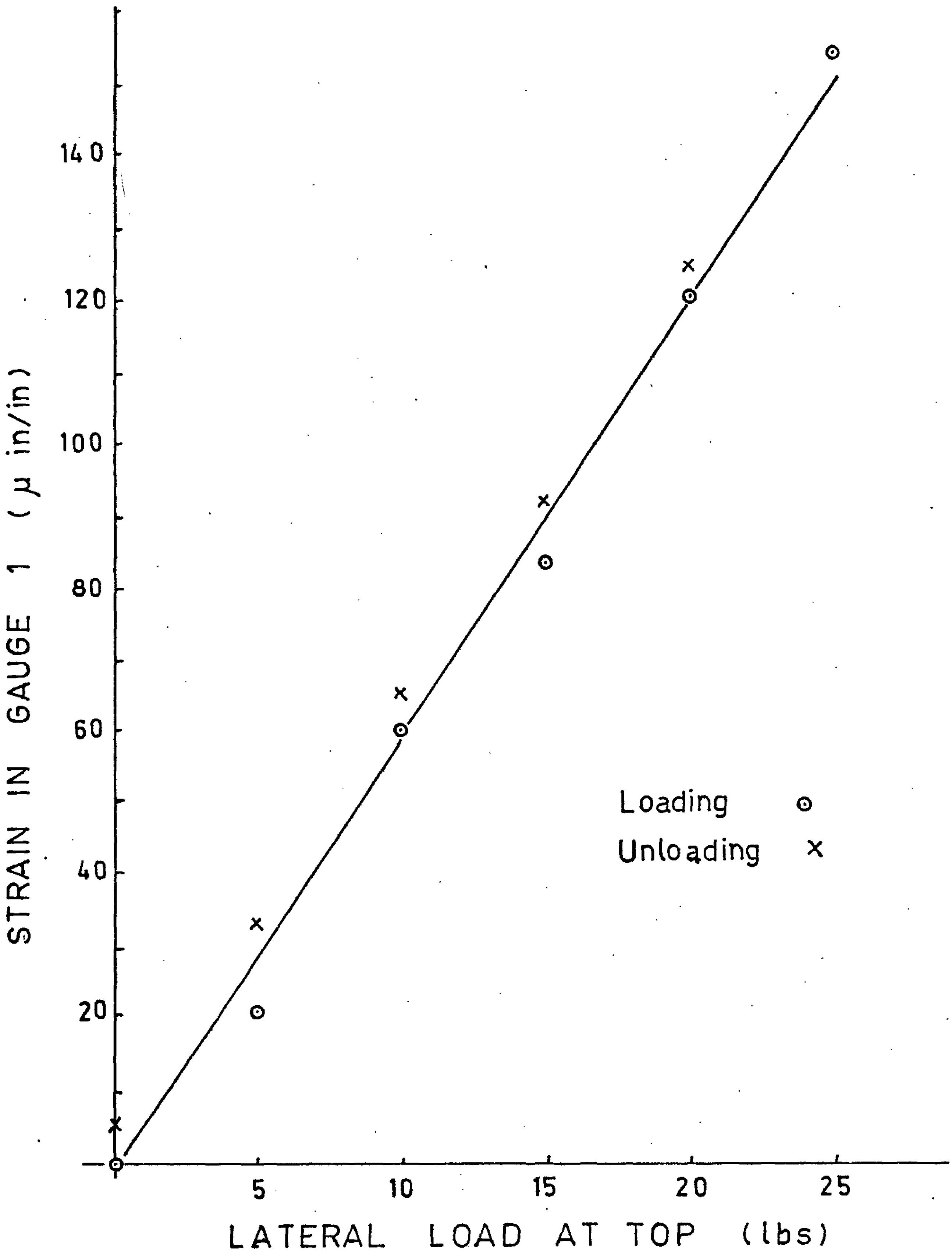

LOAD vs. STRAIN DIAGRAM FOR MODEL WITH BEAMS

FIG. 4.8.10

The effect of axial deformation of piers is found to have no effect on results for loading case with applied torque. However, the effect is considerable for in the case of lateral loading. The displacement at top decreases by 37% and rotation at top decreases by 7% as a result of neglecting axial deformation. The error introduced by neglecting axial deformation becomes significant if the axial force in the piers is large as in the case of the lateral loading. A comparison from the shear (q) plot in fig. 4.5.5 shows that the shear is about five times in the case of applied loading as compared to the case of applied torque. Since the axial force in the piers is the sum of the distributed shear q, neglecting the deformation due to axial force in the case of applied loading affect the results considerably.

In the strain diagrams (Fig. 4.5.6 to 4.5.9) the comparison between the experiment and the theory is less favourable. Since strain is a local measure, the experimental results are affected by the local imperfection of the test model. The continuum approach used in the analysis is expected to give results to the overall behaviour of the structure but with less accurate results to the local behaviour. Nevertheless, the trend of the strain distribution as predicted by the theory is varified by the experimental points.

In general it is expected that the continuum approach of analysis is best suited for structures with a large number of stories. In the present study, the model used in the experiment consists of eight floor beams only. Yet, the results obtained from the analysis compare well with the experimental points.

CHAPTER V

CONCLUSIONS AND RECOMMENDATIONS

5.1 Conclusions

The results from the static analysis and the testing of shear wall model with floors show that floor slab can provide considerable torsional stiffness by providing restraint against warping. Neglect of the floor slab stiffness will underestimate the stiffness of the structure. Moreover the actual structure is not as stiff as predicted by considering both torsional and flexural stiffness of the slabs. The bending stiffness of the slab is less effective due to the local rotation of the joints and a modified bending stiffness is to be considered. This is taken into account by a factor K in eq. 2.6.2. Theoretical values thus obtained compare reasonably well with experiments for displacement and strain measurements.

In the dynamic study of shear wall with floor slabs, the mass and mass moment of inertia of the slabs have to be considered in addition to the stiffness provided. The vibration is in general coupled. The first mode is a torsion predominant one and the second mode is bending predominant. The theoretical frequency compared reasonably with the experimental values except for the second frequency which is 16% higher. This is due to the neglect of shear deformation in the theory, which have considerable effect on the frequency for bending predominant modes.

In the static and dynamic analysis of shear walls with floors, the 'Matrix Transfer' method has been used. The method is ideal for continuous systems with discrete points. The main advantage is that the size of the matrix handled in the analysis is independent of the number of floors. An increase of the number of floors will only increase the number of matrix multiplication which can be done easily in a digital computer.

The non-planar coupled shear wall was analysed using the continuum method. It is shown that the effect of neglecting axial deformation of piers will lead to gross overestimation of stiffness of the structure for certain cases. Simplicity can be achieved by this assumption but should always be done with caution. The theoretical analysis shows reasonable agreement with the experimental results for displacements but less favourable for strains. So it can be concluded that continuum method gives good results for overall behaviour but is less accurate for local behaviour of a structure.

5.2 Recommendations

The present study of shear wall structures with special interest on floor slabs and floor beams are carried out on simple structures. The arrangement of the shear walls in an actual multi-storey building is very complex. The analysis is also complex due to various interacting elements. Simplicity can be achieved by assumption but a complete understanding of the behaviour of different interacting elements is necessary for making reasonable assumptions.

More experimental and theoretical study on the behaviour of floor slab with different geometrical arrangement is necessary. In such cases, it may not be justified to treat the floor slab as a series of beams but as an elastically supported plate.

Extension of the formulation on non-planar coupled shear wall is necessary for more generalised cases. The present analysis is applicable for two shear walls connected by a single row of beams. Extension for cases with more piers and more rows of connecting beam is required. A study on the dynamic analysis for non-planar coupled shear walls is also recomended.

In general, the analytical tools presently available to design engineers are very limited and most of the time very restricted in its applications. Therefore, more theoretical work supported by experimental data is necessary in the shear wall field to assist the practicing engineers to analyse and design structures which will be safe at the same time economic.

APPENDIX A

VLASOV'S THEORY OF THIN WALLED BEAM

The method of analysis used in the present work is based on the theory presented by Vlasov (8). Vlasov's theory is based on two geometric hypothesis:

(a) a thin walled beam of open section can be considered as a shell of rigid (undeformable) cross section.

(b) the shear deformation of the middle surface (characterising change in the angle between the co-ordinate line) can be neglected.

In shear wall structure, the concrete clear wall can be treated as thin walled beams connected by floor slabs which are normally located at regular intervals. The action of the floor slab is to prevent any deformation of the section which supports the hypothesis (a). Hypothesis (b) requires shear deformation to be negligible compared with the torsional and flexural deformations. Vlasov states that this is satisfied if for the structure shown in Fig. A.1

$$t/d \leq 0.1 \text{ and } d/\ell \leq 0.1$$

For components of tall building this conditions are satisfied.

The expression of longitudinal stress in Vlasov's theory is

$$\sigma = \frac{N}{A} - \frac{M_y \cdot x}{I_y} - \frac{M_x \cdot y}{I_x} + \frac{B \cdot \omega}{I_\omega} \tag{A.1}$$

The first three terms coincide with the equation known from elementary theory. The last term of the expression is

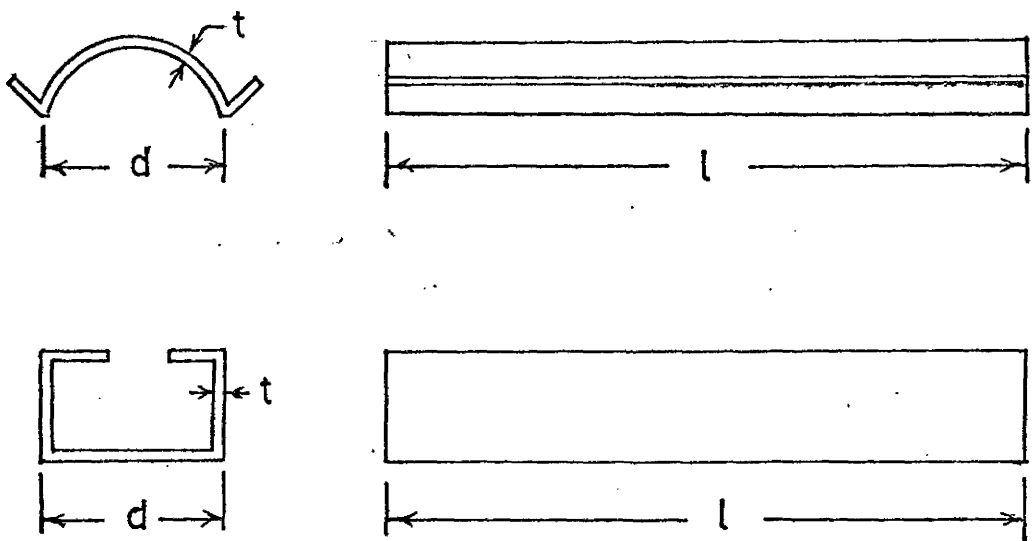

Dimensional Limitations

FIG. A 1

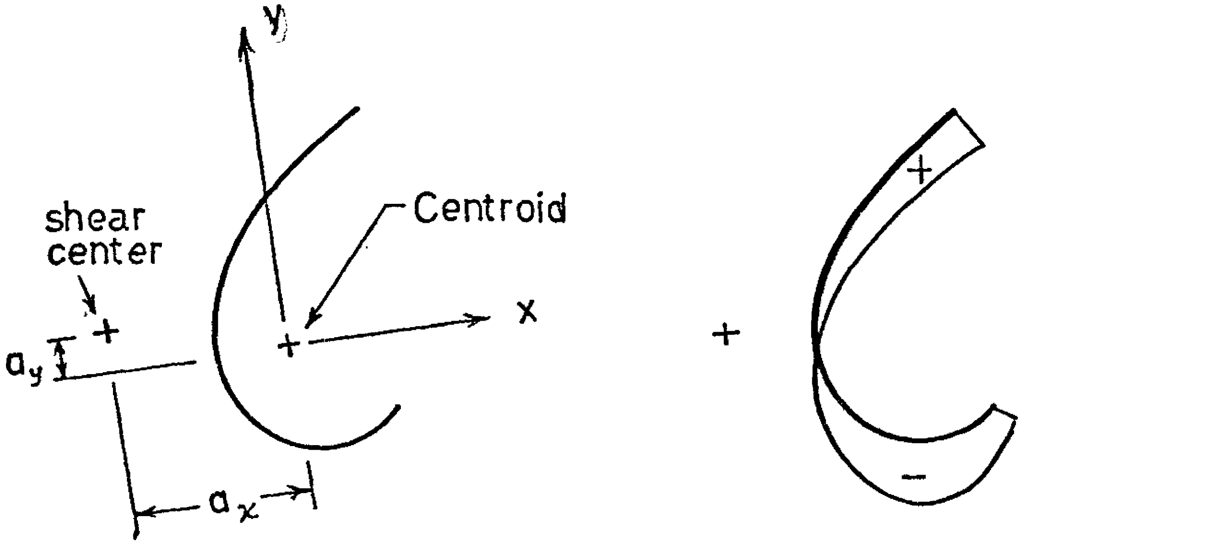

x & y Ordinates

Sectorial Coordinate ω

FIG. A 2

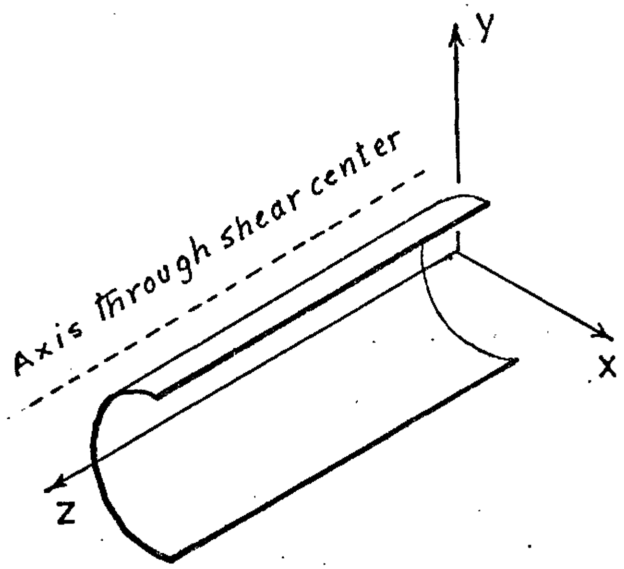

Co-ordinate System

FIG. A 3

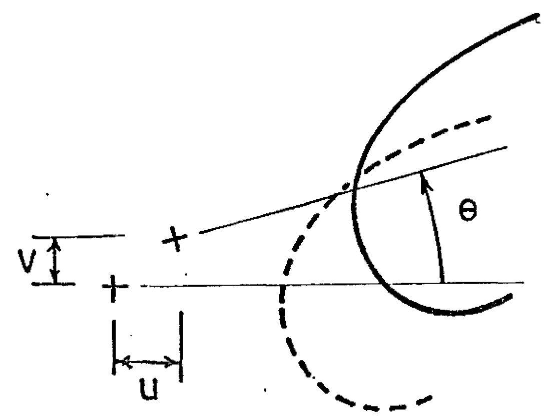

Generalised
Displacements

FIG. A 4

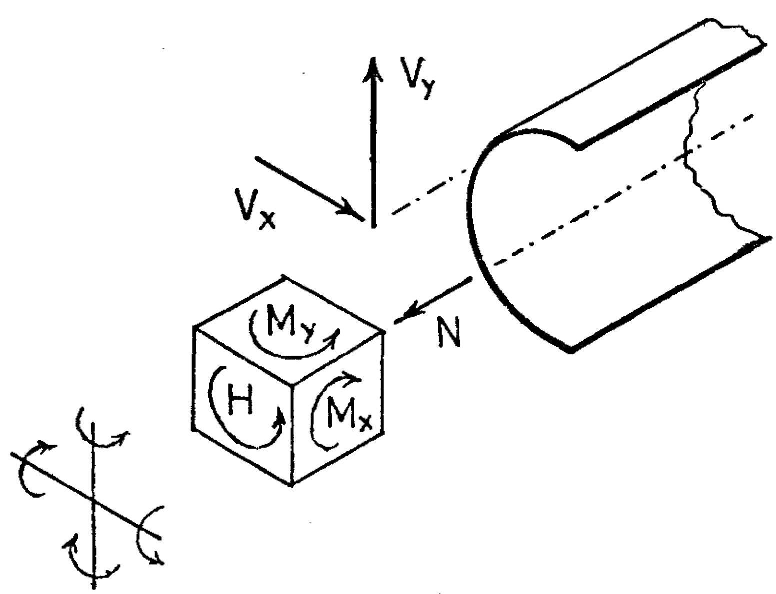

Generalised Forces

FIG. A 5

the longitudinal stress due to warping. The notations of the last terms are explained as:

Bimoment B is a generalised balanced system of forces statically equivalent to zero. Units are force x $(\text{length})^2$ e.g. lbs. in^2.

ω is the sectorial area of the point on the section where the stress is being measured. Units are $(\text{length})^2$ e.g. in^2.

I_ω is sectorial moment of Inertia of the section and is defined as $\int_A \omega^2 dA$ units are $(\text{length})^6$ e.g. in^6.

The distribution of sectorial co-ordinate for some open section is shown in Fig. A.2. Right hand co-ordinate system used in the present work (Fig. A.3). The generalised displacement variables are shear center displacements u, V and θ in xy plane and centroidal displacement s in z direction (Fig. A.4). Sign convention for generalised forces are shown in Fig. A.5.

The relation between the generalised forces and displacement variables are:

$$\left.\begin{array}{l} N = EAs', \; M_x = EI_x v'', \; M_y = EI_y u'', \\ B = -EI_\omega \theta'', \; H = -EI_\omega \theta''' + GJ\theta', \\ V_y = -EI_x v''', \; V_x = -EI_y u'''. \end{array}\right\} \quad \text{(A.2)}$$

Of these quantities, axial force and bending moments are refered to the centroid and shear forces and torque are refered to the shear center of the section.

The longitudianl stress at any point can be expressed in terms of displacement variables as:

$$\sigma = E[s' - u''x - v''y - \theta''\omega] \qquad (A.3)$$

Displacement of any point in z direction is obtained as:

$$\delta = s - u'x - v'y - \theta'\omega \qquad (A.3a)$$

Tensile stress and displacements in the direction of positive x,y & z are positive in eq. A.3 and eq. A.3a. When referred to principal generalised co-ordinates of an open section, the differential equation of a thin walled beam statically loaded at its ends are:

$$\left.\begin{aligned} EAs'' &= 0 \\ EI_x v^{IV} &= 0 \\ EI_y u^{IV} &= 0 \\ EI_\omega \theta^{IV} - GJ\theta'' &= 0 \end{aligned}\right\} \qquad (A.4)$$

Differential equations for free vibration of a thin walled beam are:

$$\left.\begin{aligned} EAs'' - \rho A\ddot{s} &= 0 \\ EI_x v^{IV} + \rho A\ddot{v} - \rho I_x \ddot{v}'' - \rho Aa_x \ddot{\theta} &= 0 \\ EI_y u^{IV} + \rho A\ddot{u} - \rho I_y \ddot{u}'' + \rho Aa_y \ddot{\theta} &= 0 \\ EI_\omega \theta^{IV} - GJ\theta'' + \rho I_p \ddot{\theta} - \rho I_\omega \ddot{\theta}'' + \rho Aa_y \ddot{u} - \rho Aa_x \ddot{v} &= 0 \end{aligned}\right\} \qquad (A.5)$$

Eq. A.4 and eq. A.5 are refered in Chapter 2 and Chapter 3 and solved accordingly as they appeared in the analysis.

APPENDIX - B

COMPUTER PROGRAMS

```
                 PROGRAM TST (INPUT,OUTPUT,TAPE5=INPUT,TAPE6=OUTPUT)
          C      STATIC ANALYSIS OF SHEAR WALL WITH FLOORS
          C      M. ENG.  THESIS  BISWAS
          C
          C             COMPUTER  NOTATIONS  USED
          C
          C             XI        MOMENT OF INERTIA OF SECTION ABOUT X AXIS
          C             YI        MOMENT OF INERTIA OF SECTION ABOUT Y AXIS
          C             WI        SECTORIAL MOMENT OF INERTIA OF SECTION
          C             DI        POLAR MOMENT OF INERTIA ABOUT SHEAR CENTER
          C             E         MODULUS OF ELASTICITY
          C             G         MODULUS OF RIGIDITY
          C             H         FLOOR HEIGHT
          C             NF        NUMBER OF STOREY
          C             DM        BIMOMENT CONTRIBUTION FACTOR
          C             PLY(I)    LATERAL LOAD AT I TH FLOOR IN Y DIRECTION
          C             PLR(I)    APPLIED TORQUE AT I TH FLOOR
          C
000003           DIMENSION P(8,8),F(8,8),PFA(8,8),PFB(8,8),PF(8,8),A(8,8),T(8,8),
                1AT(8,1),BT(8,1),N1(32),WORK(8),PLY(50),PLR(50),S(8,1),PS(8,1)
          C      INPUT DATA
000003           XI= 42.7089
000005           YI= 11.0322
000006           WI= 108.6931
000010           DI= .09767
000011           E= .4E+06
000013           PSN= .35
000014           G= E/(2.*(1.+PSN))
000020           NF= 8
000021           H= 6.
000022           DM= 20.109E+04
000024           DM= 124.909E+04
000025           DM= 0.
000026           DO 75 I=1,NF
000027           PLR(I)= 0.
000030        75 PLY(I)= 0.
000033           PLY(8)= 12.5
000035           PLR(8)= 6.2425*12.5
          C
          C      PRINTING OUT INPUT DATA
000036           WRITE (6,1)
000042         1 FORMAT (1X,* INPUT DATA *)
000042           WRITE (6,2)      NF,H,XI,YI,WI,DI,PSN,E,G,E ,DM
000074         2 FORMAT (5X,I5,10E12.4 )
000074           WRITE (6,3)
000100         3 FORMAT (1X,* FLOOR LOADS * )
000100         7 FORMAT (1X,I10,5X,3E18.6)
000100           DO 70 I=1,NF
          C      FIELD TRANSFER MATRIX F
000102        70 WRITE (6,7) I,PLY(I),PLR(I)
000116           GD= G*DI
000120           AK= H*SQRT(GD/(E*WI))
000126           AL= AK/H
000127           DO 4 I= 1,8
000130           DO 4 J= 1,8
000131           IF (I.NE.J) F(I,J)= 0.
000134         4 F(J,J)= 1.
```

```
000143          F(1,2)= H
000145          F(1,3)= -(H*H)/(2.*E*XI)
000150          F(1,4)= -(H*H*H)/(6.*E*XI)
000153          F(2,3)= -H/(E*XI)
000155          F(2,4)= -(H*H)/(2.*E*XI)
000160          F(3,4)= H
000161          F(5,6)= SINH(AK)/AL
000164          F(5,7)= (1.- COSH(AK))/GD
000170          F(5,8)= (H - SINH(AK)/AL)/GD
000175          F(6,6)= COSH(AK)
000200          F(6,7)= -(AL*SINH(AK))/GD
000204          F(6,8)= (1.- COSH(AK))/GD
000210          F(7,6)= -(GD*SINH(AK))/AL
000214          F(7,7)= COSH(AK)
000216          F(7,8)= SINH(AK)/AL
          C     POINT TRANSFER MATRIX
000221          DO 6 I= 1,8
000222          DO 6 J= 1,8
000223          IF (I.NE.J) P(I,J)= 0.
000226        6 P(J,J)= 1.
000235          P(7,6)= -DM
000237       32 CALL FLOOR(P,F,NF,A ,PFA,PFB,PF)
000246          DO 10 I= 1,8
000250       10 AT(I,1)= 0
000254          AT(4,1)= -PLY(NF)
000256          AT(8,1)= -PLR(NF)
000257          WRITE (6,9)
000263        9 FORMAT (1X,* FIELD TRANSFER MATRIX *)
000263          WRITE (6,5) (( F(I,J),J=1,8),I=1,8)
000301          WRITE (6,13)
000305       13 FORMAT (1X,* POINT TRANSFER MATRIX *)
000305          WRITE (6,5) (( P(I,J),J=1,8),I=1,8)
000323        5 FORMAT  (1X,8E15.6)
000323          NC= 1
000324       11 CALL FLOOR(P, F,NC,T,PFA,PFB,PF)
000333          NCC= NF- NC
000335          DO 12 I= 1,8
000337       12 AT(I,1)= AT(I,1)- T(I,4)*PLY(NCC)-  T(I,8)*PLR(NCC)
000352          NC= NC+1
000353          IF (NCC.EQ.1) GO TO 14
000355          GO TO 11
000355       14 DO 16 I= 1,8
000357          DO 16 J= 1,8
000360       16 A(I,J)= -A(I,J)
000367          DO 18 I= 1,4
000371          DO 18 J= 1,2
000372          K= I+4
000374          L= J+4
000375          A(I,J)= 0.
000377       18 A(K,L)= 0.
000405          A(1,1)= 1.
000407          A(2,2)= 1.
000410          A(5,5)= 1.
000411          A(6,6)= 1.
000412          CALL MINVSE(A,8,8,1.E-08,IERR,N1,WORK)
000420          IF (IERR.EQ.0 ) GO TO 30
000421       57 FORMAT (5X, * UNSUCCESSFUL  INVERSION *)
000421          WRITE (6,57)
```

```
000425           GO TO 100
000426        30 CALL GMPRD(A,AT,BT,8,8,1)
000432           BT(1,1)= 0.
000433           BT(2,1)= 0.
000434           BT(5,1)= 0.
000435           BT(6,1)= 0.
            C    BT   IS THE STATE VECTOR AT BASE
000436           WRITE (6,31)
000441        31 FORMAT (1X)
000441           WRITE (6,37)
000445        37 FORMAT (4X, *FLOOR *,10X, *DISPLACEMENT*,7X, *SLOPE*,6X,
                1 *MOMENT*,6X, *SHEAR*, 6X, *ROTATION*, 6X, *TWIST*, 6X,* BIMOMENT
                1*,6X,*TORQUE* )
000445           WRITE (6,33) ((BT(I,J),J= 1,1),I= 1,8)
000463        33 FORMAT (4X, *0*,4X,8E14.4)
000463           NA= 1
000464        17 DO  27 I= 1,8
000466        27 AT(I,1)= 0.
000472           AT(4,1)= -PLY(NA)
000474           AT(8,1)= -PLR(NA)
000475           CALL GMPRD(F,BT,S,8,8,1)
000501           WRITE (6,21) NA,((S(I,J),J= 1,1),I= 1,8)
000521        20 FORMAT (4X,I3,*  BELOW*, 8E14.4)
000521           CALL GMPRD(P,S,PS,8,8,1)
000525           DO 22 I= 1,8
000527        22 PS(I,1)= PS(I,1)+ AT(I,1)
000534           WRITE (6,21) NA,((PS(I,J),J= 1,1),I= 1,8)
000554        21 FORMAT (4X,I3,*  ABOVE *, 8E14.4)
000554           IF (NA.EQ.NF) GO TO 100
000556           DO 24 I= 1,8
000560        24 BT(I,1)= PS(I,1)
000565           NA = NA+ 1
000566           GO TO 17
000567       100 STOP
000571           END

UNUSED COMPILER SPACE
004000
```

```
              SUBROUTINE FLOOR(P,F,N,T,PFA,PFB,PF )
        C     MULTIPLICATION OF MATRICES ACCORDING TO NO OF FLOOR
        C     P, F  ARE THE INPUT MATRICES
        C     N  IS THE NO OF FLOORS
        C     T  IS THE OUTPUT MATRIX
        C     PFA, PFB, PF  ARE THE WORKING MATRICES OF SIZE 8 * 8
000012        DIMENSION P(8,8),F(8,8),T(8,8),PFA(8,8),PFB(8,8),PF(8,8)
000012        CALL MULT(P,F,PF,8)
000014        KOUNT= 1
000015        IF (N.GT.1) GO TO 4
000024        DO 10 I=1,8
000025        DO 10 J=1,8
000026     10 T(I,J)= PF(I,J)
000041        GO TO 30
000042      4 DO 5 I=1,8
000044        DO 5 J=1,8
000045      5 PFA(I,J)= PF(I,J)
000060      6 CALL MULT(PFA,PF,PFB,8)
000063        KOUNT = KOUNT+1
000065        DO 7 I=1,8
000072        DO 7 J=1,8
000073      7 PFA(I,J)= PFB(I,J)
000106        IF (KOUNT.EQ.N) GO TO 9
000110        GO TO 6
000110      9 DO 12 I=1,8
000112        DO 12 J=1,8
000113     12 T(I,J)= PFB(I,J)
000126     30 RETURN
000127        END

UNUSED COMPILER SPACE
006200
```

```
                     SUBROUTINE MULT(A,B,C,N)
             C       MULTIPLICATION OF SQUARE MARRICES
000007               DIMENSION A(N,N),B(N,N),C(N,N)
000007               DO 1 I=1,N
000010               DO 1 J=1,N
000011               C(I,J)=0.
000015               DO 1 K=1,N
000016               C(I,J)= C(I,J)+ A(I,K)*B(K,J)
000032       1       CONTINUE
000040               RETURN
000040               END

UNUSED COMPILER SPACE
006500
```

```
              PROGRAM TST (INPUT,OUTPUT,TAPE5=INPUT,TAPE6=OUTPUT)
         C    DYNAMIC ANALYSIS OF SHEAR WALL WITH FLOORS
         C    M. ENG. THESIS  BISWAS
         C                COMPUTER  NOTATIONS  USED
         C    E                     MODULUS OF ELASTICITY
         C    G                     MODULUS OF RIGIDITY
         C    PNU                   POISONS  RATIO
         C    RO                    MASS DENSITY OF MATERIAL
         C    A                     AREA OF SECTION
         C    XI                    MOMENT OF INERTIA OF SECTION ABOUT X AXIS
         C    DI                    TORSION FACTOR OF THE SECTION
         C    PI                    POLAR MOMENT OF INERTIA OF SECTION ABOUT SHEAR CENTER
         C    AX                    COORDINATE OF SHEAR CENTER
         C    NFQ                   NUMBER OF FREQUENCIS NECESSARY
         C    XJ                    MASS MOMENT OF INERTIA OF PLATE ABOUT X AXIS
         C    ZJ                    POLAR MASS MOMENT OF INERTIA OF PLATE ABOUT SHEAR CENTER
         C    AP                    DISTANCE BETWEEN SHEAR CENTER AND CENTROID OF PLATE
         C    H                     HEIGHT OF EACH STOREY
         C    NFLOOR                NUMBER OF FLOORS
         C    W                     STARTING FREQUENCY
         C    WINC                  INCREMENT OF FREQUENCY
000003        DIMENSION TS(4,4),TF(4,4)
000003        DIMENSION C(8,8),D(8,8),B(8,8)
000003        DIMENSION AA(9),RR(8),RI(8),RC(8)
000003        DIMENSION P(8,8),CD(8,8),NI(8),TEMP(8),Q(8,8)
000003        DIMENSION F(8,8),PF(8,8),PFA(8,8),PFB(8,8),T(8,8),TT(4,4)
000003        COMPLEX C,D,CD,B,Q,TEMP,RC
         C             INPUT DATA
000003        NFLOOR= 8
000004        RO= 1.11E-04
000006        DM= 46.675E+04
000007        AM= 18.4089E-04
000011        XJ= 80.7445E-04
000012        ZJ= 478.4879E-04
000014        AP= 4.4412
000015        AX= -3.3192
000017        H= 6.
000020        E= .400E+06
000022        PNU= .35
000023        G= E/(2.*(1.+PNU))
000027        A= 4.2706
000030        XI= 42.7089
000032        WI= 108.6931
000033        DI= .09767
000035        PI= 100.7907
000036        NFQ= 3
000037        W= 50.
000041        WINC= 100.
         C
         C
000042        WRITE (6,3) H,E,G,RO
000056      3 FORMAT (1X,* INPUT DATA */9X,* FLOOR HEIGHT =*,F9.4/9X,* MODULUS
             1OF ELASTICITY =*,E15.6/9X,* MODULUS OF RIGIDITY =*,E15.6/9X,* MASS
             2 DENSITY OF MATERIAL =*,E15.6)
000056        WRITE (6,7) NFLOOR
000064      7 FORMAT (9X,* NUMBER OF FLOORS = *,I4 )
000064        WRITE (6,2) A,XI,WI,DI,PI,AX,AM,XJ,ZJ,DM,AP
```

```
000116        2 FORMAT (1X,* SECTION PROPERTIES*/9X,* AREA =*,F9.4/9X,* MOMENT OF
               1INERTIA ABOUT X =*,F9.4/9X,* SECTORIAL MOMENT OF INERTIA =*,F9.4/
               29X,* TORSION FACTOR =*,F9.4/9X,* POLAR MOMENT OF INERTIA =*,F9.4/
               39X,* ORDINATE OF SHEAR CENTRE =*,F9.4/1X,* DIAPHRAGM PROPERTIES*/9
               4X,* MASS OF PLATE =*,E15.6/9X,* MASS MOMENT OF INERTIA ABOUT X =*,
               5E15.6/9X,* POLAR MASS MOMENT OF INERTIA =* ,E15.6/9X,* BIMOMENT FAC
               6TOR =*,E15.6/9X,* SHEAR CENTRE TO C.G. OF THE  PLATE =*,F9.4)
000116        1 FORMAT (6F9.4/7F9.4/3E15.6)
000116          WRITE (6,42)
000122       42 FORMAT (1X, * RESULTS FOR FIXED FREE CASE * )
000122          KKK= 333
000123          NCOUNT= 6666
000124          DETO= 0.
000125          NFREQ= 0
        C       POINT TRANSFER MATRIX  P
000126       40 DO 4 I=1,8
000130          DO 4 J=1,8
000131          IF (I.NE.J) P(I,J)=0.
000134        4 P(J,J)=1.
000143          P(3,2)= -XJ*W*W
000146          P(3,6)= -AP*AM*W*W
000150          P(4,1)=-AM*W**2
000152          P(4,5)=-AP*AM*W**2
000154          P(7,6) = -DM
000155          P(8,1)=-AP*AM*W**2
000157          P(8,5)=-ZJ*W**2
        C       COEFFECIENTS OF CHARACTERISTICS EQUATION
000161          DO 6 I=1,9
000162        6 AA(I)=0.
000165          AA(1)=-WI*XI*E**2
000170          AA(3)=DI*XI*E*G-2.*WI*XI*RO*E*W**2
000201          AA(5)=(WI*A*E+DI*XI*G+PI*XI*E)*RO*(W**2) -WI*XI*(W**4)*(RO**2)
000220          AA(7)=-DI*A*RO*G*(W**2) +(PI*XI+WI*A)*(W**4)*(RO**2)
000237          AA(9)=(-PI*A+(A*AX)**2)*(W**4)*(RO**2)
        C       SOLUTION BY SUBROUTINE BAIRST
000247          CALL BAIRST (AA,RR,RI,8)
000252          DO 5 I=1,8
000254        5 RC(I)=CMPLX(RR(I),RI(I))
        C       FIELD TRANSFER MATRIX F
000265          DO 11 J=1,8
000267          C(1,J)=CMPLX(1.,0.)
000276          C(2,J)=RC(J)
000302          C(3,J)= E*XI*(RC(J)**2)
000317          C(4,J)=-E*XI*(RC(J)**3)
000334          C(5,J)=-((E*XI)/((W**2)*RO*A*AX))*(RC(J)**4)-(XI/(A*AX))*(RC(J)**2
               1)+(1./AX)
000373          C(6,J)=-((E*XI)/((W**2)*RO*A*AX))*(RC(J)**5)-(XI/(A*AX))*(RC(J)**3
               1)+(1./AX)*RC(J)
000437          C(7,J)=(((E**2)*WI*XI)/((W**2)*RO*A*AX))*(RC(J)**6)+((E*WI*XI)/
               1(A*AX))*(RC(J)**4)-((E*WI)/AX)*(RC(J)**2)
000513          C(8,J)=(((E**2)*WI*XI)/((W**2)*RO*A*AX))*(RC(J)**7)+((E*WI*XI)/
               1(A*AX)-(E*G*DI*XI)/((W**2)*RO*A*AX))*(RC(J)**5)+(-(E*WI)/AX-(G*DI*
               2XI)/(A*AX))*(RC(J)**3)+((G*DI)/AX)*RC(J)
000611       11 CONTINUE
000613          DO 13 I=1,8
000614          DO 13 J=1,8
000615          IF (I.NE.J) D(I,J)=0.
000622          D(J,J)=CEXP(H*RC(J))
```

```
000640         13 B(I,J)=C(I,J)
000653            CALL INVCPX(B,8,8,1.E-8,IERR,NI,TEMP )
000662            CALL MATMULT(C,D,CD,8)
000665            CALL MATMULT(CD,B,Q,8)
000670            DO 24 I=1,8
000672            DO 24 J=1,8
000673         24 F(I,J)=REAL(Q(I,J))
000705            CALL FLOOR(P,F,NFLOOR,T,PFA,PFB,PF )
000713            CALL BCFXFR(T,TT)
000715            CALL DETVAL(TT,DET,4)
000720         46 PROD= DETO*DET
000722            IF (NCOUNT.EQ.5555) GO TO 47
000724            IF (PROD.GE.0.) GO TO 8
000726         44 DETN=DET
000730         45 WAP= WO+(W-WO)*DETO/(DETO-DETN)
000737            PC= (WAP-WO)/WAP
000741            IF (PC.LT..01 ) GO TO 55
000743            WT= W
000745            W= WAP
000745            NCOUNT= 5555
000746            GO TO 40
000747         47 IF (PROD.LT.0.) GO TO 44
000751            DETO= DET
000752            KKK= 222
000753            WO= W
000755            W= WT
000756            GO TO 45
000756         55 NFREQ= NFREQ+1
000760            WW= WAP/6.28
000762            WRITE (6,60) NFREQ,WW
000771         60 FORMAT (7X,*FREQ *, I3,5X,F10.4 )
000771          8 DETO= DET
000773            IF (KKK.EQ.222 ) DETO= DETN
000776            KKK= 111
000777            WO= W
001001            NCOUNT= 3333
001002            W= W+ WINC
001003            IF (NFREQ.EQ.NFQ) GO TO 50
001005            GO TO 40
001006         50 STOP
001010            END

UNUSED COMPILER SPACE
003100
```

```
                 SUBROUTINE INVCPX(A,N,NN,ZERO,IERR,NI,TEMP)
          C      REM
          C      REM      THE ROUTINE INVERTS THE MATRIX BY A PIVOTAL METHOD
          C      REM      USING THE LARGEST ELEMENT IN THE NEXT ROW AS A PIVOT.THE
          C      REM      FIRST PART DOES THE INVERSION AND THE SECOND PART
          C      REM      REARRANGES THE ROWS AND COLUMNS TO TAKE ACCOUNT OF THE
          C      REM      FACT THAT THE PIVOTS WERE NOT ON THE DIAGONAL.
          C      REM      THIS SUBROUTINE IS CALLED BY CALL INVMAT(A,N,NN,ZERO,IER,
          C      REM      NI,TEMP) WHERE A IS AN NN BY NN MATRIX IN AN N BY N ARRAY
          C      REM      ZERO IS A TEST VALUE BELOW WHICH AN ELEMENT IS CONSIDERED
          C      REM      TO BE ZERO,IER IS AN INDICATOR WHICH IS 0 IF THE INVERSE
          C      REM      IS FOUND AND NON-ZERO OTHERWISE, NI  IS A WORKING ARRAY
          C      REM      OF NN ELEMENTS AND TEMP IS ANOTHER
          C      REM
000012           DIMENSION A(N,1),NI(NN),TEMP(NN)
000012           COMPLEX A,AA,TEMP
000012           DO 10 I=1,NN
000013        10 NI(I)=0
000016           DO 20 K=1,NN
000017           AAA=0.
000020           DO 30 J=1,NN
000022           IF(NI(J).NE.0) GO TO 30
000024           C=CABS(A(K,J))
000036           IF(C.LT.AAA) GO TO 30
000041           AAA=C
000041           JJ=J
000043        30 CONTINUE
000046           IF(AAA.GT.ZERO) GO TO 70
000051           IERR=K
000052           RETURN
000052        70 NI(JJ)=K
000055           AA=A(K,JJ(
000062           A(K,JJ)=1.
000070           DO 50 J=1,NN
000072        50 A(K,J)=A(K,J)/AA
000107           DO 60 I=1,NN
000110           IF(I.EQ.K) GO TO 60
000112           AA=-A(I,JJ)
000120           A(I,JJ)=0.
000125           DO 55 J=1,NN
000126        55 A(I,J)=A(I,J)+AA*A(K,J)
000145        60 CONTINUE
000150        20 CONTINUE
000152           IERR=0
000152           DO 98 I=1,NN
000154        98 IF(NI(I).NE.I) GO TO 95
000160           RETURN
000160        95 DO 80 I=1,NN
000162           DO 79 J=1,NN
000163           K=NI(J)
000165        79 TEMP(K)=A(I,J)
000200           DO 81 J=1,NN
000201        81 A(I,J)=TEMP(J)
000214        80 CONTINUE
000216           DO 90 J=1,NN
000217           DO 89 I=1,NN
000220           K=NI(I)
```

```
000222        89  TEMP(I)=A(K,J)
000235            DO 91 I=1,NN
000236        91  A(I,J)=TEMP(I)
000253        90  CONTINUE
000255            RETURN
000256            END

UNUSED COMPILER SPACE
005600
```

```
                  SUBROUTINE FLOOR(P,F,N,T,PFA,PFB,PF )
          C       MULTIPLICATION OF MATRICES ACCORDING TO NO OF FLOOR
          C       P, F  ARE THE INPUT MATRICES
          C       N  IS THE NO OF FLOORS
          C       T  IS THE OUTPUT MATRIX
          C       PFA, PFB, PF  ARE THE WORKING MATRICES OF SIZE 8*8
000012            DIMENSION P(8,8),F(8,8),T(8,8),PFA(8,8),PFB(8,8),PF(8,8)
000012            CALL MULT(P,F,PF,8)
000014            KOUNT= 1
000015            IF (N.GT.1) GO TO 4
000024            DO 10 I=1,8
000025            DO 10 J=1,8
000026        10  T(I,J)= PF(I,J)
000041            GO TO 30
000042         4  DO 5 I=1,8
000044            DO 5 J=1,8
000045         5  PFA(I,J)= PF(I,J)
000060         6  CALL MULT(PFA,PF,PFB,8)
000063            KOUNT = KOUNT+1
000065            DO 7 I=1,8
000072            DO 7 J=1,8
000073         7  PFA(I,J)= PFB(I,J)
000106            IF (KOUNT.EQ.N) GO TO 9
000110            GO TO 6
000110         9  DO 12 I=1,8
000112            DO 12 J=1,8
000113        12  T(I,J)= PFB(I,J)
000126        30  RETURN
000127            END

UNUSED COMPILER SPACE
000200
```

```
                SUBROUTINE MATMULT (A,B,C,N)
        C       MULTIPLICATION OF COMPLEX MATRICES
000007          DIMENSION A(N,N),B(N,N),C(N,N)
000007          COMPLEX A,B,C
000007          DO 1 I=1,N
000010          DO 1 J=1,N
000011          C(I,J)=0.
000016          DO 1 K=1,N
000020          C(I,J)=C(I,J)+A(I,K)*B(K,J)
000042  1       CONTINUE
000050          RETURN
000050          END

UNUSED COMPILER SPACE
006400
```

```
                SUBROUTINE BCFXFR(T,TT)
        C       BOUNDARY CONDITION ONE END FIXED OTHER END FREE
000005          DIMENSION T(8,8),TT(4,4)
000005          DO 30 I=1,4
000006          DO 30 J=1,4
000007          K=I+2
000011          N=J+2
000012          KK=I+4
000013          NN=J+4
000014          IF (I.LE.2.AND.J.LE.2) TT(I,J)=T(K,N)
000030          IF (I.LE.2.AND.J.GT.2) TT(I,J)=T(K,NN)
000046          IF (I.GT.2.AND.J.LE.2) TT(I,J)=T(KK,N)
000064          IF (I.GT.2.AND.J.GT.2) TT(I,J)=T(KK,NN)
000101      30  CONTINUE
000105          RETURN
000106          END

UNUSED COMPILER SPACE
006300
```

```
                SUBROUTINE DETVAL(A,DET,M)
          C     EVALUATION OF DETERMINANT
000006          DIMENSION A(M,M)
000006          NE=0
000007          MM=M-1
000011          DO 8 J=1,MM
000012          JJ=J+1
000014          DO 30 JB=JJ,M
000016          IF (ABS(A(J,J)).GE.ABS(A(JB,J))) GO TO 30
000030          NE=NE+1
000032          IF (NE.EQ.2) NE=0
000034          DO 28 KK=1,M
000036          HOLD=A(J,KK)
000042          A(J,KK)=A(JB,KK)
000050       28 A(JB,KK)=HOLD
000055       30 CONTINUE
000060          DO 4 NN=JJ,M
000062          C=A(NN,J)/A(J,J)
000071          DO 4 N=1,M
000072        4 A(NN,N)=A(NN,N)-A(J,N)*C
000111        8 CONTINUE
000113          DET=1.
000114          DO 5 J=1,M
000116        5 DET=DET*A(J,J)
000125          IF (NE.EQ.I ) DET=-DET
000130          RETURN
000131          END

UNUSED COMPILER SPACE
006200
```

```
                SUBROUTINE MULT(A,B,C,N)
          C     MULTIPLICATION OF SQUARE MARRICES
000007          DIMENSION A(N,N),B(N,N),C(N,N)
000007          DO 1 I=1,N
000010          DO 1 J=1,N
000011          C(I,J)=0.
000015          DO 1 K=1,N
000016          C(I,J)=C(I,J)+A(I,K)*B(K,J)
000032    1     CONTINUE
000040          RETURN
000040          END

UNUSED COMPILER SPACE
006500
```

```
              PROGRAM TST (INPUT,OUTPUT,TAPE5=INPUT,TAPE6=OUTPUT)
        C     NON PLANAR  COUPLED  SHEAR  WALL
        C     M. ENG.   THESIS  BISWAS
        C              COMPUTER  NOTATIONS  USED
        C
        C     SX1,SX2,         MOMENT OF INERTIA OF PIERS ABOUT PARALLEL GLOBAL X TH C.G.
        C     SY1,SY2          MOMENT OF INERTIA OF PIERS ABOUT PARALLEL GLOBAL Y TH C.G.
        C     SXY1,SXY2        PRODUCT MOMENT OF INERTIA OF PIERS
        C     SW1,SW2          SECTORIAL MOMENT OF INERTIA OF PIERS W.R.T SHEAR CENTRE
        C     SJ1,SJ2          TORSION FACTORS OF PIERS
        C     EX1,EY1,EX2,EY2  COORDINATES OF C.G. OF PIERS W.R.T GLOBAL AXES
        C     CX1,CY1,CX2,CY2  COORDINATES OF S.C. OF PIERS W.R.T GLOBAL AXES
        C     A1,A2            AREA OF THE PIERS
        C     W1,W2            SECTORIAL COORDINATES
        C     E, G, PSN        MODULUS OF ELASTICITY, MODULUS OF RIGIDITY, POISONS RATIO
        C     L                CLEAR SPAN OF THE CONNECTING BEAM
        C     SB               MOMENT OF INERTIA PF CONNECTING BEAM
        C     AST              EFFECTIVE SHEAR AREA OF CONNECTING BEAM
        C     H                SPACING OF CONNECTING BEAM
        C     NF               NUMBER OF FLOORS
        C     PX               CONCENTRATED LOAD AT TOP IN X DIRECTION
        C     PY               CONCENTRATED LOAD AT TOP IN Y DIRECTION
        C     QT               CONCENTRATED TORGUE AT TOP
        C     HT               TOTAL HEIGHT OF STRUCTURE
000003        DIMENSION AAA(5,5),BBB(5)
        C
        C     INPUT DATA
000003        SX1= 9.377
000005        SX2= 9.377
000006        SY1= 2.289
000007        SY2= 2.289
000011        SXY1= -2.594
000012        SXY2=  2.594
000014        SW1= 0.
000015        SW2= 0.
000016        SJ1= .159
000017        SJ2= .159
000021        EX1= -4.313
000022        EX2=  4.313
000024        EY1= 1.687
000025        EY2= 1.687
000026        CX1= -4.804
000027        CX2=  4.804
000031        CY1= 0.
000032        CY2= 0.
000033        A1= 3.128
000034        A2= 3.128
000036        W1= 0.
000037        W2= 0.
000040        E= .4E+06
000041        PSN= .35
000043        G= E/(2.*(1.+PSN))
000047        L= 4.
000051        SB= .10997
000052        AST= .5865
000054        H= 6.
000055        NF= 8
```

```
              C
000056              PX= 25.
000060              PY= 0.
000061              QT= 0.
              C     COMPUTATION STARTS
000062              HT= FLOAT(NF)*H
000064              D= CX2*EY2- CY2*EX2+ CY1*EX1- CX1*EY1
000074              A= EX2- EX1
000075              B= EY2- EY1
000076              W= W2- W1
000100              RFACT= 1.+ (12.*E*SB)/(L*L*G*AST)
000110              SJB= SB/(H*RFACT)
000112              SJ= SJ1+ SJ2
000114              SX = SX1+ SX2
000116              SY= SY1+ SY2
000120              SXY= SXY1+ SXY2
000122              SYC= CY1*SY1+ CY2*SY2- CX1*SXY1- CX2*SXY2
000132              SXC= CX1*SX1+ CX2*SX2- CY1*SXY1- CY2*SXY2
000141              SW= CX1*CX1*SX1+ CX2*CX2*SX2+ CY1*CY1*SY1+ CY2*CY2*SY2
                   1-2.*CX1*CY1*SXY1- 2.*CX2*CY2*SXY2+ SW1+ SW2
000163              AA= SY*SXC+ SXY*SYC
000167              BB= SXY*SXC+ SX*SYC
000172              CC= A*SXC+ B*SYC
000174              SXP= SX1+ SX2
000176              SYP= SY1+ SY2
000200              SWP= SW- (SXC*SXC)/SX- (SYC*SYC)/SY
000206              IF (AA.EQ.0.) GO TO 40
000207              SX= SX- SXY*(BB/AA)
000212              SY= SY- SXY*(AA/BB)
000214              AP= A- SXY*(CC/BB)
000217              BP= B- SXY*(CC/AA)
000222              P= (SXP*SYC*SYC)/(SY*BB)+ (SXY*SXC*SXC)/(SX*AA)
000233              Q= (SYP*SXC*SXC)/(SX*AA)+ (SXY*SYC*SYC)/(SY*BB)
000244              R= (SXP*SYC*A)/(SY*BB)- (SXY*SXC*B)/(SX*AA)
000256              S= (SYP*SXC*B)/(SX*AA)-(SXY*SYC*A)/(SY*BB)
000270              GO TO 42
000271           40 SX= SXP
000273              SY= SYP
000274              AP= A
000276              BP= B
000277              P= SYC/SY
000301              Q= 0.
000302              R= A/SY
000303              S= 0.
000304           42 WP= W+ D+ (SYC*A)/SY+ (SXC*B)/SX
000315              WB=-W+ (BP*SXC)/SX- (AP*SYC)/SY  -D
000326              FF= (A*AP)/SY+ (B*BP)/SX+ 1./A1+ 1./A2
000336              F= 1./FF
000337              ALPH= (L*L)/(12.*SJB)
000345              CLTH5= ALPH*E*SWP
000347              CLTH3= -((E*SWP)/F+ ALPH*G*SJ- E*WP*WB)
000356              CLTH1= (G*SJ)/F
000360              CRMYP1= -(R*WB+P/F)
000363              CRMXP1= -(S*WB- Q/F)
000366              CRMYP3= ALPH*P
000370              CRMXP3= -ALPH*Q
000371              CRQTP2= -ALPH
000372              CRQT= 1./F
```

```
000374        WRITE (6,2) SX1,SX2,SY1,SY2,SXY1,SXY2,SW1,SW2,SJ1,SJ2,EX1,EX2,EY1,
             1EY2,CX1,CX2,CY1,CY2,A1,A2,W1,W2,E,G,PSN,L,SB,AST,H
000471        WRITE (6,3)
000475      3 FORMAT (10X)
000475        WRITE (6,2) SXC,SYC,SW,AA,BB,CC,SX,SY,SXP,SYP,AP,BP,SWP,WB,P,Q,
             1WP,F,R,S,ALPH,CLTH5,CLTH3,CLTH1,CRMYP1,CRMXP1,CRMYP3,CRMXP3,
             2CRQT,CROTP2
000575      2 FORMAT(1X,6E15.6)
000575        RAS= (-CLTH3- SQRT(CLTH3*CLTH3- 4.*CLTH5*CLTH1))/(2.*CLTH5)
000607        RBS= (-CLTH3+ SQRT(CLTH3*CLTH3- 4.*CLTH5*CLTH1))/(2.*CLTH5)
000621        RA= SQRT(RAS)
000623        RB= SQRT(RBS)
000625        CP= -(CRMYP1*PX+ CRMXP1*PY)/CLTH1 + (CRQT*QT)/CLTH1
000635        ALP= ALPH*E*SWP
000637        BET= -(ALPH*G*SJ- E*WP*WB)
000645        RA5= RA*RA*RA*RA*RA
000647        RA4= RA*RA*RA*RA
000650        RA3= RA*RA*RA
000651        RA2= RA*RA
000652        RB5= RB*RB*RB*RB*RB
000654        RB4= RB*RB*RB*RB
000655        RB3= RB*RB*RB
000656        RB2= RB*RB
000657        RAT= RA*HT
000660        RBT= RB*HT
000661        WRITE (6,5)
000664      5 FORMAT (10X)
000664        WRITE(6,2) RAS,RBS,RA,RB,CP,BET,ALP,RAT,RBT
000712        DO 4 I= 1,5
000714        DO 4 J= 1,5
000715      4 AAA(I,J)= 0
000724        AAA(1,1)= 1.
000725        AAA(1,2)= 1.
000726        AAA(1,4)= 1.
000727        AAA(2,3)= RA
000730        AAA(2,5)= RB
000732        AAA(3,3)= RA*RA*RA*E*SWP- G*SJ*RA
000737        AAA(3,5)= RB*RB*RB*E*SWP- G*SJ*RB
000745        AAA(4,2)= (ALP*RA4+ BET*RA2)*COSH(RAT)
000753        AAA(4,3)= (ALP*RA4+ BET*RA2)*SINH(RAT)
000762        AAA(4,4)= (ALP*RB4+ BET*RB2)*COSH(RBT)
000771        AAA(4,5)= (ALP*RB4+ BET*RB2)*SINH(RBT)
001000        AAA(5,2)= RA2*COSH(RAT)
001004        AAA(5,3)= RA2*SINH(RAT)
001007        AAA(5,4)= RB2*COSH(RBT)
001012        AAA(5,5)= RB2*SINH(RBT)
001015        BBB(1)= 0.
001016        BBB(2)= -CP
001017        BBB(3)= G*SJ*CP-P*PX+ Q*PY   -QT
001027        BBB(4)= 0.
001030        BBB(5)= 0.
001031        WRITE (6,7) AAA
001036      7 FORMAT (3X,5E18.6)
001036        WRITE (6,7) BBB
001044        CALL SIMQ(AAA,BBB,5,KS)
001047        WRITE (6,9) KS
001055      9 FORMAT (20X,I3)
001055        WRITE (6,7) BBB
```

```
001063        C1= BBB(1)
001065        C2= BBB(2)
001066        C3= BBB(3)
001070        C4= BBB(4)
001071        C5= BBB(5)
001073        Z= 0.
001074        WRITE (6,11)
001077     11 FORMAT(10X)
001077     10 RAZ= RA*Z
001101        RBZ= RB*Z
001103        THET= C1+ C2*COSH(RAZ)+ C3*SINH(RAZ)+ C4*COSH(RBZ)+ C5*SINH(RBZ)+
             1CP*Z
001126        THETP1= C2*RA*SINH(RAZ)+ C3*RA*COSH(RAZ)+ C4*RB*SINH(RBZ)+ C5*
             1RB*COSH(RBZ)+ CP
001150        THETP2= C2*RA2*COSH(RAZ)+ C3*RA2*SINH(RAZ)+ C4*RB2*COSH(RBZ)+
             1C5*RB2*SINH(RBZ)
001172        THETP3= C2*RA3*SINH(RAZ)+ C3*RA3*COSH(RAZ)+ C4*RB3*SINH(RBZ)+
             1C5*RB3*COSH(RBZ)
001214        WRITE (6,12) THET,THETP1,THETP2,THETP3
001230     12 FORMAT (1X,6E20.6)
001230        IF(Z.EQ.HT) GO TO 13
001232        Z= Z+H
001234        GO TO 10
001234     13 B1= (C2*(-E*SWP*RA3+ G*SJ*RA))/WB
001244        B2= (C3*(-E*SWP*RA3+ G*SJ*RA))/WB
001253        B3= (C4*(-E*SWP*RB3+ G*SJ*RB))/WB
001262        B4= (C5*(-E*SWP*RB3+ G*SJ*RB))/WB
001271        B5= (G*SJ*CP-P*PX+ Q*PY -QT)/WB
001302        D1= -B1/RA
001304        D2=-B2/RA
001305        D3= -B3/RB
001307        D4= -B4/RB
001311        D5= -B5
001312        D6= (B1*COSH(RAT)+ B2*SINH(RAT))/RA+ (B3*COSH(RBT)+ B4*SINH(RBT))
             1/RB+ B5*HT
001337        Z= 0.
001340        WRITE (6,19)
001343     19 FORMAT (10X)
001343     15 RAZ= RA*Z
001345        RBZ= RB*Z
001347        FQ= B1*SINH(RAZ)+ B2*COSH(RAZ)+ B3*SINH(RBZ)+ B4*COSH(RBZ)+ B5
001367        FT= D1*COSH(RAZ)+ D2*SINH(RAZ)+ D3*COSH(RBZ)+ D4*SINH(RBZ)+
             1  D5*Z+ D6
001412        THET= C1+ C2*COSH(RAZ)+ C3*SINH(RAZ)+ C4*COSH(RBZ)+ C5*SINH(RBZ)+
             1CP*Z
001436        THETP1= C2*RA*SINH(RAZ)+ C3*RA*COSH(RAZ)+ C4*RB*SINH(RBZ)+ C5*
             1RB*COSH(RBZ)+ CP
001460        THETP2= C2*RA2*COSH(RAZ)+ C3*RA2*SINH(RAZ)+ C4*RB2*COSH(RBZ)+
             1C5*RB2*SINH(RBZ)
001502        THETP3= C2*RA3*SINH(RAZ)+ C3*RA3*COSH(RAZ)+ C4*RB3*SINH(RBZ)+
             1C5*RB3*COSH(RBZ)
001524        BIMNT1= -E*SW1*THETP2
001527        BIMNT2= -E*SW2*THETP2
001531        TRQ1= -E*SW1*THETP3+ G*SJ1*THETP1
001536        TRQ2= -E*SW2*THETP3+ G*SJ2*THETP1
001544        WRITE (6,17) FQ,FT,BIMNT1,BIMNT2,TRQ1,TRQ2
001563     17 FORMAT(1X,6E16.6)
001563        IF (Z.EQ.HT) GO TO 29
```

```
001565          Z= Z+H
001567          GO TO 15
001567       29 Z1= (SYC*C2*RA2)/SY-  (AP*D1)/(E*SY)
001600          Z2= (SYC*C3*RA2)/SY-(AP*D2)/(E*SY)
001611          Z3= (SYC*C4*RB2)/SY- (AP*D3)/(E*SY)
001622          Z4= (SYC*C5*RB2)/SY- (AP*D4)/(E*SY)
001633          Z5= -(AP*D5)/(E*SY)- (SXP*SYC*PX)/(E*SY*BB)+ (SXY*SYC*PY)/(E*SY*BB
               1 )
001652          Z6= -(AP*D6)/(E*SY)+ (SXP*SYC*HT*PX)/(E*SY*BB)-(SXY*SYC*HT*PY)
               1/(E*SY*BB)
001672          Z7= -Z2/RA- Z4/RB
001676          Z8= -Z1/RA2-  Z3/RB2
001702          E1=-(SXC*C2*RA2)/SX- (BP*D1)/(E*SX)
001713          E2=-(SXC*C3*RA2)/SX- (BP*D2)/(E*SX)
001724          E3=-(SXC*C4*RB2)/SX- (BP*D3)/(E*SX)
001735          E4=-(SXC*C5*RB2)/SX- (BP*D4)/(E*SX)
001746          IF (AA.EQ.0.) GO TO 50
001747          E5= -(BP*D5)/(E*SX)+ (SXY*SXC*PX)/(E*SX*AA)- (SYP*SXC*PY)/
               1  (E*SX*AA)
001765          E6= -(BP*D6)/(E*SX)- (SXY*SXC*HT*PX)/(E*SX*AA)+ (SYP*SXC*HT*PY)
               1 /(E*SX*AA)
002005          GO TO 52
002005       50 E5= -PY/(E*SX)
002010          E6= (PY*HT)/(E*SX)
002014       52 E7= -E2/RA- E4/RB
002020          E8= -E1/RA2- E3/RB2
002024          Z= 0.
002025          WRITE(6,22)
002031       22 FORMAT(10X)
002031       20 RAZ= RA*Z
002033          RBZ= RB*Z
002035          ZETP2= Z1*COSH(RAZ)+ Z2*SINH(RAZ)+ Z3*COSH(RBZ)+ Z4*SINH(RBZ)+
               1 Z5*Z+ Z6
002057          ZETP1= (Z1/RA)*SINH(RAZ)+ (Z2/RA)*COSH(RAZ)+ (Z3/RB)*SINH(RBZ)+
               1 (Z4/RB)*COSH(RBZ)+ (Z5/2.)*Z*Z+ Z6*Z+ Z7
002113          ZET= (Z1/RA2)*COSH(RAZ)+ (Z2/RA2)*SINH(RAZ)+ (Z3/RB2)*COSH(RBZ)+
               1  (Z4/RB2)*SINH(RBZ)+ (Z5/6.)*Z*Z*Z+ (Z6/2.)*Z*Z+ Z7*Z+ Z8
002153          ETAP2= E1*COSH(RAZ)+ E2*SINH(RAZ)+ E3*COSH(RBZ)+ E4*SINH(RBZ)+
               1 E5*Z+ E6
002176          ETAP1= (E1/RA)*SINH(RAZ)+ (E2/RA)*COSH(RAZ)+ (E3/RB)*SINH(RBZ)
               1 + (E4/RB)*COSH(RBZ)+ (E5/2.)*Z*Z+ E6*Z+ E7
002232          ETA= (E1/RA2)*COSH(RAZ)+(E2/RA2)*SINH(RAZ)+ (E3/RB2)*COSH(RBZ)+
               1 (E4/RB2)*SINH(RBZ)+ (E5/6.)*Z*Z*Z+ (E6/2.)*Z*Z+E7*Z+ E8
002272          WRITE (6,37) ZET,ZETP1,ZETP2,       ETA,ETAP1,ETAP2
002312       37 FORMAT (1X, 6E13.4)
002312          IF (Z.EQ.HT) GO TO 26
002314          Z= Z+H
002316          GO TO 20
002316       26 STOP
002320          END

UNUSED COMPILER SPACE
010700
```

APPENDIX-C

EXPERIMENTAL DATA

TABLE C1

STRAIN DATA FOR MODEL WITH FLOORS

strain in μ in/in for load at 8th floor

Strain Gauge No.	Loading 2.5 lbs.	5 Lbs.	7.5 lbs.	10 lbs.	12.5 lbs.
1	-30	-56	-92	-116	-140
2	+24	+48	+68	+86	+106
3	-28	-56	-84	-110	-130
4	+14	+38	+64	+94	+118
5	-30	-56	-84	-114	-138
6	+18	+50	+80	+112	+142
7	+15	+30	+48	+60	+76
8	0	-10	-22	-34	-46
9	*				
10	-22	-48	-74	-100	-126
11	+5	+5	+7	+8	+9
12	-12	-25	-40	-55	-68
13	-20	-44	-72	-96	-120
14	+14	+36	+48	+60	+70
15	-14	-36	-52	-64	-78
16	-3	-7	-11	-15	-20
17	-14	-28	-38	-42	-54
18	+6	+16	+32	+48	+60
19	-8	-24	-42	-56	-70
20	+25	+58	+98	+134	+170
21	-28	-58	-90	-118	-148
22	+16	+38	+60	+84	+108
23	+6	+12	+20	+28	+34
24	+14	+36	+56	+78	+98

* Strain Gauge out of order

TABLE C1 (continued)

STRAIN DATA FOR MODEL WITH FLOOR

Strain in μ in/in for load at 8th floor

Strain Gauge No.	Loading 10 lbs.	7.5 lbs.	5 lbs.	2.5 lbs.	0
1	-114	-84	-50	-25	-2
2	+90	+70	+50	+28	+2
3	-114	-94	-74	-52	-26
4	+94	+70	+40	+14	0
5	-114	-90	-62	-34	-6
6	+116	+84	+62	+28	+8
7	+62	+48	+36	+20	+2
8	-38	-24	-10	-2	0
10	-104	-80	-54	-26	0
11	+8	+8	+6	+4	0
12	+56	+44	+30	+16	+2
13	-100	-74	-50	-26	-2
14	+60	+52	+42	+26	+10
15	-64	-54	-40	-26	-12
16	-15	-12	-8	-5	-2
17	-44	-36	-23	-13	-2
18	+50	+46	+24	+12	0
19	-60	-46	-32	-22	-11
20	+138	+106	+72	+36	+6
21	-124	-94	-66	-38	-10
22	+86	+62	+40	+14	0
23	+28	+18	+12	+4	+2
24	+80	+58	+40	+16	+3

* Strain Gauge out of order

TABLE C2

DEFLECTION DATA FOR MODEL WITH FLOOR

Deflection in inch for load at 8th floor

Dial Gauge No.	Loading 2.5 lbs.	5 lbs.	7.5lbs	10 lbs.	12.5 lbs.
1	.011	.032	.055	.079	.097
2	.0285	.0725	.118	.1695	.2125
3	.009	.026	.043	.062	.084
4	.025	.066	.108	.151	.187
5	.007	.022	.041	.061	.083
6	.020	.053	.086	.122	.152
7	.003	.010	.022	.024	.030
8	.010	.030	.048	.069	.085
9	.002	.004	.006	.009	.011
10	.004	.011	.0175	.025	.031

Dial Gauge No.	10 lbs.	7.5 lbs.	5 lbs.	2.5 lbs.	0
1	.082	.063	.040	.016	.005
2	.1715	.1325	.0885	.040	.010
3	.066	.049	.032	.014	.005
4	.153	.120	.080	.036	.006
5	.064	.047	.028	.011	.003
6	.124	.097	.064	.028	.003
7	.025	.020	.013	.005	.001
8	.070	.054	.036	.015	.003
9	.008	.007	.005	.002	.001
10	.025	.020	.013	.090	.002

TABLE C3

STRAIN DATA FOR MODEL WITH FLOORS

Strain in μ in/in for load at 6th floor

Strain Gauge No.	2.5 lbs.	5 lbs.	7.5 lbs.	10 lbs.	12.5 lbs.
1	-24	-44	-62	-84	-98
2	+24	+44	+66	+86	+106
3	-24	-46	-70	-92	-116
4	+4	+18	+36	+56	+78
5	-18	-40	-60	-80	-100
6	+4	+18	+40	-60	+80
7	+8	+20	+30	+42	+52
8	0	-4	-12	-24	-36
9	*				
10	----------------no reading----------------				
11	-4	-8	-12	-17	-22
12	+6	+10	+16	+26	+30
13	-4	-12	-22	-34	-44
14	+10	+18	+28	+36	+42
15	+2	+4	+5	+6	+8
16	-10	-22	-36	-50	-66
17	+5	+10	+18	+26	+34
18	-6	-16	-24	-30	-38
19	0	-2	-12	-24	-42
20	+14	+32	+50	+72	+92
21	-14	-32	-48	-68	-86
22	+5	+14	+24	+34	+44
23	+12	+32	+46	+62	+78
24	-2	-4	-5	-6	-6

* Strain Gauge out of order

TABLE C3 (continued)

STRAIN DATA FOR MODEL WITH FLOORS

Strain in μ in/in for load at 6th floor

Strain Gauge No.	Loading 10 lbs.	7.5 lbs.	5 lbs.	2.5 lbs.	0
1	-88	-72	-56	-22	-6
2	+88	+68	+46	+26	0
3	-96	-74	-52	-28	-6
4	+60	+38	+22	+10	+2
5	-82	-64	-44	-26	-6
6	-58	-44	-16	-8	0
7	+42	+34	+24	+12	0
8	-28	-18	-12	-2	0
9	*				
10	----------------no reading-----------------				
11	-18	-13	-9	-4	-2
12	+26	+20	+14	+8	+4
13	-36	-24	-18	-6	-2
14	+34	+28	+20	+10	0
15	+6	+4	+2	0	0
16	-58	-42	+32	-14	+4
17	+30	+20	+14	+6	0
18	-30	-25	-18	-10	-2
19	-42	-22	-12	-2	0
20	+76	+54	+38	+14	+2
21	-72	-54	-36	-18	-4
22	+34	+24	+15	+6	0
23	+62	+48	+32	+14	0
24	-4	-4	-4	-2	0

* Strain Gauge out of order

TABLE C4

DEFLECTION DATA FOR MODEL WITH FLOORS

Deflection in inch for load at 6th floor

Dial Gauge No.	Loading 2.5 lbs.	5 lbs.	7.5 lbs.	10lbs.	12.5 lbs.
1	.005	.024	.030	.043	.058
2	.015	.0525	.072	.100	.129
3	.004	.020	.0255	.036	.047
4	.014	.052	.060	.097	.1245
5	.004	.018	.023	.033	.046
6	.012	.043	.059	.081	.105
7	.002	.010	.012	.017	.022
8	.007	.026	.036	.050	.064
9	.001	.004	.005	.006	.008
10	.003	.011	.014	.019	.025

Dial Gauge No.	10 lbs.	7.5 lbs.	5 lb.s	2.5 lbs.	0
1	.044	.032	.019	.008	0
2	.105	.076	.047	.020	.001
3	.038	.027	.016	.006	0
4	.101	.074	.046	.019	.001
5	.036	.024	.014	.005	.001
6	.085	.062	.038	.016	.001
7	.018	.014	.008	.003	0
8	.052	.038	.023	.009	0
9	.007	.005	.003	.001	0
10	.020	.015	.009	.004	0

TABLE C5

STRAIN DATA FOR MODEL WITH FLOORS

Strain in μ in/in for load at 4th floor

Strain Gauge No.	Loading 2.5 lbs.	5 lbs.	7.5 lbs.	10 lbs.	12.5 lbs.
1	-21	-36	-54	-68	-84
2	+18	+40	+60	+82	+100
3	-14	-34	-50	-68	-84
4	0	+6	+18	+34	+50
5	-12	-26	-28	-50	-62
6	0	+6	+14	+26	+40
7	+8	+20	+30	+42	+52
8	----------------no reading----------------------				
9	*				
10	-7	-18	-30	-40	-52
11	-4	-8	-12	-17	-22
12	+6	+10	+16	+22	+26
13	-4	-12	-22	-34	-44
14	+10	+18	+28	+36	+42
15	-2	-4	-5	-6	-8
16	-10	-22	-36	-50	-66
17	+5	+10	+18	+26	+34
18	-6	-16	-24	-30	-38
19	0	-2	-12	-24	-42
20	+14	+32	+50	+72	+92
21	-14	-32	-48	-68	-86
22	+5	+14	+24	+34	+44
23	+12	+32	+46	+62	+78
24	-2	-4	-5	-6	-6

* Strain Gauge out of order

TABLE C5 (continued)

STRAIN DATA FOR MODEL WITH FLOORS

Strain in μ in/in for load at 4th floor

Strain Gauge No.	10 lbs.	7.5 lbs.	5 lbs.	2.5 lbs.	0
1	-72	-56	-44	-28	-10
2	+78	+58	+34	+14	+2
3	-70	-54	-36	-18	-4
4	+40	+34	+24	+10	+6
5	-52	-40	-30	-16	-6
6	+32	+20	+12	+4	0
7	+42	+34	+24	+12	0
8	--------------no reading------------------				
9	*				
10	-43	-32	-22	-10	-4
11	-18	-13	-10	-5	0
12	+22	+16	+10	+4	0
13	-32	-20	-14	-4	0
14	+34	+28	+20	+10	0
15	-6	-4	-2	-2	0
16	-58	-42	-32	-14	-4
17	+30	+20	+14	+8	0
18	-30	-22	-17	-10	-2
19	-42	-22	-12	-2	0
20	+76	+54	+38	+14	+2
21	-72	-54	-36	-18	-4
22	+34	+25	+15	+6	0
23	+62	+48	+32	+14	0
24	-4	-4	-4	-2	0

TABLE C6

DEFLECTION DATA FOR MODEL WITH FLOOR

Deflection in inch for load at 4th floor

Dial Gauge No.	Loading 2.5 lbs.	5 lbs.	7.5 lbs.	10 lb.s	12.5 lbs.
1	.001	.008	.012	.020	.029
2	.008	.025	.037	.054	.073
3	.001	.008	.012	.018	.026
4	.007	.024	.037	.055	.074
5	.001	.007	.011	.017	.025
6	.006	.020	.032	.047	.064
7	.001	.005	.008	.011	.015
8	.005	.015	.023	.034	.046
9	0	.002	.003	.005	.006
10	.002	.007	.010	.015	.020

Dial Gauge No.	Loading 10 lbs.	7.5 lbs.	5 lbs.	2.5 lbs.	0
1	.023	.017	.012	.007	0
2	.060	.046	.031	.020	.003
3	.021	.016	.011	.007	0
4	.060	.048	.031	.019	.003
5	.019	.014	.010	.006	.001
6	.052	.040	.026	.016	.003
7	.012	.0095	.007	.004	.001
8	.037	.029	.019	.011	.001
9	.005	.004	.003	.0015	0
10	.016	.012	.008	.006	.001

TABLE C7

STRAIN DATA FOR MODEL WITH BEAMS

Strain in μ in/in for lateral load at top

Strain Gauge No.	5 lbs.	10 lbs.	15 lbs.	20 lbs.	25 lbs.
1	-20	-60	-82	-120	-152
2	-18	-42	-72	-104	-132
3	-16	-40	-76	-112	-140
4	no strain				
5	-12	-24	-46	-52	-64
6	-22	-46	-74	-98	-124
11	+8	+24	+38	+52	+64
12	+22	+42	+62	+82	+110
13	+35	+63	+83	+103	+123
14	+16	+38	+62	+88	+114
15	+14	+24	+34	+44	+54
16	no strain				
17	-14	-29	-44	-59	-73
18	+18	+42	+76	+114	+160
19	-16	-33	+50	-66	-84
20	+10	+30	+40	+54	+70
21	-54	-138	-230	-326	+410

TABLE C7 (continued)

STRAIN DATA FOR MODEL WITH BEAMS

strain in μ in/in for lateral load at top

Strain Gauge No.	Loading 20 lbs.	15 lbs.	10 lbs.	5 lbs.	0
1	-124	-92	-64	-34	-6
2	-106	-76	-46	-22	0
3	-120	-86	-56	-26	-4
4	no strain				
5	-54	-42	-26	-14	-2
6	-104	-80	-56	-30	-5
11	+56	+44	+30	+14	0
12	+90	+72	+52	+28	+2
13	+99	+79	+65	+41	+6
14	+94	+76	+50	+26	+4
15	+46	+36	+26	+16	+2
16	no strain				
17	-62	-46	-30	-13	-2
18	+130	+98	+68	+36	+10
19	-70	-52	-34	-14	0
20	-60	-50	-34	-20	-2
21	-336	-252	-182	-76	-8

TABLE C8

DEFLECTION DATA FOR MODEL WITH FLOORS

Deflection in inch for lateral load at top

Dial Gauge No.	Loading 5 lbs.	10 lbs.	15 lbs.	20 lbs.	25 lbs.
1	.015	.030	.052	.064	.079
2	.013	.024	.046	.056	.061
3	.013	.020	.037	.042	.053
4	.007	.012	.019	.026	.030
5	.0036	.0069	.0095	.0119	.0127
6	.024	.060	.100	.132	.167
7	.019	.050	.086	.113	.144
8	.016	.042	.071	.100	.121
9	.009	.026	.045	.060	.077
10	.0051	.0115	.0206	.0270	.0336

Dial Gauge No.	Loading 20 lbs.	15 lbs.	10 lbs.	5 lbs.	0
1	.066	.054	.035	.020	.004
2	.057	.046	.029	.016	.006
3	.045	.039	.033	.014	.004
4	.029	.021	.015	.010	.003
5	.0124	.0099	.0073	.0048	.0013
6	.147	.115	.085	.046	.011
7	.127	.099	.074	.038	.009
8	.107	.083	.063	.032	.007
9	.068	.054	.039	.019	.006
10	.0289	.0230	.0178	.0121	.0043

TABLE C9

STRAIN DATA FOR MODEL WITH BEAMS

Strain in μ in/in for torque at top

Strain Gauge No.	Loading 25 lb-in	50 lb-in	75 lb-in	100 lb-in	125lb-in
1	-72	-164	-248	-356	-446
2	-30	-66	-116	-158	-200
3	no strain				
4	-34	-76	-124	-168	-200
5	-12	-24	-38	-50	-60
6	+6	+22	+36	+52	+60
11	-10	-28	-48	-70	-88
12	+15	+38	+58	+79	+101
13	+50	+113	+173	+233	+301
14	-11	-24	-36	-49	-62
15	+10	+23	+35	+52	+65
16	+25	+55	+83	+114	+142
17	+30	+70	+108	+154	+184
18	+26	+54	+89	+117	+145
19	+10	+23	+36	+48	+64
20	-14	-22	-34	-47	-62
21	-20	-32	-42	-56	-70

TABLE C9 (continued)

STRAIN DATA FOR MODEL WITH BEAMS

Strain in μ in/in for torque at top

Strain Gauge No.	Loading 100lb-in	75lb-in	50lb-in	25lb-in	0
1	-380	-308	-212	-92	-15
2	-172	-134	-96	-56	-6
3	no strain				
4	-174	-144	-108	-74	-4
5	-50	-38	-28	-14	0
6	+54	+38	+25	+16	+2
11	-76	-64	-46	-28	-8
12	+82	+62	+42	+22	+2
13	+236	+176	+118	+60	+4
14	-51	-39	-27	-15	-2
15	-50	-38	-26	-14	-3
16	+116	+89	+60	+30	+2
17	+160	+128	+100	+62	+6
18	+119	+92	+56	+30	+3
19	+52	+39	+25	+14	+2
20	-54	-38	-26	-10	0
21	-50	-43	-33	-22	-2

TABLE C10

DEFLECTION DATA FOR MODEL WITH FLOORS

Deflection in inch for torque at top

Dial Gauge No.	Loading 25lb-in	50lb-in	75lb-in	100lb-in	125lb-in
1	.004	.008	.018	.023	.031
2	.003	.007	.016	.022	.028
3	.003	.0005	.013	.018	.025
4	.002	.004	.008	.011	.015
5	.0006	.0018	.0041	.0054	.0071
6	.017	.059	.101	.139	.180
7	.013	.043	.081	.110	.146
8	.009	.035	.066	.091	.121
9	.006	.023	.043	.059	.078
10	.0023	.0099	.019	.0262	.0354

Dial Gauge No.	Loading 100lbs-in	75lb-in	50lb-in	25lb-in	0
1	.026	.018	.011	.008	.003
2	.023	.016	.010	.007	.004
3	.021	.014	.008	.005	.002
4	.013	.009	.005	.003	.001
5	.006	.0042	.0024	.0018	.0009
6	.149	.111	.072	.045	.008
7	.119	.094	.056	.035	.007
8	.099	.073	.046	.029	.004
9	.064	.047	.030	.018	.003
10	.0284	.0208	.0125	.0071	.001

BIBLIOGRAPHY

1. AFSAR, M.
"Lateral Loading of Shear Wall Models", M. Eng. Thesis, August 1967.

2. QURESHI, A.A.
"Behaviour of Shear Wall Models with Circular Wall Openings", M. Eng. Thesis, February 1968.

3. SPEIRS, J.W.
"Lateral Loading of Small Scale Shear Wall Building with Floor Slab", M. Eng. Thesis, March 1969.

4. RAINA, R.K.
"Dynamic Response of Thin Wall Shear Wall Model", M. Eng. Thesis, January 1970.

5. SWIFT, R.D.
"Analysis of Asymmetrical Coupled Shear Wall Structures", M. Eng. Thesis, April 1970.

6. COULL, A. and SMITH, S.B.
"Analysis of Shear Wall Structures", A review of previous research, Symposium of Tall Buildings, pp. 138-58. April 1966.

7. WINOKUR, A. and GLUCK, J.
"Lateral Loads in Asymmetric Multi-storey Structures", Journal of the Structural Division, Proc. of the Am. Soc. of Civil Eng., V. 94, n. ST. 3, March 1968.

8. VLASOV, V.Z.
"Thin Walled Elastic Beams", Published for the National Science Foundation, Washington D.C. by the Israel Program for Scientific Translations, Jerusulem 1961 (First edition published in original Russian 1940).

9. ZBIROHOWSKI-KOSCIA
"Thin Walled Beams--from Theory to Practice", Crosby-Lockwood, London 1969.

10. QADEER, A.
"The Interaction of Floor Slabs and Shear Walls", Ph.D. Thesis at University of Southamption, October 1968.

11. QADEER, A. and SMITH, S.B.
"The Bending Stiffness of Slabs Connecting Shear Walls", ACI Journal, June 1969.

12. TARANATH, B.S.
"The Torsional Behaviour of Open Section Shear Wall Structures", Ph.D. Thesis at University of Southampton, October 1968.

13. BECK, H.
"Contribution to the Analysis of Shear Walls", Journal of the American Concrete Institute, V.59, pp 1055-69 1962.

14. ROSMAN, R.
"Approximate Analysis of Shear Wall Subjected to Lateral Loads". Journal of the American Concrete Institute, V.61, pp 717-32, 1964.

15. COULL, A. and CHOUDHURY, J.R.
"Stresses and Deflections in Coupled Shear Walls", Journal of the American Concrete Insitute, pp. 65-72, February 1967.

16. COULL, A. and CHOUDHURY, J.R.
"Analysis of Coupled Shear Walls", Journal of the American Concrete Institute, pp. 587-93, September 1967.

17. CHOUDHURY, J.R.
"Analysis of Plane Spatial System of Interconnected Shear Walls", Ph.D. Thesis. University of Southampton, October 1968.

18. MICHAEL, D.
"Torsional Coupling of Core Walls in Tall Buildings", The Structural Engineer, N.2, V 47, February 1969.

19. JENKINS, W.M. and HARRISON, T.
" Analysis of Tall Buildings with Shear Wall Under Bending and Torsion", Tall Buildings, pp. 413-49.

20. HOLMES, M. And ASTILL, A.W.
"Experimental Stresses and Deflections of a Model Shear Wall Structure", Journal of the American Concrete Institute, pp. 667-76, August 1969.

21. ROSMAN, R.
"Analysis of Pierced Torsion Boxes", Acta Techniac Scientiarum Hungaricae, Tomus 65 (3-4), pp.365-97, 1969.

22. GLUCK, J.
"Lateral Load Analysis of Asymmetric Multistorey Structures", Journal of the Structural Division, Proc. of the Am. Soc. of Civil Eng., ST2, pp. 317-33, February 1970.

23. MACLEOD, I.A.
"Connected Shear Wall of Unequal Width", Journal of American Concrete Institute, pp. 408-12, May 1970.

24. BISWAS, J.K. and TSO, W.K.
Discussion of Ref. (22), Journal of Structural Division Proceedings Am. Soc. of Civil Engineers, ST 11, pp. 2540-44, November 1970.

25. HOLTZER, H.
Die Berechnung der Drehshwingunnen, Springer-Verllag, Berlin 1921.

26. MYKLESTAD, N.O.
"New Methods of Calculating Natural Modes of Coupled Bending Torsion Vibration of Beam", Tran. ASME, Vol. 67 pp. 61-67, 1945.

27. THOMSON, W.T.
"Matrix Solution of Vibration of Nonuniform Beam", Jour. Appl. Mech. Vol. 17, No. 3, pp.337-339, 1950.

28. COULL, A. and IRWIN, A.W.
"Analysis of Load Distribution in Multistorey Shear Wall Structures", The Structural Engineer, N.8, V.48, August 1970.

29. TSO, W.K.
"Coupled Vibration of Thin-Walled Elastic Bars",
J. Engineering Mechanics Division, A.S.C.E. Vol. 91
EM3 1965 pp.33-52.